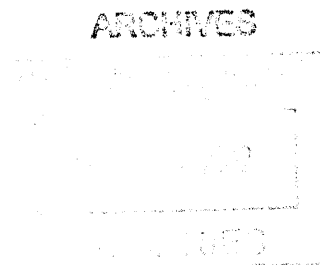


Structure-function Characterization and Engineering of Polysaccharides and Antibodies with Therapeutic Activity

by

Luke Robinson

B.S., University of Minnesota (2006)



Submitted to the Department of Biological Engineering
in partial fulfillment of the requirements for the degree of

Doctor of Philosophy in Biological Engineering
at the

MASSACHUSETTS INSTITUTE OF TECHNOLOGY

September 2012


© 2012 Massachusetts Institute of Technology. All Rights Reserved.

Author

.....


Luke Robinson
Department of Biological Engineering
August 16, 2012

Certified by

.....


Ram Sasisekharan, Ph.D.
Alfred H. Caspary Professor of Biological Engineering
Thesis Supervisor

Accepted by

.....


Forest M. White, Ph.D.
Associate Professor of Biological Engineering
Chair, Graduate Program

This doctoral thesis has been examined by a committee of the Department of Biological Engineering as follows:

Pete Dedon, M.D., Ph.D.
Professor of Toxicology and Biological Engineering
Deputy Director, MIT Center for Environmental Health Sciences
Thesis Committee Chair

Ram Sasisekharan, Ph.D.
Alfred H. Caspary Professor of Biological Engineering
Thesis Supervisor

Zach Shriver, Ph.D.
Vice President of Research
Visterra, Inc.

Rahul Raman, Ph.D.
Research Scientist
Department of Biological Engineering

Structure-function Characterization and Engineering of Polysaccharides and Antibodies with Therapeutic Activity

by

Luke Robinson

Submitted to the Department of Biological Engineering on August 16, 2012 in Partial Fulfillment of the Requirements for the Degree of Doctor of Philosophy in Biological Engineering

ABSTRACT

Proteins and polysaccharides are of growing importance as a source for novel therapeutic compounds and target a range of diseases, from cancer to infections from pathogens. However, owing to their large and complex structures, they face a unique set of challenges, compared to small molecules, in their discovery and development as safe, efficacious drugs. Towards addressing these challenges, we describe in this thesis the implementation of structure-function relationship approaches to characterize and engineer polysaccharides and antibodies to improve their therapeutic profiles.

The plant polysaccharide pectin, when modified, has demonstrated significant anticancer activity in animal models and small-scale clinical trials. Its development has been hampered, however, due to its complex structure and lack of structure-activity correlates. Using an integrated approach, we engineer a modified pectin that exhibits significant *in vivo* anticancer activity, which we link to specific structural attributes and cellular functional mechanisms. These results improve our structure-function understanding of anticancer modified pectin, an important step towards the clinical use of this complex polysaccharide.

Applying what we learned from pectin, we develop an integrated framework to identify a contaminant in batches of heparin, a polysaccharide anticoagulant drug, associated with an outbreak of allergic-type reactions in 2007-2008. Employing orthogonal analytical approaches to overcome challenges of characterizing structurally complex pharmaceutical heparin, we determine that the structurally related glycan, oversulfated chondroitin sulfate, is the major contaminant. We link its presence to activation of the contact pathway, thereby establishing a structure-function understanding of contaminated heparin and improving the safety profile of this polysaccharide drug.

Transitioning knowledge gained from the structure-function characterization of polysaccharides, we engineer, by structure-based design, a broad spectrum neutralizing antibody to dengue virus, which yearly infects more than 200 million people, causing approximately 21,000 deaths. We incorporate complementary approaches of energetics and empirical informatics

methods to rationally redesign an existing antibody for greater breadth and potency, resulting in an engineered antibody with binding to all four virus serotypes and good *in vitro* potency.

Overall, this thesis provides important insights into structure-function approaches through the use of complementary methods to characterize and engineer therapeutic polysaccharides and antibodies.

Thesis Supervisor: Ram Sasisekharan

Title: Alfred H. Caspary Professor of Biological Engineering

Acknowledgements

First, I would like to express my most sincere gratitude to my advisor Professor Ram Sasisekharan for all the guidance and support he has so generously provided me. Entering graduate school, I would not have imagined the variety of positive and meaningful opportunities he has graciously entrusted me to be a part of, ranging from cutting-edge exciting research projects, to tackling a real-time public health outbreak, to global translational research collaborations, and an undergraduate international exchange program, among others. His positive energy, infectious optimism, exuberance for impactful research, and dedication to improving global health through science have been true sources of inspiration to me. He has instilled in me a passion to create change for the betterment of others through science and by working collaboratively with others. Lastly, I thank Professor Sasisekharan for his genuine, unqualified support of my growth and development scientifically, professionally, and personally.

I would also like to thank the other members of my thesis committee. My committee Chair, Professor Pete Dedon, has been truly supportive and encouraging of me and my research, and I appreciate his insightful comments towards the guidance and completion of my thesis work. I would like to thank Dr. Zach Shriver, a committee member, for his earnest support and insightful feedback throughout my research work. Enlightening discussions with him were instrumental in helping me better understand, develop and efficiently implement scientific plans towards key goals. I would also like to thank Dr. Rahul Raman, a committee member, for his support and for encouraging me to think more broadly and critically about my research work.

The success of this research and the good times I had during the process would not have been possible without such an excellent group of labmates. I would like to thank all those who contributed to or were involved with some aspects of the work presented here, assisted me with training/protocols/etc., or just provided helpful and/or fun conversation: Dave Eavarone, Akila Jayaraman, Vidya Subramanian, Karunya Srinivasan, Kannan Tharakaraman, Troy Rurak, Samira Daswani, Tom Haller, Uday Aich, Carol Koh, Aarthi Chandresekharan, Aravind Srinivasan, Boris Gavrilov, Andrew Hatas, Yi-Ling Chen, Jing Li, Nathan Stebbins, Ido Bachelet, and others I probably have missed (sorry). I would like to extend a special thanks to Chalermchai (“Beam”) Artpradit for not only his excellent research contributions but also as a kind, caring, and fun friend to have throughout much of my graduate research. I would also like to thank the lab administrator and extraordinary Ada Ziolowski for her tireless and very positive assistance with all research and MIT endeavors.

I would like to thank the entire BE program, and especially Professor Doug Lauffenburger, for the opportunity to be a part of such a motivated, intelligent, creative, and fun community. I was fortunate to TA for Professor John Essigmann, during which I learned much; I appreciate his support and positive involvement, both at MIT and with collaborative efforts in Thailand. I owe a huge thanks to the many wonderful people I’ve met in BE and the great friendships I’ve established.

A special thanks to Ta, Phil, Scott, Chris and my other classmates for the many great times and the support they provided.

It would not have been possible for me to be where I am without the support and encouragement of my family. I would like to thank my mom for her unconditional love and teaching me so many important life values, and for always listening to and following my research despite not being a scientist herself. Also big thanks to my siblings, Jon, Missy, and Tom, for their guidance, perspective, love, and just “being there” for me when I needed it.

Last and most of all, I would like to thank my wife, Liza Robinson. Her unwavering support and boundless love through the ups and downs of my graduate program not only provided essential help during these times, but reminded me every day how lucky I am to have her in my life.

Table of Contents

Abstract	5
Acknowledgements	7
Table of Contents	9
List of Figures	13
List of Tables	15
1. Background	17
1.1. Motivation.....	17
1.2. Anticancer Modified Pectin	18
1.2.1. Pectin structure	18
1.2.2. Anticancer modified pectin.....	20
1.3. Anticoagulant Heparin.....	23
1.3.1. Heparin.....	23
1.3.2. Outbreak of allergic-type reactions in people undergoing dialysis	25
1.4. Dengue.....	26
1.4.1. Dengue disease	26
1.4.2. Dengue virus	30
1.4.3. The humoral response to dengue infection	32
1.4.4. Passive antibody therapy as an antiviral treatment modality	33
1.5. Thesis Outline and Specific Aims	35
1.6. References	36

2. Structure-function characterization of anticancer modified citrus pectin. 43

2.1. Introduction and motivation.....	43
2.2. Methods.....	44
2.2.1. Pectin preparation.....	44
2.2.2. Capillary electrophoresis.....	45
2.2.3. ¹ H-NMR.....	46
2.2.4. <i>In vivo</i> tumor studies.....	46
2.2.5. Cell viability.....	46
2.2.6. Chemoinvasion through matrigel.....	46
2.2.7. Western blotting.....	47
2.2.8. Cloning of human Gal-1 and Gal-3.....	47
2.2.9. Gal-1 and Gal-3 interaction with pectin.....	47
2.2.10. <i>In Vitro</i> cell binding.....	48
2.2.11. Adhesion.....	48
2.2.12. Flow cytometry.....	48
2.2.13. siRNA knockdown.....	49
2.2.14. MALDI-MS.....	49
2.3. Results.....	50
2.3.1. Anticancer ACP is generated directly from lemon NCP.....	50
2.3.2. ACP is enriched for liberated neutral oligosaccharides.....	53
2.3.3. Galectin-1 and galectin-3 preferentially bind to ACP.....	56
2.3.4. Galectins modulate ACP activity through AKT signaling.....	57
2.3.5. Tumor PTEN is necessary for ACP-induced signaling.....	57
2.4. Discussion.....	59
2.5. References.....	62

3. Identification of a contaminant in heparin by structure-function characterization 65

3.1. Summary and overall significance.....	95
4. Engineering of a broad spectrum neutralizing antibody to dengue virus by structure-guided rational design	99
4.1. Introduction and motivation.....	99
4.2. Methods	101
4.2.1. Cells & viruses	101
4.2.2. Focus forming assay	101
4.2.3. Expression and purification of antibodies and EDIII proteins.....	102
4.2.4. Indirect ELISA.....	103
4.2.5. Competition ELISA	103
4.2.6. Surface plasmon resonance	104
4.2.7. Focus reduction neutralization test (FRNT).....	104
4.2.8. Ala-scanning.....	105
4.3. Results	106
4.3.1. Generation of 4E11-EDIII structural model and design of affinity-enhancing mutations	106
4.3.2. Experimental assessment of DV4 affinity-enhancing mutations	107
4.3.3. Affinity and neutralizing activity of engineered mAb 4E-5A.....	110
4.3.4 Structural analysis of 4E-5A antibody	115
4.4. Discussion.....	117
4.4.1. Summary	117
4.4.2. Potent cross-reactive antibodies to DV.....	118
4.4.3. Molecular mechanisms of antibody neutralization potency.....	119
4.4.4. Computational and experimental method developments	120
4.4.5. Therapeutic potential of 4E-5A.....	123
4.4.6. Overall significance and future directions.....	126
4.5. References	127

5. Summary and significance..... 131

List of Abbreviations..... 134

List of Figures

Figure 1.1 Schematic representation of the basic structure of pectin	20
Figure 1.2 Main disaccharide unit of heparin.....	24
Figure 1.3 Model of antibody-dependent enhancement (ADE) of DV infection	28
Figure 1.4 Structure of DV and E protein.....	31
Figure 2.1 Effect of ACP on tumor growth and metastasis <i>in vivo</i>	50
Figure 2.2 Anti-tumor efficacy of ACP <i>in vitro</i>	51
Figure 2.3 Capillary electrophoresis and ¹ H-NMR analysis.....	53
Figure 2.4 MALDI-MS analysis of ACP and NCP.....	55
Figure 2.5 Role of galectins in ACP anti-tumor activity	56
Figure 2.6 Pathway analysis of ACP anti-tumor activity.....	58
Figure 4.1 Structure of DV and E protein.....	100
Figure 4.2 Affinity-enhancing mutations localize to the periphery of the 4E11:EDIII-DV4 interface	109
Figure 4.3 Affinities of single mutant antibodies with increased EDIII-DV4 affinity and similar EDIII- DV1-3 affinities relative to 4E11 WT	110
Figure 4.4 In vitro neutralizing activity of antibodies assessed by FRNT	113
Figure 4.5 Structural prediction of 4E-5A and contacts formed by its five mutations	115
Figure 4.6 Alignment of 4E11:EDIII structural model with solved co-crystal structure.	116

Figure 5.1 Summary of broader implications from this thesis regarding structure-function relationships of complex biopolymers.....133

List of Tables

Table 2.1 CE monosaccharide composition of charge-separated ACP and NCP fractions.....	54
Table 4.1 Mutations with increased EDIII-DV4 affinity and similar affinity to EDIII-DV1-3 relative to WT 4E11, as determined by EDIII indirect ELISA.....	108
Table 4.2 Affinities of 4E11 WT and combined mutant antibody 4E-5A determined by competition ELISA.....	111
Table 4.3 Free energy assessment of individual mutant antibodies and the combination mutant antibody 4E-5A.....	111
Table 4.4 Kinetic binding parameters and dissociation constant for WT 4E11 and 4E-5A determined by SPR.....	112
Table 4.5 Quantification of antibody neutralizing activity by FRNT ₅₀	114
Table 4.6 Predicted hydrogen bond, salt bridge, and hydrophobic packing contacts formed by mutations in 4E-5A to EDIII-DV4.....	116
Table 4.7 Summary of studies employing rational design methods for antibody affinity improvement.....	122

1. Background

1.1. Motivation

Proteins and complex carbohydrates are of growing importance as a source for novel therapeutic compounds for drug discovery and development, in part, due to their exquisite biological specificity, range of functionalities, and accumulating evidence of their clinical efficacy and safety [1]. Indeed, there are over 300 pharmaceutical recombinant proteins and antibodies approved in the US and/or Europe, with a current market of approximately \$100 billion and an estimated 15-18% annual growth [2]. Examples of protein and carbohydrate drugs include enzymes, antibodies, hormones, cytokines, growth factors, sulfated glycosaminoglycans, and glycomimetics [1, 3-5]. Proteins and polysaccharides in their natural form may demonstrate interesting “lead” activities by, for example, binding a therapeutic target. However, as natural proteins and carbohydrates have not evolved for use as drugs, improvement in their properties, such as activity, affinity, specificity, and stability, among others, may be necessary to convert them to clinically viable compounds [6-11].

Development of structure-function relationships provides an effective and common strategy to rationally modify *small molecule* natural compounds for improved activities and properties towards their development as drugs [12-16]. However, proteins and polysaccharides, owing to their large and complex structures, are faced with a unique set of challenges in applying a similar approach to improve their properties for therapeutic development. Complete structural characterization, including 3D conformation and microheterogeneities (e.g., variable glycan chain structures), is frequently an arduous process, and sometimes not possible, for proteins and polysaccharides [17]. Instead, structure-characterization techniques, such as NMR and mass spectrometry (MS), are often most useful for providing information regarding structural *attributes* or *properties* of proteins and polysaccharides rather than complete structural elucidation. Furthermore, when it is possible to determine complete 3D structures, such as with proteins by X-ray crystallography, substantial time and resources are required, which limits the ability to rapidly

relate multiple different structures to their respective activities. In addition to structure-determination challenges, direct structural modification techniques for proteins and polysaccharides often lack the precision possible with small molecules. For example, adding specific functional groups at particular sites on proteins or complex carbohydrates becomes exceedingly challenging due to the variety and abundance of chemical groups already present in these natural biopolymers. Collectively, significant challenges exist to developing robust structure-function relationships for characterizing and rationally engineering proteins and complex carbohydrates for their therapeutic development.

Motivated by these challenges, this thesis work is aimed to further develop and implement structure-function relationship approaches to characterize and engineer polysaccharides and antibodies with therapeutic activity. Three different molecules are explored in this thesis. First, a modified plant polysaccharide, pectin, which exhibits anticancer activity, is characterized using an integrative approach to develop a structure-function relationship towards its development as a clinically relevant therapeutic. Second, an existing polysaccharide drug, heparin, is characterized by structure-function approaches to identify a contaminant associated with an outbreak of adverse clinical events. And third, structure-function approaches are utilized to rationally engineer a broad spectrum neutralizing antibody to dengue virus. Development and application of structure-function approaches to characterize and engineer therapeutic proteins and polysaccharides would aid not only our understanding of these complex biopolymers but also directly support the development of new protein and carbohydrate therapeutics. The remainder of “Chapter 1: Background” provides an introduction to the three biopolymers – pectin, heparin, and dengue antibodies – investigated in this thesis.

1.2. Anticancer Modified Pectin

1.2.1. Pectin structure

Pectins are a family of large, complex polysaccharides found in the cell walls of terrestrial plants where they participate in diverse functions such as plant growth, mechanical support,

development, and plant defense [18]. Pectins are structurally defined as a group of polysaccharides rich in covalently linked galacturonic acid (GalA), though they exhibit substantial diversity in fine structural features [19-21]. Due to their gelling and stabilizing properties, pectins are extensively used in the food industry, such as in the production of jams and jellies. Gelling properties and the high safety profile of pectins have encouraged their use in other areas, such as biomedical matrices for wound bandaging [22] and drug delivery applications [23]. Dietary pectin has also been linked to positive health effects such as decreasing cholesterol levels [24-26], heavy metal detoxification [27-29], and immune system stimulation [30, 31].

Broadly, pectin is composed of “smooth” and “hairy” regions (**Figure 1.1**) [18, 21]. Smooth regions, termed homogalacturonan (HG), are composed of a linear polymer of poly-1-4 linked α -D-GalA moieties with varying degrees of methyl-esters and *O*-acetyl-esters. HG comprises approximately 65% of pectin, although this varies by pectin source [19]. The GalA backbone can be found modified by different chemical groups: partial methylesterification at the *C*-6 carboxyl and *O*-acetylation at *O*-2 and *O*-3 positions. The hairy regions, which show greater structural diversity than HG, are divided into two distinct domains termed rhamnogalacturonan I (RGI) and rhamnogalacturonan II (RGII). RGI, which represents about 25% of pectin, contains a backbone of $[-\alpha\text{-D-GalA-1,2-}\alpha\text{-L-Rha-1-4-}]_n$. Each rhamnose (Rha) residue serves as a potential branch point for additional glycan chains, leading to a high degree of structural variability. RGI branched chains are largely composed of homo- and heteropolymers of galactose and arabinose. RGII is the most complex domain of pectin, possessing multiple branch points with at least 13 different types of sugars, and over 20 types of different linkages. RGII makes up about 10% of pectin and, in contrast to RGI, its structure is largely conserved across plant species. The fine structural features of pectin vary substantially and are influenced by plant tissue source, development state, and modification during storage of plants (e.g., fruit ripening), among other conditions [32]. Collectively, pectins represent a group of large polysaccharides with highly heterogeneous structural features, including diversity of monosaccharides, chain length, amount of and location of branching, glycosidic linkages, and chemical modifications.

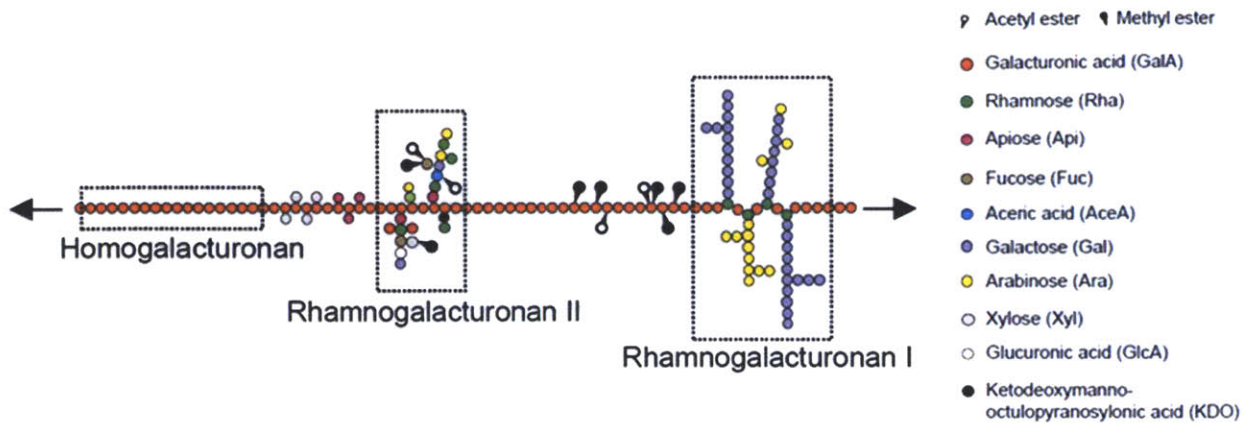


Figure 1.1 Schematic representation of the basic structure of pectin. The major domains of pectin include homogalacturonan, rhamnogalacturonana I, and rhamnogalacturonan II. Pectin structure exhibits a high level of heterogeneity in terms of size, composition, linkages, and chemical modifications. Adapted from [20].

1.2.2. Anticancer modified pectin

There is growing evidence that pectins, when structurally modified, can exhibit significant anticancer activity, with therapeutic benefit being demonstrated in multiple animal models [33-37] as well as in small-scale clinical trials [38-42]. Indeed, one such modified pectin product, GCS-100, is reported to have been evaluated in nine phase I and II clinical trials involving more than 140 human subjects in which results demonstrated initial signals of anti-tumor activity and good tolerability [43]. Despite the evidence of anticancer efficacy and safety of modified pectins accumulated during the past ~20 years, clinical realization of a viable pectin therapeutic product has been met with significant challenge, stemming much from the structural complexity of pectins and associated lack of structure-function understanding of therapeutic pectin products. A fundamental understanding of the structural motifs of modified pectin responsible for anticancer activity as well as their mechanism of action is central to the development of clinically relevant efficacious anticancer pectin.

The generation of anticancer pectin typically involves modification of citrus pectins by various combinations of heat, pH, and enzyme treatments. Starting material often reported in the literature is a commercial-grade pectin (e.g., from Sigma pectin) [35-37, 44], however such material is prone to considerable structural variability depending on the plant source(s) and method of

pectin extraction [32]. Pectin modification schemes described in the literature and patents vary considerably but typically involve heat and/or pH treatment with rare incorporation of digestion by pectin-degrading enzymes. Combinations of heat and pH treatments of pectin have been shown to modify pectin structure in characteristic ways [45-47]. High temperature treatment of pectin under acidic conditions favors hydrolysis of glycosidic linkages [45]. Neutral glycan chains, however, are more susceptible to acid-catalyzed hydrolysis, and therefore preferential degradation of pectin hairy regions will occur while leaving smooth regions more intact under high temperature acidic conditions. In contrast, alkaline conditions favor the chemical processes of de-esterification and depolymerization of the HG backbone [46]. The reaction can be biased towards increased de-esterification or depolymerization by temperature control: low temperature alkaline conditions favor de-esterification while high temperature with base favors depolymerization of HG [47]. The first pectins with reported anti-tumor activity were generated from various commercial citrus pectin powders extensively fragmented through a combination of heat, alkaline, and acid [35-37], though additional approaches have been reported [34, 48]. The high variability in both starting material and modification procedures reported for the generation of anticancer modified pectin further complicates a consensus understanding of the structural motifs responsible for mediating pectin activity.

Previous studies have demonstrated pectin to modulate molecular and cellular activities involving galectin-3 and have thus implicated a galectin-3-mediated mechanism of modified pectin anticancer activity [44, 49-52]. Galectins are a family of lectins characterized by their ability to recognize β -galactose-containing glycan structures by a conserved carbohydrate recognition domain (CRD). The family of galectins consists of 15 members, with multiple galectins implicated in tumorigenic processes, including apoptosis, tumor cell transformation, and cell-cycle regulation [53]. The implication of galectin-3 in tumorigenic processes coupled with evidence of pectin binding to galectin-3 makes a galectin-3-mediated therapeutic mechanism appealing, however evidence directly connecting pectin-galectin-3 interaction with anticancer activity is lacking.

Moreover, mechanistic details beyond direct binding to galectin-3, such as downstream signaling of galectin-3 and possible involvement of other galectins, remain largely unknown.

Structural studies of modified pectin, while providing new insights, have not elucidated a definitive link between the presence of specific structural motifs and functional anticancer activity. One study has demonstrated through multiple binding assays that pectin, and specifically galactans, are able to directly bind galectin-3 [49], however further functional studies were lacking to connect binding with anticancer activity. The direct role of galactans in binding galectin-3 was also demonstrated by Gao and coworkers, however they determined that the GalA-containing fraction of modified pectin was also able to bind galectin-3 [51]. In a separate study, Sathisha and coworkers tested various pectic polysaccharides for effects on breast cancer cell apoptosis and invasion, and found a general correlation between the presence of arabinose and galactose with activity [50], though no specific bioactive structural motifs were identified. While these studies implicate the hairy region structures in mediating activity, another study by Jackson and coworkers identified non-methylester, base-sensitive glycan structures as correlating with apoptosis activity, and that bioactive motifs could be generated or enriched for by acid treatment of citrus pectin [48]. Since neutral branched chains of pectin (i.e., galactan and arabinan) are not highly sensitive to base and their structures would be depolymerized by acidic conditions, the results from Jackson et al. suggest other structures than galactans and arabinans as likely responsible for activity. Collectively, previous studies have not connected specific structural motifs with anticancer activity, and inconsistency exists among implicated bioactive structures.

To address the challenges inherent to establishing a structure-function relationship of modified pectin with anticancer activity, an integrated approach combining complementary analytical techniques with molecular, cellular, and animal model functional studies is undertaken. Results demonstrate structural attributes of modified citrus pectin that distinguish it from native citrus pectin, and that these attributes correspond to *in vivo* anticancer activity as well as specific modulation of intracellular signaling cascades linked to galectin binding. Improved understanding

of the structural motifs mediating activity and the associated mechanism of action will allow the generation and development of more effective and consistent anticancer pectin agents.

1.3. Anticoagulant Heparin

1.3.1. Heparin

Heparin is a potent anticoagulant agent widely used in a variety of clinical settings, including acute coronary syndrome, venous thromboembolism, pulmonary embolism, and hemodialysis [54-56]. Pharmaceutical heparin, also termed unfractionated heparin (UFH) to distinguish it from low molecular weight heparins (LMWHs), is composed of a heterogeneous mixture of highly sulfated linear polysaccharides isolated from biological sources, typically porcine intestine currently. UFH exerts its major anticoagulant activity by inactivating thrombin and factor Xa through an antithrombin III (AT)-dependent mechanism [57]. Heparin, via a specific pentasaccharide sequence, binds AT, which induces a conformational change in AT leading to its activation [58]. Activated AT subsequently inhibits thrombin (factor IIa) and factor Xa, among other coagulation factors. Inhibition of factor Xa requires only activated AT, however inhibition of thrombin requires the formation of the ternary complex composed of heparin and AT with thrombin to inactivate thrombin.

Heparin is a complex linear polysaccharide belonging to the glycosaminoglycan (GAG) family. Broadly, it is composed of repeating disaccharide units consisting of a glucosamine and uronic acid which have variable sulfation. Produced biosynthetically, heparin is found exclusively as chains attached to the proteoglycan serglycin in connective-tissue-type mast cells where it participates in the storage of mass cell granular components such as histamine, proteases and inflammatory mediators [59]. The biosynthesis of heparin occurs by extension of copolymers of D-N-acetylglucosamine (GlcNAc) linked to D-glucuronic acid (GlcA) as $\text{GlcNAc}\alpha 1-4\text{GlcA}\beta 1-4$. During the biosynthetic process, extensive modification of the base chain occurs by the coordination of a variety of enzymes, including multiple sulfotransferases, an epimerase, and a deacetylase [60, 61]. Arising from this biosynthetic process, heparin exhibits substantial structural heterogeneity,

including chain length, degree and location of sulfates, and epimer differences [62]. The most abundant disaccharide unit of heparin is 2-*O*-sulfonated iduronic acid (IdoA) 1 → 4 linked to a 6-*O*, *N*-sulfonated glucosamine (GlcNS) (**Figure 1.2**). Overall, heparin demonstrates the greatest negative charge density of any known biological macromolecule and exhibits substantial heterogeneity.

Starting material for pharmaceutical heparin is first isolated from the biological source of pig intestine, usually from China. A series of steps are applied to isolate crude heparin from tissue:

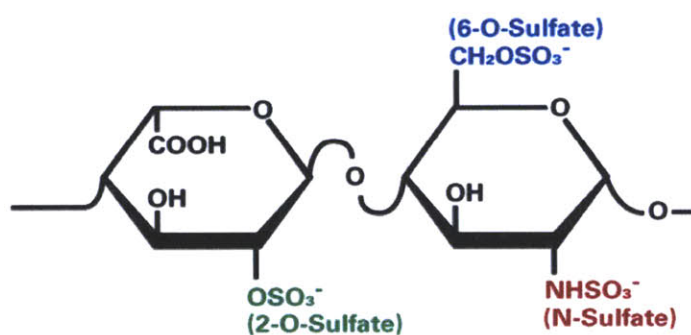


Figure 1.2 Main disaccharide unit of heparin.

physical separation of mucosa from the intestine, solubilization by addition of proteases, and multiple precipitation/solubilization steps [63]. Crude heparin material then undergoes cGMP purification steps involving selective precipitations, ion exchange, chemical treatments, and

filtrations [63]. The final pharmaceutical heparin product demonstrates significant polydispersity and complexity, having a MW range of 5,000 – 40,000 Da (average ~15,000 Da), variable chain length, significant sequence heterogeneity (the major trisulfated disaccharide constitutes ~75% of the composition), and substantial sulfation variability (average ~2.6 sulfates/disaccharide). In addition, pharmaceutical heparin is known to frequently contain impurities, most notably dermatan sulfate, also a GAG, in amounts up to 7%, which is considered tolerable as it does not affect heparin anticoagulant activity [64].

The structural complexity of heparin coupled with its high heterogeneity challenges elucidation of its structure. The complexity precludes any single current analytical technique from complete characterization, and thus integration of results from a set of orthogonal techniques which provide complementary information provides an effective approach to thorough characterization – a subject described in depth in our recent review article [17]. In this regard,

analytical techniques including capillary electrophoresis (CE), HPLC, mass spectrometry (MS), NMR, and enzymatic digestion have been effectively adapted for a variety of glycan analyses, including heparin [17, 65, 66]. The direct combination of these methods in the form of a separation technique coupled with a detection method (so-called “hyphenated techniques”), such as LC-MS, CE-MS, CE-NMR, LC-NMR, provide further advantages of improved resolution and sensitivity [67]. Indeed, the application of an integrated approach using complementary, high-resolution analytical techniques was critical to the successful identification and characterization of a contaminant in batches of heparin associated with adverse events, as described below.

1.3.2. Outbreak of allergic-type reactions in people undergoing dialysis

Beginning in late 2007, a series of acute, allergic-type reactions in patients undergoing heparin therapy during kidney dialysis was reported. The sharp increase in allergic-like responses was reported to the CDC, which notified the FDA on Jan 4, 2008. Initial investigations focused on the clinical settings as the possible cause of the reactions, however no link to adverse reactions was identified. Instead, a connection was made to certain lots of heparin manufactured by Baxter Healthcare, and subsequently suspect lots and eventually all of Baxter’s heparin products were recalled by February 28, 2012. As a result, the number of adverse reactions to heparin therapy returned to basal levels by April 2008 [68].

The adverse responses were anaphylactoid in nature, with signs and symptoms including hypotension, facial flushing, breathing difficulty, tachycardia, nausea, and fainting. In some cases, the severity of the reaction resulted in severe hypotension and, altogether, over 200 deaths worldwide were eventually linked to the outbreak [69]. The immediacy and severity of adverse reactions to heparin therapy coupled with heparin’s widespread and essential use in a variety of clinical settings necessitated an understanding of the cause(s) of the adverse events to prevent future occurrences. Initial investigations by the FDA of heparin batches associated with adverse events using enzymes, CE, and ¹H-NMR revealed “heparin-like” molecule(s) [68]. As described above, the high structural complexity and substantial heterogeneity complicates complete characterization of all structural components in heparin. Moreover, molecules having similar

physicochemical properties as heparin (e.g., “heparin-like” contaminant molecules), when mixed with heparin, become exceedingly difficult to structurally elucidate due to the presence of overlapping signals and properties, which challenges resolving foreign structures from the natural heterogeneity of heparin product.

Further complicating the circumstances around the heparin mystery was an outbreak in 2006-2007 of a highly virulent form of porcine reproductive and respiratory syndrome virus (PRSSV) in Chinese pigs, the principal source material for crude heparin [70, 71]. A key feature of infection with PRSSV is the activation of macrophages [72], and activated monocytes and macrophages are known to produce highly sulfated chondroitin sulfate (type E) on the serglycin proteoglycan [59, 73]. Concern thus arose that PRSSV infections in pigs may be leading to the production of impurities (e.g., highly sulfated chondroitin sulfate) that could be copurified with heparin during the process of generating pharmaceutical heparin product.

In order to address these issues, help identify the contaminant(s), and correlate presence of the contaminant(s) to the observed anaphylactoid responses, a team of scientists from academic labs and the pharmaceutical industry was enlisted to work with the FDA. I was fortunate to participate in the ensuing investigations and to be a part of such an intelligent and motivated team consisting of scientific, medical, and regulatory experts all working in concert to rapidly resolve the heparin crisis.

1.4. Dengue

1.4.1. Dengue disease

Dengue is the most common vector-borne viral disease in humans, with an estimated 3.6 billion people at risk for infection. Globally, more than 200 million dengue infections occur each year, resulting in approximately 21,000 deaths [74]. The high morbidity associated with dengue leads to significant public health, social, and economic impact on populations and countries where dengue is endemic [75]. The disease, transmitted to humans by mosquitos, is endemic to much of the tropical and subtropical regions of the world. Dengue has been described as an emerging

disease, with an increasing number of cases, their severity, and the geographical spread of dengue [76]. The World Health Organization (WHO) has reported a 30-fold increase in dengue incidence in the past 50 years concomitant with a geographical increase from a few to now over 100 countries with endemic dengue [77]. Central to the emergence of dengue is the increased human population growth and urbanization, expanded travel, globalized economy, and lack of effective mosquito control [78]. Currently, no approved vaccine or specific therapy exists for dengue.

Dengue illness is caused by infection with one of the four dengue virus serotypes (DV1-4), which are antigenically and genetically related. The disease is endemic to many tropical and subtropical regions, including Southeast Asia, the Pacific, and the Americas, with human transmission caused by the transfer of virus from an infected *Aedes* mosquito, principally the urban-adapted *Aedes aegypti* species, which also has a preference for biting humans. Infection with dengue virus causes a spectrum of clinical signs and symptoms, ranging from subclinical infection, to mild febrile symptoms, to severe life-threatening hemorrhagic disease. Classical form of the disease, termed dengue fever (DF), presents as acute febrile illness lasting 3-7 days and is accompanied by symptoms that can include fever, headache, muscle and joint pain, nausea, rash, and vomiting. While most DF cases are acute and self-limiting, in about 1% of cases, the disease progresses to more severe forms, a progression which cannot be reliably predicted. More severe disease forms, termed dengue hemorrhagic fever (DHF) and dengue shock syndrome (DSS), occur during defervescence and are characterized by plasma leakage; multifactorial hemostatic abnormalities, including marked thrombocytopenia; and hemorrhagic symptoms [77]. Severe plasma leakage can lead to hypotension and circulatory collapse, causing potential organ failure and death. Despite the name, many DHF patients experience only minor bleeding symptoms, although in some cases severe hemorrhagic manifestations do occur. Clinical management of DHF/DSS is limited to supportive care, which focuses on appropriate and careful fluid replacement to prevent shock and organ failure [77].

The most significant single risk factor for development of severe disease is previous infection by a heterologous serotype. The leading theory to explain this and related observations is termed antibody-dependent enhancement (ADE), in which non-neutralizing and cross-neutralizing antibodies promote virus infection and replication in cells bearing antibody receptors on their surface (**Figure 1.3**). Uptake of virus-antibody complexes occurs more efficiently than free virus

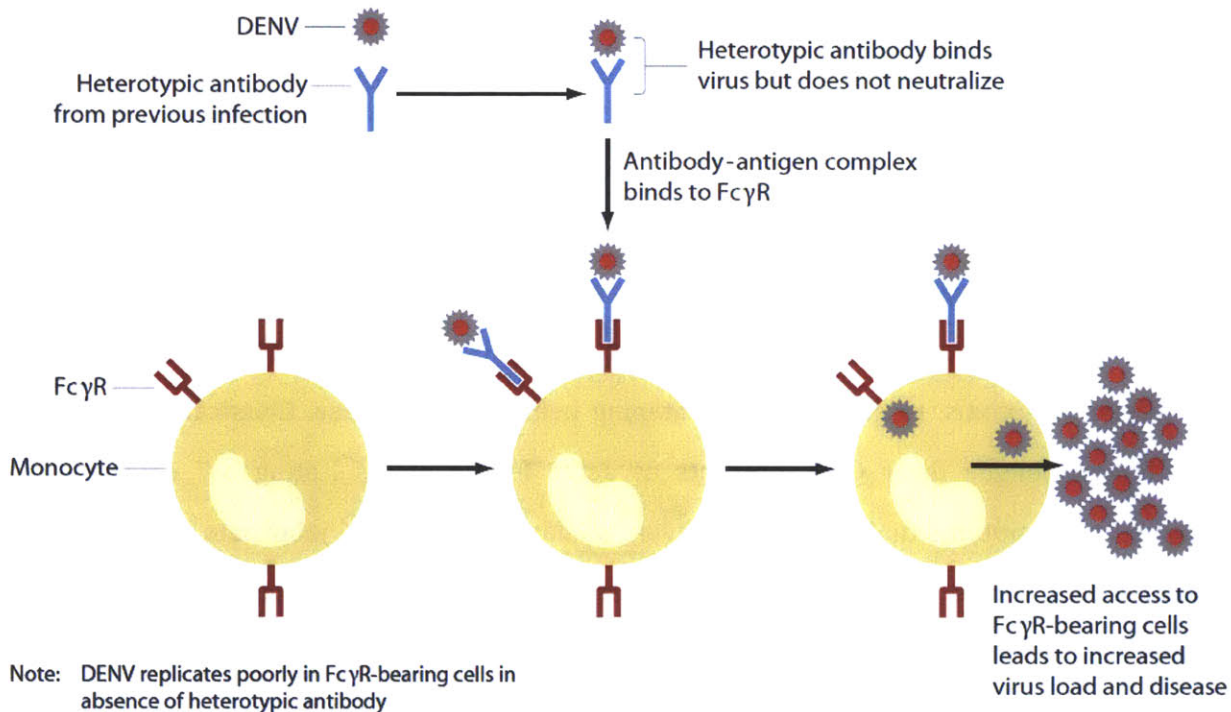


Figure 1.3 Model of antibody-dependent enhancement (ADE) of DV infection. Non-neutralizing or cross-neutralizing (heterotypic) antibodies at subneutralizing concentrations can bind dengue virions and enable increased infection of Fcγ receptor-bearing cells such as monocytes. Increased infection leads to augmented viral replication and exacerbated disease presentation (adapted from [95]).

causing increased replication of virus. The higher occurrence of DHF during primary DV infection in the first year of life in children born to DV-immune mothers, and who therefore acquire antibody against DV transplacentally, further supports the implication of antibodies in causing increased disease severity [79]. Importantly, these observations in young infants shows that at ages less than 6 months, the infants are protected from disease, but as antibody titers wane, there is increased risk for disease [80]. Based on these observations as well as *in vitro* experiments of ADE,

neutralizing antibodies at subneutralizing concentrations, in addition to non-neutralizing antibodies, appear to be able to mediate ADE. Additional support for the ADE hypothesis stems from direct experimental studies in which antibodies can confer increased virus levels both *in vitro* as well as *in vivo* in mouse and non-human primate models [81]. Antibody-mediated increased replication of DV is believed to be able to cause increased disease burden based on the observed positive correlation between peak viremia titer and disease severity in humans [82-84]. However, cases of DHF/DSS in non-infant individuals who experience primary DV infections indicates that additional factors beyond ADE can lead to severe disease. In addition to previous heterotypic infection, other risk factors for severe disease include the strain and serotype of the infecting virus, age, genetic background of the individual, and degree of viremia [84, 85].

The pathogenesis underlying severe dengue disease is not well understood, though immunopathological mechanisms rather than direct tissue damage by virus are believed to be largely involved [86]. The immunopathological response is characterized as excessive immune activation leading to heightened levels of pro-inflammatory cytokines and T-cell activation, however the exact mediators and their mechanisms remain largely undefined [87, 88]. Such immunopathological mechanisms are thought to cause increased capillary permeability and/or coagulation dysfunction, thereby leading to observed clinical signs of plasma leakage and increased hemorrhaging.

An effective vaccine for dengue remains elusive despite more than 50 years of development efforts. Increased understanding of the disease, immunity, and the virus has shown that a unique set of challenges are faced for the development of a safe and efficacious dengue vaccine based on the existence of four serotypes combined with increased risk of disease severity in secondary infections [89, 90]. An effective vaccine must provide robust, long-term protective immunity against all four serotypes simultaneously while not causing severe disease, and the leading strategy to accomplish these goals is the use of attenuated live viruses of each of the four serotypes [91, 92]. Vaccines which cause a weak antibody response to one or multiple serotypes could, due to ADE, increase vaccinee risk for development of severe disease above the risk associated with no vaccine.

Additionally, there is a lack of animal models that faithfully capture the human disease as well as a lack of validated immunological correlates of immunity, thus significantly challenging efforts to assess the safety and efficacy of vaccine candidates in preclinical settings. The challenges associated with development of a dengue vaccine further motivate the need for other disease intervention methods, including antiviral therapies and passive immunization strategies.

1.4.2. Dengue virus

Dengue virus is a member of the *Flaviviridae* family and contains a single-stranded RNA genome of positive polarity. 'Dengue virus' does not refer to a single virus but rather a group of four antigenically and genetically related viruses which share disease phenotypes in human infection. The four viruses, termed serotypes (DV 1-4), although related, share about 65% of their genomes, which is a similar degree of relatedness of other flaviviruses to each other, such as West Nile Virus (WNV) to Japanese Encephalitis Virus (JEV). The RNA genome encodes a single open reading frame that is translated as a single polyprotein and is cleaved by viral and host proteases to produce ten viral proteins, which includes three structural proteins (core [C], premembrane/membrane [prM]/[M], and envelope [E]) and seven nonstructural (NS) proteins. The dengue virion particle is approximately 50 nm in diameter with an icosahedral symmetry, and is composed of the RNA genome; C, prM/M, and E proteins; and a host cell-derived lipid bilayer.

Dengue virus enters host cells by binding to yet unidentified host cell receptors followed by receptor-mediated endocytosis. Though no consensus exists regarding the identity of the receptor(s) used by DV, a variety of putative receptors have been described, with heparan sulfate (HS) identified across a multitude of studies (reviewed in [93]). In a body of work separate from this thesis, I am participating in studies to further characterize the role of HS as a DV receptor using recombinant subviral particles of clinical isolate strains. Upon the acidification of the endosome, the E protein rearranges from dimeric to a trimeric conformation, resulting in fusion of the host cell and viral membranes. Nucleocapsid is subsequently released into the cytoplasm, and after dissociation of C protein and the RNA genome, RNA replication and protein translation begin. Particle assembly occurs in the lumen of the endoplasmic reticulum (ER). Particles are first

assembled as fully immature virions presenting intact prM, which prevents fusion of new particles with ER and Golgi membranes during the egress process. Cleavage of prM in the trans-Golgi network along with increased lumen pH induces the rearrangement of E protein into dimeric form

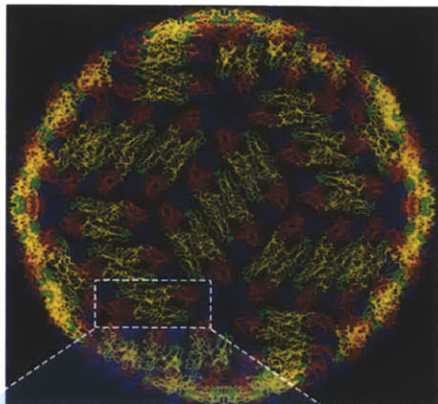


Figure 1.4 Structure of DV and E protein. DV surface structure is composed of 90 dimers of E protein arranged with icosahedral symmetry. The E protein is composed of three domains: EDI (red), EDII (yellow), and EDIII (blue). Cross-reactive neutralizing epitopes are marked: EDII fusion loop (green) and EDIII A-strand (magenta). Adapted from [76].

and the conversion of a particle from immature to an infectious, mature virion. DV particles are subsequently released into the extracellular environment. Importantly, the cleavage of prM is not an efficient process, which leads to the generation of immature, partially mature, and fully mature populations of particles.

EDII harbors the fusion loop, a conserved sequence of hydrophobic residues responsible for insertion into host cell endosomal membrane to mediate fusion. EDIII has an immunoglobulin-like fold and is likely involved in host cell attachment by recognition of yet unidentified receptors [94]. Conservation of the E protein amino acid sequence is high within serotypes, with identities between 90-96%. However, between serotypes, E protein sequences typically only share approximately 60-70% identity, reflecting the sequence and evolutionary divergence between the

The major DV surface protein is the E protein, which is arranged as 90 dimers on the virus surface positioned horizontally to the lipid bilayer thus creating a smooth, spike-less particle (**Figure 1.4**). The E protein is composed of three domains (EDI-III) (**Figure 1.4**). EDI comprises the central region nested between EDII and EDIII. EDII, the dimerization domain, makes contacts with EDII of its dimeric E protein partner. At its distal end,

four serotypes. Being the major virus surface protein, the E protein is the primary target of the humoral response to DV infection.

1.4.3. The humoral response to dengue infection

The adaptive immune response to dengue infection participates in both protective and pathologic aspects of disease. Infection with one serotype leads to long-term protective immunity to that serotype as well as transient protection to heterologous serotypes. However, cross-protection wanes rapidly (~3-6 months), after which individuals are at risk for increased disease severity upon infection by heterotypic DV. The leading hypothesis to explain this observation is increased viral replication by ADE, as described above, thus directly implicating the humoral response in pathologic progression of disease. Concomitantly, however, neutralizing antibodies against E protein are primary mediators of protection against DV infection [95]. A robust antibody response against an infecting serotype provides long-term protection against reinfection of the same serotype [96]. The role of the humoral response in conferring protection is also supported by experimental studies in which passive transfer of antibodies against E protein confer protection in mice challenged with DV infection [97-99] as well as in non-human primate models of DV infection [100]. Additionally, maternally transferred antibodies provide protection to infants less than six months old [101].

The antibody response to dengue infection is primarily directed towards E, prM, and non-structural protein 1 (NS1), with the principal neutralizing response being against E protein. Antibodies recognizing prM tend to have high cross-reactivity and cause enhanced infectivity *in vitro*, with little neutralizing activity [102]. The antibody response directed against E protein targets all three domains. EDI-specific antibodies tend to have low or no neutralizing activity, and antibodies against EDII tend to be weakly neutralizing but highly cross-reactive. Such antibodies typically recognize the highly conserved fusion loop and neutralize DV by inhibition of fusion with host cell endosomal membrane. However, the fusion loop is largely inaccessible in the intact virion structure which limits neutralizing activity of antibodies which target this epitope [103]. Antibodies directed to EDIII tend to have high neutralizing activity but are generally serotype-specific [94, 104-

107]. Studies have identified cross-reactive EDIII antibodies which have moderate to high neutralizing activity, however these antibodies tend to neutralize only 2-3 serotypes [108-113]. Studies of the humoral response to DV infection in mice indicated that EDIII-specific antibodies play a major role in neutralizing activity against DV from serum [99, 104, 105, 111]. However, recent studies of the humoral response in humans indicates that EDIII-specific antibodies bear little of the serum DV neutralizing activity [114], and instead antibodies which bind complex, quaternary epitopes on the surface of DV appear to be largely responsible for DV neutralizing activity in human infection [115, 116].

Studies characterizing mechanisms influencing neutralization potency of E protein-specific antibodies towards flaviviruses have demonstrated that neutralization is a 'multi-hit' phenomenon in which multiple antibodies must bind a single virion particle to render it non-infectious (reviewed in [117]). Factors governing potency include the accessibility of the neutralizing epitope, the level of antibody occupancy of its epitopes, and affinity of the antibody for the epitope [118]. Serotype-specific antibodies directed against EDIII tend to have greater neutralizing activity than cross-reactive antibodies against EDIII. Biochemical investigations of this observation have indicated that while these two classes of antibodies have similar affinities for their epitopes, cross-reactive antibodies require a higher level of occupancy to neutralize virion particles [118, 119], which may be explained by the differing accessibility of their epitopes in an intact virion.

1.4.4. Passive antibody therapy as an antiviral treatment modality

No specific therapy exists for dengue, however efforts to develop antivirals, particularly in the form of small molecules, is of interest as a means to combat the disease. A growing therapeutic modality for antivirals is the use of neutralizing monoclonal antibodies (mAbs) [120-125]. MAbs offer several advantages as a source for the development of novel antivirals. First, they have high biochemical specificity for their targets, thus decreasing or limiting off-target effects. Second, the clinical use of therapeutic mAbs for other indications, such as oncology, has helped define their pharmacokinetic (PK) profiles, information which can be used to more reliably predict PK parameters for mAb products in development. In addition, mAbs can elicit both direct and indirect

activities against viral infections: direct activity via binding and neutralizing virus particles, and indirect activity by recruiting and activating additional immune response via effector functions mediated by mAb Fc binding to cognate receptors on immune cells and activation of complement molecules.

The serum half-life of antibodies is high (~21 days for IgG 1, 2, and 4) compared to many other molecule classes, particularly small molecules. This long half-life translates into a longer window of therapeutic activity from a single drug administration. Importantly, mAb long half-life enables prophylactic, in addition to therapeutic, applications. Indeed, the only currently approved antiviral mAb, palivizumab (Synagis), is for prophylactic treatment of respiratory syncytial virus. Many viral diseases show epidemic cycles characterized by rapid increases in the number and geographical spread of disease. Antiviral prophylactics, including mAbs, would provide significant public health benefit in potential curbing outbreaks as well as protecting individuals in high risk areas, such as residents who are unable to vacate and medical personnel.

While mAbs offer much promise as an emerging modality for therapeutic and prophylactic intervention of viral diseases, challenges do exist to their successful development. First, the development and manufacture of mAbs can be more expensive than that of small molecules, making antiviral therapeutics potentially more expensive. Additional costs arise from the biological nature of mAbs compared to purely synthetic small molecules. The increased use of mAbs as therapies, such as in oncology, has helped foment increased efficiency and decreased costs in mAb development and manufacture, thus contributing towards cost reductions.

Another significant challenge to the development of effective antiviral mAbs stems from the high antigenic variability present for many viruses. Much of viral antigenic variability arises from immune pressure combined with the ability of viruses to evolve rapidly, as observed with notable examples of HIV and influenza virus. Substantial challenges thus exist in identification of mAbs with potent neutralizing activity across the many subtypes/genotypes of a virus. One approach to address this challenge is the utilization of multiple mAbs (a mAb 'cocktail') which have complementary activity towards different strains, thereby enabling high breadth of targeting.

Multiple mAbs per drug product can significantly increase regulatory challenges as well as development and manufacture expenses, with the latter already being a substantial barrier to market realization of antiviral mAb therapeutics. Therefore, a single broadly neutralizing mAb may be preferred for many viral disease areas. A critical, and often limiting, challenge to successful development of mAb therapeutics for antiviral diseases rests in the identification of potent, broadly neutralizing mAbs.

1.5. Thesis Outline and Specific Aims

This thesis aims to utilize structure-function approaches to characterize and engineer complex biopolymers – polysaccharides and antibodies – towards improving their therapeutic profiles. A structure-function approach is applied to two polysaccharides – pectin as a potentially new drug and an established drug, heparin – and to an antibody directed against dengue virus having therapeutic potential. Towards this thesis, three specific aims are investigated:

- 1. Establish a robust structure-function understanding of modified pectin having anticancer activity. (Chapter 2)***
- 2. Develop a structure-function approach to define a contaminant in batches of heparin associated with an outbreak of adverse clinical events. (Chapter 3)***
- 3. Employ structure-function-based rational design to engineer a broad spectrum neutralizing antibody to dengue virus having therapeutic potential. (Chapter 4)***

1.6. References

1. Leader, B., Q.J. Baca, and D.E. Golan, *Protein therapeutics: a summary and pharmacological classification*. Nat Rev Drug Discov, 2008. **7**(1): p. 21-39.
2. Langer, E.S., *Biomanufacturing Outsourcing Outlook*. BioPharm International, 2012. **25**(2): p. 15-16.
3. Sasisekharan, R. and K. Viswanathan, *Functional Glycomics and the Future of Glycomic Drugs*, in *Drug Efficacy, Safety, and Biologics Discovery*. 2008, John Wiley & Sons, Inc. p. 277-300.
4. Ernst, B. and J.L. Magnani, *From carbohydrate leads to glycomimetic drugs*. Nat Rev Drug Discov, 2009. **8**(8): p. 661-677.
5. Lever, R. and C.P. Page, *Novel drug development opportunities for heparin*. Nat Rev Drug Discov, 2002. **1**(2): p. 140-148.
6. Carter, P.J., *Potent antibody therapeutics by design*. Nat Rev Immunol, 2006. **6**(5): p. 343-357.
7. Lazar, G.A., et al., *Designing proteins for therapeutic applications*. Current Opinion in Structural Biology, 2003. **13**(4): p. 513-518.
8. Marshall, S.A., et al., *Rational design and engineering of therapeutic proteins*. Drug Discovery Today, 2003. **8**(5): p. 212-221.
9. Szymkowski, D.E., *Rational optimization of proteins as drugs: a new era of 'medicinal biology'*. Drug Discovery Today, 2004. **9**(9): p. 381-383.
10. Carter, P.J., *Introduction to current and future protein therapeutics: A protein engineering perspective*. Experimental Cell Research, 2011. **317**(9): p. 1261-1269.
11. Caravella, J. and A. Lugovskoy, *Design of next-generation protein therapeutics*. Current Opinion in Chemical Biology, 2010. **14**(4): p. 520-528.
12. Andricopulo, A.D. and C.A. Montanari, *Structure-Activity Relationships for the Design of Small-Molecule Inhibitors*. Mini Reviews in Medicinal Chemistry, 2005. **5**(6): p. 585-593.
13. Mann, J., *Natural products in cancer chemotherapy: past, present and future*. Nat Rev Cancer, 2002. **2**(2): p. 143-148.
14. Haustedt, L., et al., *Rational approaches to natural-product-based drug design*. Curr Opin Drug Discov Devel, 2006. **9**(4): p. 445-462.
15. Koehn, F.E. and G.T. Carter, *The evolving role of natural products in drug discovery*. Nat Rev Drug Discov, 2005. **4**(3): p. 206-220.
16. Paterson, I. and E.A. Anderson, *The Renaissance of Natural Products as Drug Candidates*. Science, 2005. **310**(5747): p. 451-453.
17. Robinson, L.N., et al., *Harnessing glycomics technologies: Integrating structure with function for glycan characterization*. Electrophoresis, 2012. **33**(5): p. 797-814.
18. Caffall, K.H. and D. Mohnen, *The structure, function, and biosynthesis of plant cell wall pectic polysaccharides*. Carbohydr Res, 2009. **344**(14): p. 1879-900.
19. Mohnen, D., *Pectin structure and biosynthesis*. Curr Opin Plant Biol, 2008. **11**(3): p. 266-77.
20. Willats, W.G.T., et al., *Pectin: cell biology and prospects for functional analysis*. Plant Molecular Biology, 2001. **47**(1): p. 9-27.
21. Willats, W.G.T., J.P. Knox, and J.D. Mikkelsen, *Pectin: new insights into an old polymer are starting to gel*. Trends in Food Science & Technology, 2006. **17**(3): p. 97-104.
22. Liu, L., et al., *Pectin/poly(lactide-co-glycolide) composite matrices for biomedical applications*. Biomaterials, 2004. **25**(16): p. 3201-3210.

23. Liu, L., M. Fishman, and K. Hicks, *Pectin in controlled drug delivery – a review*. Cellulose, 2007. **14**(1): p. 15-24.
24. Bell, L.P., et al., *Cholesterol-lowering effects of soluble-fiber cereals as part of a prudent diet for patients with mild to moderate hypercholesterolemia*. The American Journal of Clinical Nutrition, 1990. **52**(6): p. 1020-6.
25. Fernandez, M.L., et al., *Citrus pectin and cholesterol interact to regulate hepatic cholesterol homeostasis and lipoprotein metabolism: a dose-response study in guinea pigs*. The American Journal of Clinical Nutrition, 1994. **59**(4): p. 869-78.
26. Terpstra, A.H.M., et al., *Dietary Pectin with High Viscosity Lowers Plasma and Liver Cholesterol Concentration and Plasma Cholesteryl Ester Transfer Protein Activity in Hamsters*. The Journal of Nutrition, 1998. **128**(11): p. 1944-1949.
27. Kohn, R., *Binding of toxic cations to pectin, its oligomeric fragments and plant tissues*. Carbohydrate Polymers, 1982. **273**(2).
28. Eliaz, I., et al., *The effect of modified citrus pectin on urinary excretion of toxic elements*. Phytotherapy Research, 2006. **20**(10): p. 859-864.
29. Zhao, Z.Y.M.D., et al., *THE ROLE OF MODIFIED CITRUS PECTIN AS AN EFFECTIVE CHELATOR OF LEAD IN CHILDREN HOSPITALIZED WITH TOXIC LEAD LEVELS*. Alternative Therapies in Health and Medicine, 2008. **14**(4): p. 34-8.
30. Salman, H., et al., *Citrus pectin affects cytokine production by human peripheral blood mononuclear cells*. Biomedicine & Pharmacotherapy, 2008. **62**(9): p. 579-582.
31. Lim, B.O., et al., *Dietary Fibers Modulate Indices of Intestinal Immune Function in Rats*. The Journal of Nutrition, 1997. **127**(5): p. 663-667.
32. Schols, H.A. and A.G.J. Voragen, *The chemical structure of pectins*, in *Pectins and their Manipulation*, G.B. Seymour and J.P. Knox, Editors. 2002, Blackwell Publishing Ltd: Oxford. p. 1-29.
33. Liu, H.Y., et al., *Inhibitory effect of modified citrus pectin on liver metastases in a mouse colon cancer model*. World J Gastroenterol, 2008. **14**(48): p. 7386-91.
34. Han, S.B., et al., *Pectic polysaccharide isolated from Angelica gigas Nakai inhibits melanoma cell metastasis and growth by directly preventing cell adhesion and activating host immune functions*. Cancer Lett, 2006. **243**(2): p. 264-73.
35. Platt, D. and A. Raz, *Modulation of the lung colonization of B16-F1 melanoma cells by citrus pectin*. J Natl Cancer Inst, 1992. **84**(6): p. 438-42.
36. Pienta, K.J., et al., *Inhibition of spontaneous metastasis in a rat prostate cancer model by oral administration of modified citrus pectin*. J Natl Cancer Inst, 1995. **87**(5): p. 348-53.
37. Nangia-Makker, P., et al., *Inhibition of human cancer cell growth and metastasis in nude mice by oral intake of modified citrus pectin*. J Natl Cancer Inst, 2002. **94**(24): p. 1854-62.
38. Guess, B.W., et al., *Modified citrus pectin (MCP) increases the prostate-specific antigen doubling time in men with prostate cancer: a phase II pilot study*. Prostate Cancer Prostatic Dis, 2003. **6**(4): p. 301-4.
39. Azemar, M., et al., *Clinical Benefit in Patients with Advanced Solid Tumors Treated with Modified Citrus Pectin: A Prospective Pilot Study*. Clinical Medicine Insights: Oncology, 2007. **1**(CMO-1-Azémar-et-al): p. 73.
40. Cotter, F., et al., *Single-agent activity of GCS-100, a first-in-class galectin-3 antagonist, in elderly patients with relapsed chronic lymphocytic leukemia*. J Clin Oncol, 2009. **27**(15s): p. abst 7006.
41. Cotter, F., et al. *Caspase activation as a surrogate biomarker for treating chronic lymphocytic leukemia with GCS-100, a novel carbohydrate, in a phase II trial*. in *2008 Molecular Markers*. 2008.

42. Springate CF, C.T., Belt R, Redfern C, Stuart K, *Phase II study of GBC-590 in patients with relapsing or refractory colorectal cancer*. Am Soc Clin Oncol, 2001. **20**: p. 2226a.
43. La Jolla Pharmaceutical Company. *GCS-100 Technology*. 2012 [cited 2012 July 22]; Available from: <http://www.ljpc.com/technology-gcs100technology.html>.
44. Inohara, H. and A. Raz, *Effects of natural complex carbohydrate (citrus pectin) on murine melanoma cell properties related to galectin-3 functions*. Glycoconj J, 1994. **11**(6): p. 527-32.
45. Thibault, J.-F., Renard, C.M.G.C, Axelos, M., Roger, P., and Crepeau, M.J., *Studies on the length of homogalaturonic regions in pectins by acid-hydrolysis*. Carbohydr Res, 1993. **238**: p. 271-286.
46. Renard, C.M.G.C. and J.-F. Thibault, *Degradation of pectins in alkaline condition: kinetics of demethylation*. Carbohydr Res, 1996. **286**: p. 139-150.
47. Kravtchenko, T.P., et al., *Improvement of the selective depolymerization of pectic substances by chemical b-elimination in aqueous solution*. Carbohydrate Polymers, 1992. **19**: p. 237-242.
48. Jackson, C.L., et al., *Pectin induces apoptosis in human prostate cancer cells: correlation of apoptotic function with pectin structure*. Glycobiology, 2007. **17**(8): p. 805-19.
49. Gunning, A.P., R.J. Bongaerts, and V.J. Morris, *Recognition of galactan components of pectin by galectin-3*. Faseb J, 2008.
50. Sathisha, U.V., et al., *Inhibition of galectin-3 mediated cellular interactions by pectic polysaccharides from dietary sources*. Glycoconj J, 2007. **24**(8): p. 497-507.
51. Gao, X., et al., *Analysis of the neutral polysaccharide fraction of MCP and its inhibitory activity on galectin-3*. Glycoconjugate Journal, 2012. **29**(4): p. 159-165.
52. Glinsky, V.V. and A. Raz, *Modified citrus pectin anti-metastatic properties: one bullet, multiple targets*. Carbohydrate Research, 2009. **344**(14): p. 1788-1791.
53. Liu, F.-T. and G.A. Rabinovich, *Galectins as modulators of tumour progression*. Nat Rev Cancer, 2005. **5**(1): p. 29-41.
54. Krishnaswamy, A., A.M. Lincoff, and C.P. Cannon, *The Use and Limitations of Unfractionated Heparin*. Critical Pathways in Cardiology, 2010. **9**(1): p. 35-40 10.1097/HPC.0b013e3181d29713.
55. Hirsh, J., et al., *Mechanism of Action and Pharmacology of Unfractionated Heparin*. Arteriosclerosis, Thrombosis, and Vascular Biology, 2001. **21**(7): p. 1094-1096.
56. Fischer, K.-G., *Essentials of anticoagulation in hemodialysis*. Hemodialysis International, 2007. **11**(2): p. 178-189.
57. Gray, E., J. Hogwood, and B. Mulloy, *The Anticoagulant and Antithrombotic Mechanisms of Heparin*, in *Heparin - A Century of Progress*, R. Lever, B. Mulloy, and C.P. Page, Editors. 2012, Springer Berlin Heidelberg. p. 43-61.
58. Lindahl, U., et al., *Structure of the antithrombin-binding site in heparin*. Proceedings of the National Academy of Sciences, 1979. **76**(7): p. 3198-3202.
59. Kolset, S. and H. Tveit, *Serglycin – Structure and biology*. Cellular and Molecular Life Sciences, 2008. **65**(7): p. 1073-1085.
60. Carlsson, P. and L. Kjellén, *Heparin Biosynthesis*, in *Heparin - A Century of Progress*, R. Lever, B. Mulloy, and C.P. Page, Editors. 2012, Springer Berlin Heidelberg. p. 23-41.
61. Esko, J., K. Kimata, and U. Lindahl, *Proteoglycans and Sulfated Glycosaminoglycans*, in *Essentials of Glycobiology. 2nd edition.*, A. Varki, et al., Editors. 2009, Cold Spring Harbor Laboratory Press: Cold Spring Harbor.
62. Sugahara, K. and H. Kitagawa, *Heparin and Heparan Sulfate Biosynthesis*. IUBMB Life, 2002. **54**(4): p. 163-175.
63. Liu, H., Z. Zhang, and R.J. Linhardt, *Lessons learned from the contamination of heparin*. Natural Product Reports, 2009. **26**(3): p. 313-321.

64. Neville, G.A., et al., *Monitoring the purity of pharmaceutical heparin preparations by high-field 1H-nuclear magnetic resonance spectroscopy*. Journal of Pharmaceutical Sciences, 1989. **78**(2): p. 101-104.
65. Shriver, Z., et al., *Heparin and Heparan Sulfate: Analyzing Structure and Microheterogeneity*, in *Heparin - A Century of Progress*, R. Lever, B. Mulloy, and C.P. Page, Editors. 2012, Springer Berlin Heidelberg. p. 159-176.
66. Mulloy, B., *Structure and Physicochemical Characterisation of Heparin*, in *Heparin - A Century of Progress*, R. Lever, B. Mulloy, and C.P. Page, Editors. 2012, Springer Berlin Heidelberg. p. 77-98.
67. Hung, S.L., et al., *Analysis of the steps involved in Dengue virus entry into host cells*. Virology, 1999. **257**(1): p. 156-67.
68. U.S. Food and Drug Administration. *Information on heparin*. July 22, 2012]; Available from: <http://www.fda.gov/Drugs/DrugSafety/PostmarketDrugSafetyInformationforPatientsandProviders/UCM112597>.
69. Beni, S., J. Limtiaco, and C. Larive, *Analysis and characterization of heparin impurities*. Analytical and Bioanalytical Chemistry, 2011. **399**(2): p. 527-539.
70. Tian, K., et al., *Emergence of Fatal PRRSV Variants: Unparalleled Outbreaks of Atypical PRRS in China and Molecular Dissection of the Unique Hallmark*. PLoS ONE, 2007. **2**(6): p. e526.
71. Zhou, Y.J., et al., *Highly Virulent Porcine Reproductive and Respiratory Syndrome Virus Emerged in China*. Transboundary and Emerging Diseases, 2008. **55**(3-4): p. 152-164.
72. Van Breedam, W., et al., *Porcine reproductive and respiratory syndrome virus entry into the porcine macrophage*. Journal of General Virology, 2010. **91**(7): p. 1659-1667.
73. Uhlin-Hansen, L., T. Eskeland, and S.O. Kolset, *Modulation of the expression of chondroitin sulfate proteoglycan in stimulated human monocytes*. Journal of Biological Chemistry, 1989. **264**(25): p. 14916-14922.
74. Beatty, M., G. Letson, and H. Margolis, *Estimating the global burden of dengue*. Am J Trop Med Hygiene, 2009. **81**(5): p. 231.
75. Gubler, D.J., *Epidemic dengue/dengue hemorrhagic fever as a public health, social and economic problem in the 21st century*. Trends in Microbiology, 2002. **10**(2): p. 100-103.
76. Mackenzie, J.S., D.J. Gubler, and L.R. Petersen, *Emerging flaviviruses: the spread and resurgence of Japanese encephalitis, West Nile and dengue viruses*. Nat Med, 2004.
77. World Health Organization (WHO), *Dengue: Guidelines for Diagnosis, Treatment, Prevention and Control—New Edition*. 2009, UNICEF, UNDP, World Bank: Geneva.
78. Gubler, D.J., *Dengue, Urbanization and Globalization: The Unholy Trinity of the 21st Century*. Tropical Medicine and Health, 2011. **39**(4SUPPLEMENT): p. S3-S11.
79. Kliks, S.C., et al., *Evidence That Maternal Dengue Antibodies Are Important in the Development of Dengue Hemorrhagic Fever in Infants*. The American Journal of Tropical Medicine and Hygiene, 1988. **38**(2): p. 411-419.
80. Libraty, D.H., et al., *A Prospective Nested Case-Control Study of Dengue in Infants: Rethinking and Refining the Antibody-Dependent Enhancement Dengue Hemorrhagic Fever Model*. PLoS Med, 2009. **6**(10): p. e1000171.
81. Halstead, S.B., *In Vivo Enhancement of Dengue Virus Infection in Rhesus Monkeys by Passively Transferred Antibody*. Journal of Infectious Diseases, 1979. **140**(4): p. 527-533.
82. Libraty, D.H., et al., *Differing Influences of Virus Burden and Immune Activation on Disease Severity in Secondary Dengue-3 Virus Infections*. Journal of Infectious Diseases, 2002. **185**(9): p. 1213-1221.

83. Murgue, B., et al., *Prospective study of the duration and magnitude of viraemia in children hospitalised during the 1996–1997 dengue-2 outbreak in French Polynesia*. Journal of Medical Virology, 2000. **60**(4): p. 432-438.
84. Vaughn, D.W., et al., *Dengue Viremia Titer, Antibody Response Pattern, and Virus Serotype Correlate with Disease Severity*. Journal of Infectious Diseases, 2000. **181**(1): p. 2-9.
85. Guzmán, M.G. and G. Kouri, *Dengue: an update*. The Lancet Infectious Diseases, 2002. **2**(1): p. 33-42.
86. Green, S. and A. Rothman, *Immunopathological mechanisms in dengue and dengue hemorrhagic fever*. Current Opinion in Infectious Diseases, 2006. **19**(5): p. 429-436
10.1097/01.qco.0000244047.31135.fa.
87. Rothman, A.L., *Immunity to dengue virus: a tale of original antigenic sin and tropical cytokine storms*. Nat Rev Immunol, 2011. **11**(8): p. 532-543.
88. Martina, B.E.E., P. Koraka, and A.D.M.E. Osterhaus, *Dengue Virus Pathogenesis: an Integrated View*. Clinical Microbiology Reviews, 2009. **22**(4): p. 564-581.
89. Thomas, S.J. and T.P. Endy, *Critical issues in dengue vaccine development*. Current Opinion in Infectious Diseases, 2011. **24**(5): p. 442-450 10.1097/QCO.0b013e32834a1b0b.
90. Coller, B.-A.G. and D.E. Clements, *Dengue vaccines: progress and challenges*. Current Opinion in Immunology, 2011. **23**(3): p. 391-398.
91. Murrell, S., S.-C. Wu, and M. Butler, *Review of dengue virus and the development of a vaccine*. Biotechnology Advances, 2011. **29**(2): p. 239-247.
92. Guzman, M.G., et al., *Dengue: a continuing global threat*. Nat Rev Micro, 2010. **8**(12(Suppl)): p. S7-16.
93. Hidari, K.I.P.J. and T. Suzuki, *Dengue virus receptor*. Tropical Medicine and Health, 2011. **39**(4SUPPLEMENT): p. S37-S43.
94. Crill, W.D. and J.T. Roehrig, *Monoclonal Antibodies That Bind to Domain III of Dengue Virus E Glycoprotein Are the Most Efficient Blockers of Virus Adsorption to Vero Cells*. Journal of Virology, 2001. **75**(16): p. 7769-7773.
95. Murphy, B.R. and S.S. Whitehead, *Immune Response to Dengue Virus and Prospects for a Vaccine**. Annual Review of Immunology, 2011. **29**(1): p. 587-619.
96. Innis, B., *Antibody responses to dengue virus infection*, in *Dengue and Dengue Hemorrhagic Fever*, D. Gubler and G. Kuno, Editors. 1997, CAB Int.: New York. p. 221-243.
97. Kaufman, B.M., et al., *Monoclonal Antibodies against Dengue 2 Virus E-Glycoprotein Protect Mice against Lethal Dengue Infection*. The American Journal of Tropical Medicine and Hygiene, 1987. **36**(2): p. 427-434.
98. Sukupolvi-Petty, S., et al., *Structure and Function Analysis of Therapeutic Monoclonal Antibodies against Dengue Virus Type 2*. Journal of Virology, 2010. **84**(18): p. 9227-9239.
99. Brien, J.D., et al., *Genotype-Specific Neutralization and Protection by Antibodies against Dengue Virus Type 3*. Journal of Virology, 2010. **84**(20): p. 10630-10643.
100. Lai, C.-J., et al., *Epitope Determinants of a Chimpanzee Dengue Virus Type 4 (DENV-4)-Neutralizing Antibody and Protection against DENV-4 Challenge in Mice and Rhesus Monkeys by Passively Transferred Humanized Antibody*. Journal of Virology, 2007. **81**(23): p. 12766-12774.
101. Pengsaa, K., et al., *Dengue Virus Infections in the First 2 Years of Life and the Kinetics of Transplacentally Transferred Dengue Neutralizing Antibodies in Thai Children*. Journal of Infectious Diseases, 2006. **194**(11): p. 1570-1576.
102. Dejnirattisai, W., et al., *Cross-Reacting Antibodies Enhance Dengue Virus Infection in Humans*. Science, 2010. **328**(5979): p. 745-748.

103. Cherrier, M.V., et al., *Structural basis for the preferential recognition of immature flaviviruses by a fusion-loop antibody*. The EMBO journal, 2009. **28**(20): p. 3269-3276.
104. Gromowski, G.D. and A.D.T. Barrett, *Characterization of an antigenic site that contains a dominant, type-specific neutralization determinant on the envelope protein domain III (ED3) of dengue 2 virus*. Virology, 2007. **366**(2): p. 349-360.
105. Roehrig, J.T., R.A. Bolin, and R.G. Kelly, *Monoclonal Antibody Mapping of the Envelope Glycoprotein of the Dengue 2 Virus, Jamaica*. Virology, 1998. **246**(2): p. 317-328.
106. Sukupolvi-Petty, S., et al., *Type- and Subcomplex-Specific Neutralizing Antibodies against Domain III of Dengue Virus Type 2 Envelope Protein Recognize Adjacent Epitopes*. Journal of Virology, 2007. **81**(23): p. 12816-12826.
107. Roehrig, J.T., *Antigenic Structure of Flavivirus Proteins*, in *Advances in Virus Research*. 2003, Academic Press. p. 141-175.
108. Lok, S.-M., et al., *Binding of a neutralizing antibody to dengue virus alters the arrangement of surface glycoproteins*. Nat Struct Mol Biol, 2008. **15**(3): p. 312-317.
109. Gromowski, G.D., N.D. Barrett, and A.D.T. Barrett, *Characterization of Dengue Virus Complex-Specific Neutralizing Epitopes on Envelope Protein Domain III of Dengue 2 Virus*. Journal of Virology, 2008. **82**(17): p. 8828-8837.
110. Thullier, P., et al., *Mapping of a dengue virus neutralizing epitope critical for the infectivity of all serotypes: insight into the neutralization mechanism*. Journal of General Virology, 2001. **82**(8): p. 1885-1892.
111. Shrestha, B., et al., *The Development of Therapeutic Antibodies That Neutralize Homologous and Heterologous Genotypes of Dengue Virus Type 1*. PLoS Pathog, 2010. **6**(4): p. e1000823.
112. Matsui, K., et al., *Characterization of dengue complex-reactive epitopes on dengue 3 virus envelope protein domain III*. Virology, 2009. **384**(1): p. 16-20.
113. Midgley, C.M., et al., *Structural Analysis of a Dengue Cross-Reactive Antibody Complexed with Envelope Domain III Reveals the Molecular Basis of Cross-Reactivity*. The Journal of Immunology, 2012. **188**(10): p. 4971-4979.
114. Wahala, W.M.P.B., et al., *Dengue virus neutralization by human immune sera: Role of envelope protein domain III-reactive antibody*. Virology, 2009. **392**(1): p. 103-113.
115. de Alwis, R., et al., *Identification of human neutralizing antibodies that bind to complex epitopes on dengue virions*. Proceedings of the National Academy of Sciences, 2012. **109**(19): p. 7439-7444.
116. Teoh, E.P., et al., *The Structural Basis for Serotype-Specific Neutralization of Dengue Virus by a Human Antibody*. Science Translational Medicine, 2012. **4**(139): p. 139ra83.
117. Pierson, T.C., et al., *Structural Insights into the Mechanisms of Antibody-Mediated Neutralization of Flavivirus Infection: Implications for Vaccine Development*. Cell Host & Microbe, 2008. **4**(3): p. 229-238.
118. Pierson, T.C., et al., *The Stoichiometry of Antibody-Mediated Neutralization and Enhancement of West Nile Virus Infection*. Cell host & microbe, 2007. **1**(2): p. 135-145.
119. Gromowski, G.D., et al., *Mutations of an antibody binding energy hot spot on domain III of the dengue 2 envelope glycoprotein exploited for neutralization escape*. Virology, 2010. **407**(2): p. 237-246.
120. Law, M. and L. Hangartner, *Antibodies against viruses: passive and active immunization*. Current Opinion in Immunology, 2008. **20**(4): p. 486-492.
121. Zhu, Z., et al., *Development of human monoclonal antibodies against diseases caused by emerging and biodefense-related viruses*. Expert Review of Anti-infective Therapy, 2006. **4**(1): p. 57-66.

122. Dimitrov, D., *Human monoclonal antibodies against HIV and emerging viruses*, in *National Institute of Allergy and Infectious Disease: Frontiers in Research*, V. Georgiev, K. Western, and J. McGowan, Editors. 2008, Humana Press: Totowa, NJ. p. 299-308.
123. Meulen, J.t., *Monoclonal antibodies for prophylaxis and therapy of infectious diseases*. *Expert Opinion on Emerging Drugs*, 2007. **12**(4): p. 525-540.
124. Casadevall, A., E. Dadachova, and L.-a. Pirofski, *Passive antibody therapy for infectious diseases*. *Nat Rev Micro*, 2004. **2**(9): p. 695-703.
125. Marasco, W.A. and J. Sui, *The growth and potential of human antiviral monoclonal antibody therapeutics*. *Nat Biotech*, 2007. **25**(12): p. 1421-1434.

2. Structure-function characterization of anticancer modified citrus pectin

2.1. Introduction and motivation

Pectin is a structurally complex, naturally occurring polysaccharide that is a major component of plant primary cell walls [1, 2]. In its native state in plants, pectin has well characterized roles in plant growth, development, and defense. Dietary pectin has shown to exhibit multiple potential health benefits, including lowering cholesterol, stimulation of the immune system, and modulation of glucose metabolism [2]. This gelling, non-toxic polysaccharide has additionally been adapted for application in a wide range of industries including food, cosmetics, adhesives, and medical devices. More recently, modified pectins have come under extensive investigation for their promising role as cancer therapeutics [3-10].

Pectin may be broadly characterized as a carbohydrate network consisting of interconnected linear polysaccharides rich in galacturonic acid (GalA) interspersed with structurally diverse neutral oligosaccharide branches [1]. Fragmentation of the pectin network with alkali, acid, heat, and/or pectin-degrading enzymes yields modified pectin formulations with distinct physical, chemical, and biological properties [11-13]. The effects of these treatments are distinct but interconnected: high temperature and alkaline treatment primarily fragment and de-esterify the linear GalA-rich pectin backbone [13, 14] while acid treatment favors hydrolysis of glycosidic linkages within the neutral oligosaccharide branches [12]. The first pectins with reported anti-tumor activity were generated from citrus pectin powders extensively fragmented through a combination of heat, alkaline, and acid treatments [5-7], though other activation approaches have recently been reported [4, 10]. Consequent digestion and increased solubilization of the pectin network is hypothesized to enhance binding of pectin structures to galectin-3 (Gal-3) [7, 15, 16], a β -galactose-binding lectin that is a multi-faceted regulator of tumor progression [17, 18]. Modified

pectins have been demonstrated to reduce tumor growth and/or metastasis in a range of models including melanoma [4, 5, 16], breast [7], colon [3], and prostate cancer [6, 8].

Anticancer modified pectins show promise for clinical translation and have undergone small phase I and II trials which have demonstrated initial activity and a good safety profile [8, 19-23]. However, despite showing promising signs of clinical efficacy, little is still known regarding the link between pectin structure and anticancer activity. This is likely due, at least in part, to the high structural complexity and heterogeneity of pectin, varied starting pectin sources used in studies, and paucity of structural characterization reported with biological activities. In turn, this has led to variable and sometimes conflicting reports regarding the activities of modified pectins [3-7, 9, 10]. As a result, the identity of the bioactive pectin fragments, effective modification procedures, and pectin's anticancer mechanism of action remain poorly understood. To advance this promising area of cancer research and drug development, we describe here an integrated approach combining complementary analytical techniques with molecular, cellular and animal model functional studies to establish a modified pectin structure-function relationship. We generated a modified pectin termed activated citrus pectin (ACP) directly from lemon peel-derived native citrus pectin (NCP), a non-modified pectin. ACP demonstrated marked anticancer activity when compared to NCP and exhibited distinct structure features compared to NCP. Collectively, we demonstrate an integrative approach for the analysis of anticancer pectin and provide a new link between structure, function and *in vivo* outcome of therapeutic pectins.

2.2. Methods

2.2.1. Pectin preparation

The following citrus pectin powders were obtained for compositional analysis: Sigma P-9135 Lot #098K0032 [P1], Lot #99H0029 [P2], Lot #013K0007 [P3], and Fluka 76280 [P4]. NCP was isolated from lemon peels by a modification of a published procedure [24]. Briefly, albedo was separated from fresh lemon peels, suspended in distilled water (pH 2) and microwaved for 20 sec

in a 23 mL General Purpose Acid Digestion Bomb (Parr Instruments). Crude pectin solution was filtered and precipitated before pellet recovery by centrifugation. Typical yield of pectin (NCP) extraction was 1 mg of pectin per 1 mL of crude extract. NCP (10 mg/mL in distilled water) was pre-heated to 80°C for 4 minutes and incubated with 50 mM NaOH at 80°C for 90 minutes with mixing every 15 minutes. The resulting pectin was cooled to RT, adjusted to pH 5 with HCl, and concentrated by lyophilization. Isolation of the ACP fraction was achieved by HPLC (10 mM ammonium acetate pH 6.9, 1 mL/min flow rate) on a YMC-Pack Diol-200 (300 x 8 mm ID, S-5 μ m, 20 nm; YMC, Inc.) size exclusion column. ACP eluted between 9.5 – 15 min and was collected. Pectins were filter sterilized and pH adjusted for biological assays. ACP and NCP were fractionated for structural analysis after passage through a CarboPac PA1 column (10 mM potassium acetate pH 6, 0.9 mL/min flow rate) and collection of unbound material in void volume. Charged fractions were obtained by isolating material that required more than 800 mM potassium acetate to elute from the same column.

2.2.2. Capillary electrophoresis

Pectins (40 μ L, 20 μ g) were partially depolymerized by incubation with 200 mM TFA at 80°C for 72 h. The resulting hydrolysates were lyophilized and resuspended in 30 μ L of 60 mM sodium acetate (pH 5) containing 3 mM CaCl₂. Two μ L of dialyzed pectinase mixture (Sigma, 0.3 U / mL) were added, and the sample was incubated for 48 hours at 45°C to achieve full depolymerization [25]. The pectinase reaction products were lyophilized and labeled with 8-aminopyrene-1,3,6-trisulfonic acid trisodium salt (APTS) according to a modified procedure [26]. Briefly, 15 μ L of 25 mM APTS in 15 % acetic acid and 5 μ L of 1 M NaBH₃CN were added to dry pectin powder. The mixture was incubated at 55°C for 90 min before stopping the reaction by adding 500 μ L of distilled water. Monosaccharide standards representing the composition of pectin were also labeled with APTS as described. Capillary electrophoresis analysis of APTS-labeled pectin components was performed with a ProteomeLab PA 800 (Beckman-Coulter Inc.) with a 40 cm bare-fused silica capillary (Polymicro Technologies) running 42 mM sodium tetraborate buffer (pH 10.2) with Ar laser detection.

2.2.3. ¹H-NMR

¹H-NMR was performed at 80°C using a Bruker 400 MHz instrument with an average of 256 measurements. Sodium 3-(trimethylsilyl)propionate-2,2,3,3-d₄ (TMSP) (Cambridge Isotope Laboratories Inc.) was used as a reference. Pectin was prepared for NMR by lyophilization and resuspension in D₂O. Pectin concentrations were 10 mg / mL, pD of the solution was 4. Methodology for calculating pectin methylation and relative amount of 4,5-dehydrogalacturonic acid have been previously described [27, 28].

2.2.4. *In vivo* tumor studies

For primary tumor growth studies, 2.5 x 10⁵ B16F10 melanoma cells were implanted in the left flank of male C57/BL6 mice on day 0. ACP (20 mg / kg) or NCP (20 mg / kg) were diluted in 100 μL PBS and injected s.c. every third day starting on day 7 when the tumors had reached 100 mm³ in volume. All mice were sacrificed as required by control tumor burden on day 17. For experimental metastasis studies, 5 x 10⁵ B16F10 melanoma cells were treated with 0.5% NCP (40 mg / kg), 0.5% ACP (40 mg / kg) or PBS for 30 minutes and injected into the tail vein of C57/BL6 mice on day 0 similarly to previously described [5]. On day 10, mice were sacrificed and the lungs were excised and fixed in Bouin's solution. Metastatic nodules were counted with the aid of a dissecting microscope.

2.2.5. Cell viability

Cell viability was measured using the WST-1 reagent (Roche) according to manufacturer's instructions. Briefly, B16F10 cells were seeded in a 96 well plate such that they were 50% confluent after 24 h. Cells were then treated with 1 mg/mL NCP, 1 mg/mL ACP, or PBS control. After an additional 24 hours, cells were incubated with 10% WST-1 reagent and cell viability was quantified by absorbance at 450 nm.

2.2.6. Chemoinvasion through matrigel

A measure of chemoinvasion was performed similarly to that described previously [29]. Briefly, Transwell inserts (Corning Inc; 8 μm pore size, 6.5 mm diameter) were coated with 15 μg of

Matrigel (Becton Dickinson) and allowed to dry overnight in a sterile laminar flow hood. Serum-deprived (0.1% FBS, overnight) B16F10 cells (2×10^5) were treated with APC or NPC at various concentrations and then added to the top of inserts. Reservoirs below inserts contained growth medium (500 μ l) supplemented with growth factor (40 ng/mL HGF) as a chemoattractant. After 40 h incubation, non-invaded cells were removed using cotton swabs, and invaded cells were fixed using 2.5% glutaraldehyde in PBS. Invaded cells were stained with crystal violet and counted with a Zeiss Axiovert 200M microscope using 9 fields of view per insert.

2.2.7. Western blotting

Cell monolayers were lysed in sample buffer and resolved on a 4–12% gradient SDS-polyacrylamide-gel electrophoresis gel. The proteins were transferred to a nitrocellulose membrane, blocked, and probed with primary antibodies to phospho-Akt(Thr308), phospho-PTEN(Ser380), and AKT (Cell Signaling) as well as actin as a loading control (Santa Cruz Biotechnology). Proteins were detected by chemiluminescence after incubation with the appropriate secondary horseradish peroxidase-labeled antibodies and visualized with a Kodak 2000 gel-imaging system.

2.2.8. Cloning of human Gal-1 and Gal-3

Gal-1 and Gal-3 were cloned using cDNA isolated from HUVECs. The galectin genes were cloned into the *NheI* / *Sall* restriction sites of pET-28a(+) vector (Novagen). Protein expression was carried out using *E. coli* Rosetta2 (DE3) (Novagen) and purified by IMAC using a HiTrap Chelating HP column (GE Healthcare). Proteins were dialyzed through a 2000 MWCO membrane (Spectrum Laboratories Inc.) against PBS and concentrated with 3000 MWCO Centriplus Centrifugal Filter Devices (Millipore) at 4 °C. Histidine tags were removed with thrombin (Sigma) treatment. Galectins were labeled with CFSE fluorescent label from Fluka. Proteins at 0.5 mg /mL in 50% PBS buffer were incubated with 1.5 mg/mL CFSE (in DMSO) in 9:1 ratio (v/v) for 2 h at RT and subsequently dialyzed.

2.2.9. Gal-1 and Gal-3 interaction with pectin

Colorless polystyrene microspheres (3.0 μm diameter, Polysciences) were passively adsorbed with either ACP or NCP by incubation ($\sim 10^9$ microspheres) with 50 μg of ACP/NCP in carbonate/bicarbonate buffer (50mM, pH 9.6) at 37 $^\circ\text{C}$ for 3 h. Microparticles were then washed with water. Treated microparticles ($\sim 10^6$) were probed by incubation with recombinant, fluorescein-labeled Gal-1 or Gal-3 (1 $\mu\text{g}/\text{mL}$) in the presence of increasing concentrations of lactose in PBS on ice for 30 min. Microparticles were then washed and analyzed by flow cytometry.

2.2.10. *In Vitro* cell binding

To measure cellular binding of ACP, B16F10 cells were incubated with 8-aminopyrene 1,3,6-trisulfonic acid (APTS)-labeled ACP at various concentrations in the presence or absence of 10 mM lactose or glucose in PBS ($\text{CaCl}_2/\text{MgCl}_2$ supplemented) for 30 minutes and cells were analyzed by flow cytometry.

2.2.11. Adhesion

Untreated 96-well plates (Becton Dickinson) were coated with matrigel (25 $\mu\text{g}/\text{ml}$), laminin (50 $\mu\text{g}/\text{ml}$), or fibronectin (50 $\mu\text{g}/\text{ml}$) and incubated at 4 $^\circ\text{C}$ for 18 hrs prior to blocking with 1% BSA (1 hr, 37 $^\circ\text{C}$). 4×10^4 pretreated (1 mg/mL ACP or NCP, 15-60 minutes, 37 $^\circ\text{C}$) B16F10 cells in 100 μl basal medium containing 0.1% BSA were added to each well and incubated for 15-60 minutes at 37 $^\circ\text{C}$. Non-adherent cells were removed by gently washing cells three times. To quantify adhesion, adherent cells were fixed with 2.5% glutaraldehyde in PBS and stained with crystal violet. Excess dye was washed away before solubilizing with 2% SDS and measuring absorbance at 550 nm. Alternatively wells were first coated with a confluent monolayer of HUVECs before addition of pretreated and fluorescently labeled (Vybrant CFDA SE cell tracer, Invitrogen) B16F10 cells for 30 minutes. Adherent cells were quantified by fluorescence (excitation 485 nm, emission 538 nm).

2.2.12. Flow cytometry

Intracellular quantification of protein phosphorylation by flow cytometry was performed as previously described [30, 31]. Following treatment with ACP, NCP, PBS, or LY294002 in the presence or absence of Gal-3/-1 antibodies for 30 minutes, cells were gently detached from the

culture plate with 0.02% EDTA in PBS, immediately fixed with 2.5% v/v formaldehyde in PBS for 5 minutes on ice, and permeabilized in 100% methanol for 10 minutes on ice. The following primary antibodies were used at 5 µg/mL or diluted 1:75 in FX buffer (0.1% w/v BSA, 0.05% w/v NaN₃ in PBS, pH 7.4), 25 minutes on ice: phospho-Akt(Thr308), phospho-PTEN(Ser380), PTEN (Cell Signaling), phospho-PI3K(Tyr508) (Santa Cruz Biotechnology), and rabbit IgG (Sigma) as an isotype control. Cells were washed and stained with Alexa 488-conjugated anti-rabbit or anti-goat antibodies (Invitrogen), 5 µg/mL in FX buffer, 20 minutes on ice. Data acquisition was performed on a Beckman-Coulter Cell Lab Quanta SC flow cytometer equipped with MPL robot. Means and coefficients of variance produced by the Quanta Analysis™ software were used for statistical evaluations.

2.2.13. siRNA knockdown

PTEN expression was reduced using the SignalSilence PTEN siRNA kit (Cell Signaling) according to manufacturer's instructions. Briefly, B16F10 cells were plated in a 96 well plate such that they would reach ~50% confluence after 24 hours. At this time, PTEN expression was knocked down using the targeted siRNA constructs with the supplied transfection reagent overnight. Media was replaced and cells were treated with NCP (1 mg/mL), ACP (1 mg/mL) or PBS control for 30 minutes before harvesting for protein analysis. Intracellular flow cytometry quantification of protein phosphorylation was performed as described above.

2.2.14. MALDI-MS

MALDI-MS was performed with a Voyager-DE STR BioSpectrometry Workstation (PerSeptive Biosystems) typically detecting mass range of 500 – 7000 Da. Samples were irradiated with a N₂ laser (337 nm) using laser intensity 2200 and 100 shots were averaged for every mass spectrum. Negative and positive mode MALDI-MS were performed using an ATT/Nafion and 2,5 dehydroxybenzoic acid (DHB) matrix respectively. The matrix was mixed in a 1:1 ratio with 2 mg/mL pectin and added to a stainless steel MALDI probe. The spots were dried at atmospheric humidity. In order to identify structures represented by MALDI-MS, peaks were annotated with all

theoretically possible mass identities. Theoretical identities were ranked according to mathematical fits based on data from NMR and CE, and the set that best satisfied data collected from CE and NMR experiments was selected for final structure assignment.

2.3. Results

2.3.1. Anticancer ACP is generated directly from lemon NCP

NCP from the homogeneous citrus source of lemons, a common source of citrus pectin [11], was used as the starting material for isolating anticancer modified pectin fractions. Heat and base

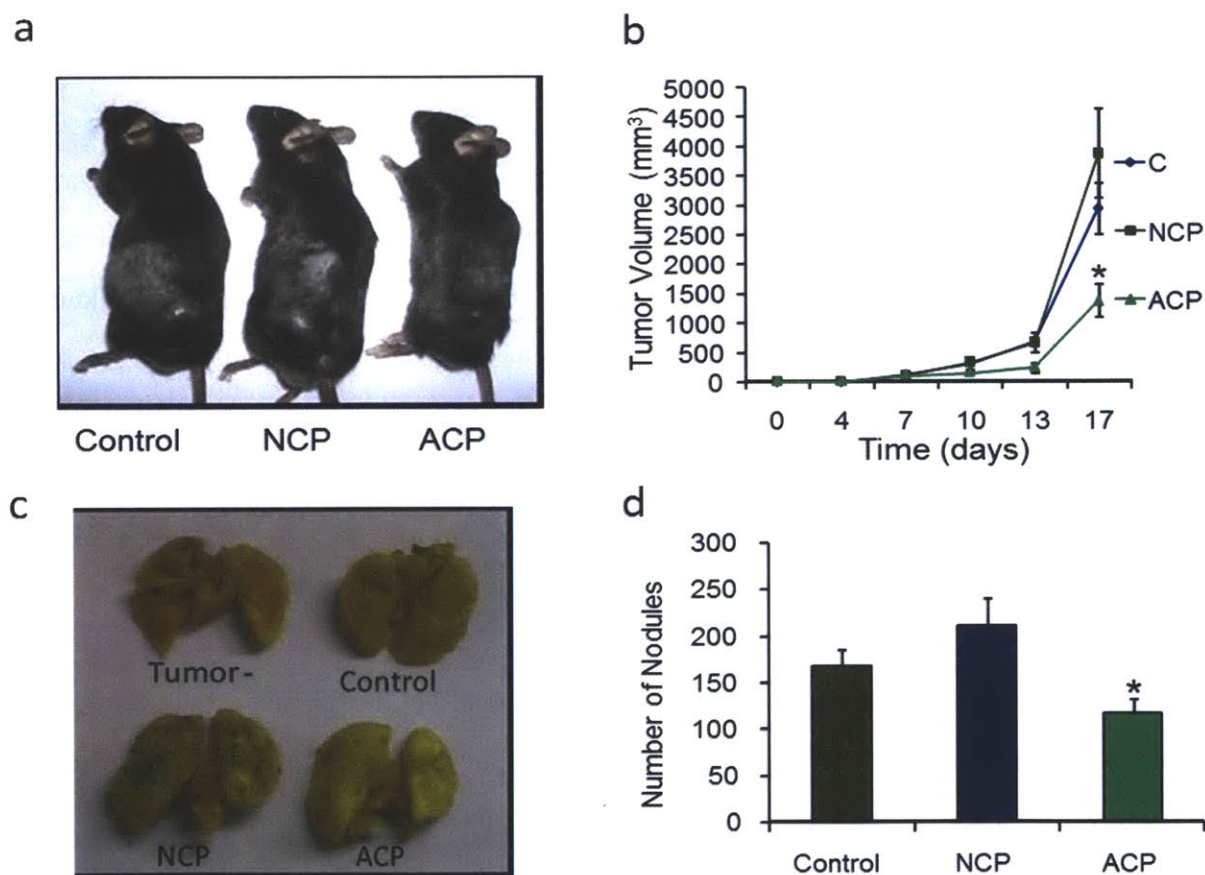


Figure 2.1 Effect of ACP on tumor growth and metastasis *in vivo*. (a),(b) B16F10 primary site tumor growth following treatment with NCP (20 mg / kg), ACP (20 mg / kg), and PBS control every third day after tumors reached 100 mm³ in volume. (c),(d) Number of metastatic lung nodules following tail vein injection of 5×10^5 B16F10 melanoma cells treated with NCP (40 mg / kg), ACP (40 mg / kg) or PBS. On day 10, mice were sacrificed and metastatic nodules counted with the aid of a dissecting microscope. Results are presented as means \pm s.e.m. * $p < 0.05$ vs. control.

were employed to promote the demethylation and fragmentation of the GalA backbones (see Methods). A regularly employed acid treatment step was omitted to preserve the structural integrity of the neutral oligosaccharide branched regions which may be responsible for galectin binding [15, 16, 32]. The resultant formulation was separated by HPLC-SEC to increase the solubility of the partially digested pectin and to divide the material into defined fractions for testing.

A low molecular weight fraction, termed ACP, demonstrated notably higher anticancer

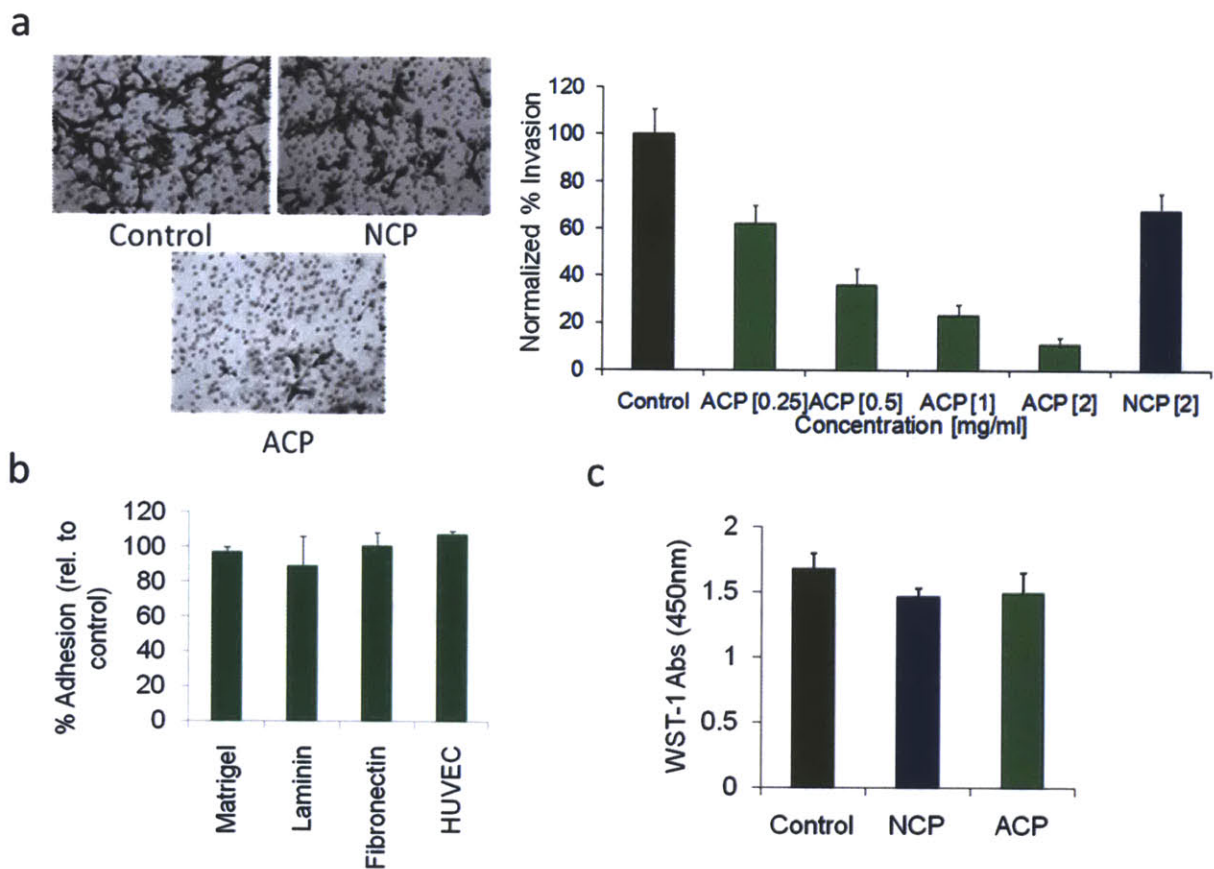


Figure 2.2 Anti-tumor efficacy of ACP *in vitro*. (a) Quantification of B16F10 cell chemoinvasion through matrigel after treatment with designated concentrations of NCP, ACP, and PBS control. (b) B16F10 cell adhesion to matrigel, laminin, fibronectin, and HUVECs after pretreatment with ACP (1mg / mL). Results expressed as percentage of adhesion compared to B16F10 cells pretreated with NCP (1mg / mL). (c) Measure of cell viability using the WST-1 reagent. Adherent B16F10 cells at 50% confluence were treated with NCP (1mg / mL), ACP (1mg / mL), or PBS and evaluated for cell viability after 24 hours.

activity compared to NCP both *in vitro* and *in vivo*. To assess the role of ACP on primary tumor growth, B16F10 cells were implanted s.c. into C57/BL6 mouse flanks. Treatment every third day with ACP inhibited tumor growth by ~50% over the course of our study when compared to control (**Figure 2.1a,b**). To assess the role of ACP on tumor metastasis, ACP-treated B16F10 cells were injected i.v. into C57/BL6 mice. ACP treatment inhibited the formation of lung metastatic nodules by ~30% compared to control (**Figure 2.1c,d**). The *in vivo* efficacy was corroborated *in vitro*, with ACP exhibiting a dose-dependent inhibition of B16F10 chemoinvasion through matrigel (**Figure 2.2a**). Interestingly, ACP treatment demonstrated no significant effect on B16F10 cell adhesion to multiple basement membrane matrix proteins or to human umbilical vein endothelial cells (HUVECs) (**Figure 2.2b**) in contrast to some previous modified pectin formulations [5, 16]. ACP also did not inhibit B16F10 cell proliferation compared to NCP (**Figure 2.2c**) under *in vitro* culture conditions. Collectively, these results demonstrate that ACP is a potent *in vivo* anti-tumor and anti-metastatic agent and that this activity is not due to direct *in vitro* tumor cytotoxicity.

One hindrance to developing a reproducible, clinically relevant anticancer pectin formulation is the potential for structural heterogeneity in the modified pectin formulations reported across studies. The pre-processed pectin powders currently used as starting materials [5-7, 16] are often mixed in citrus composition and may differ in processing conditions, and structural information is not always known or reported [33]. We analyzed the compositions of pectin powders available from common laboratory vendors to determine the extent of any compositional diversity (**Figure 2.3a**). The pectin powders analyzed contained similar relative concentrations of the major monosaccharide constituents (GalA, rhamnose, and galactose), however greater differences were noted in the relative concentrations of the minority monosaccharide components of the neutral side chains (glucose, mannose, and arabinose). These differences were observed both in pectin powders purchased from different vendors as well as between lots from the same vendor (**Figure 2.3a**). Since the bioactive structures within modified pectins remain largely unknown, these compositional differences could impact the bioactivity of modified pectins and may be responsible

for the variable reports of anti-tumor pectin function. The use of NCP as a starting material enables the generation of a standardizable pectin for comparison across studies.

2.3.2. ACP is enriched for liberated neutral oligosaccharides

To characterize structural differences between NCP and ACP, we first investigated modifications to the GalA pectin backbone. $^1\text{H-NMR}$ analysis revealed that 70% of GalA residues are

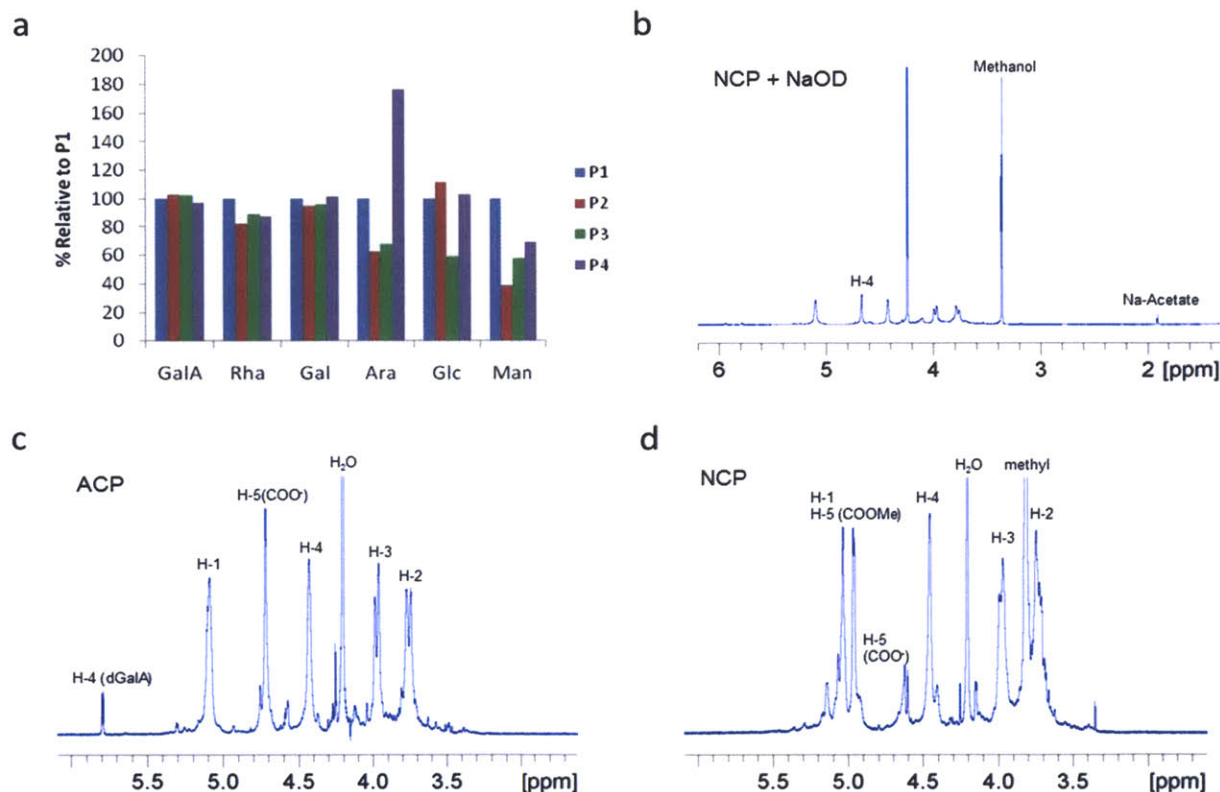


Figure 2.3 Capillary electrophoresis and $^1\text{H-NMR}$ analysis. (a) Monosaccharide compositional analysis of commercial citrus pectin powders by capillary electrophoresis. Pectins were depolymerized and enzymatically digested prior to analysis as described in the Methods. All results were normalized relative to levels of pectin powder P1 for purposes of comparison. P1 = Sigma P-9135 Lot #098K0032, P2 = Sigma P-9135 Lot #99H0029, P3 = Sigma P-9135 Lot #013K0007, P4 = Fluka 76280. (b) Measurement of acetylation and methylation of NCP. The 400 MHz $^1\text{H-NMR}$ spectra of NCP shows formation of methanol and Na-acetate. Amounts of methylation and acetylation were calculated by comparing ratios of H-4 of GalA (4.44 ppm) and H-4 of dGalA (5.78 ppm) with those of methanol (3.3 ppm) and Na-acetate (1.9 ppm). (c), (d): 400 MHz $^1\text{H-NMR}$ spectra of ACP and NCP demonstrate differences in the amounts of dGalA and methylation state. H-4 of GalA (4.44 ppm) and H-4 of dGalA (5.78 ppm) were used to determine the relative amount of dGalA present.

methyated in NCP and that ACP is free of methylation (**Figure 2.3b**) [27]. ¹H-NMR was also used to demonstrate the extent of GalA backbone fragmentation through monitoring the formation of 4,5-dehydro-galacturonic acid (dGalA) after β-elimination [28]. dGalA is not present in NCP, however over 8% of GalA was converted to dGalA in ACP, indicating significant fragmentation (**Figure 2.3c,d**). Collectively these results demonstrate that de-esterification and fragmentation of the GalA backbone distinguish ACP from NCP.

Table 2.1 CE monosaccharide composition of charge-separated ACP and NCP fractions.

	ACP-N	NCP-N	ACP-C
Rha (%)	0.79 ± 0.05	0.02 ± 0.02	0.21 ± 0.02
Man (%)	10.73 ± 0.27	14.22 ± 0.25	0.06 ± 0.01
Glc (%)	6.35 ± 0.61	3.91 ± 0.05	0.03 ± 0.04
Xyl (%)	7.89 ± 0.33	3.14 ± 0.09	0.27 ± 0.05
Ara (%)	14.35 ± 0.4	43.22 ± 0.12	0.24 ± 0.05
Gal (%)	58.71 ± 0.27	17.45 ± 0.19	0.13 ± 0.03
GalA + dGalA (%)	1.18 ± 0.04	18.03 ± 0.33	99.07 ± 0.12

We next compared structures of the branched regions of ACP and NCP. ACP and NCP were charge fractionated by HPLC-AEC into the least charged and most charged components corresponding primarily to the branched and linear regions of pectin, respectively. Monosaccharide composition by CE (**Table 2.1**) shows the presence of 99.07% GalA in the most charged fraction of ACP (ACP-C) and only 1.18% GalA in the neutral fraction (ACP-N), indicating that the branched regions of ACP were nearly completely liberated from the homogalacturonan regions. To confirm these findings from ¹H-NMR and CE, we next compared structures of ACP and NCP by MALDI-MS. Peak assignments from negative mode MALDI-MS indicate that the charged region of ACP consists only of unbranched GalA (**Figure 2.4a**). NCP retains a structurally complex spectrum consistent with an intact network of neutral polysaccharide branches and the charged

GalA backbone (**Figure 2.4b**). Positive mode MALDI-MS of ACP demonstrates that the branched regions of ACP consist of oligosaccharides composed primarily of neutral pentoses and hexoses (**Figure 2.4c**), results consistent with the predominance of galactans, arabinans, and arabinogalactans of hairy regions [2]. Positive mode analysis of NCP however reveals peaks corresponding to methylated GalA (**Figure 2.4d**). Taken together, our data demonstrate that ACP

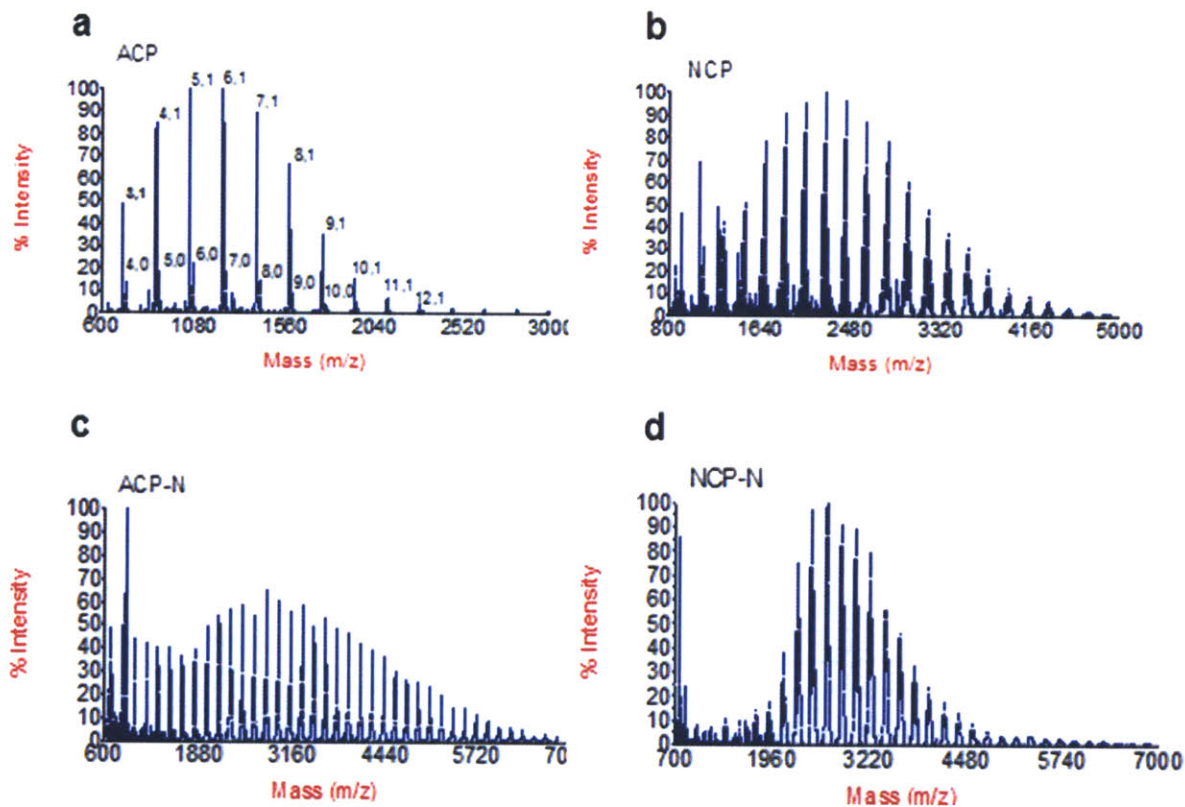


Figure 2.4 MALDI-MS analysis of ACP and NCP. (a),(b) Negative mode MALDI-MS spectra of ACP and NCP, respectively. All major spectral peak masses of ACP are consistent with structures consisting of only GalA and dGalA as annotated (number of GalA, number of dGalA). The major spectral peak masses of NCP can be described as a mixed combination of charged and neutral constituents found within the pectin network. (c), (d) Positive mode MALDI-MS spectra of the neutral components of ACP (ACP-N) and NCP (NCP-N), respectively.

consists of demethylated, fragmented GalA backbones, and that the branched regions of ACP have been liberated from these backbones while retaining intact, structurally complex neutral oligosaccharide structures.

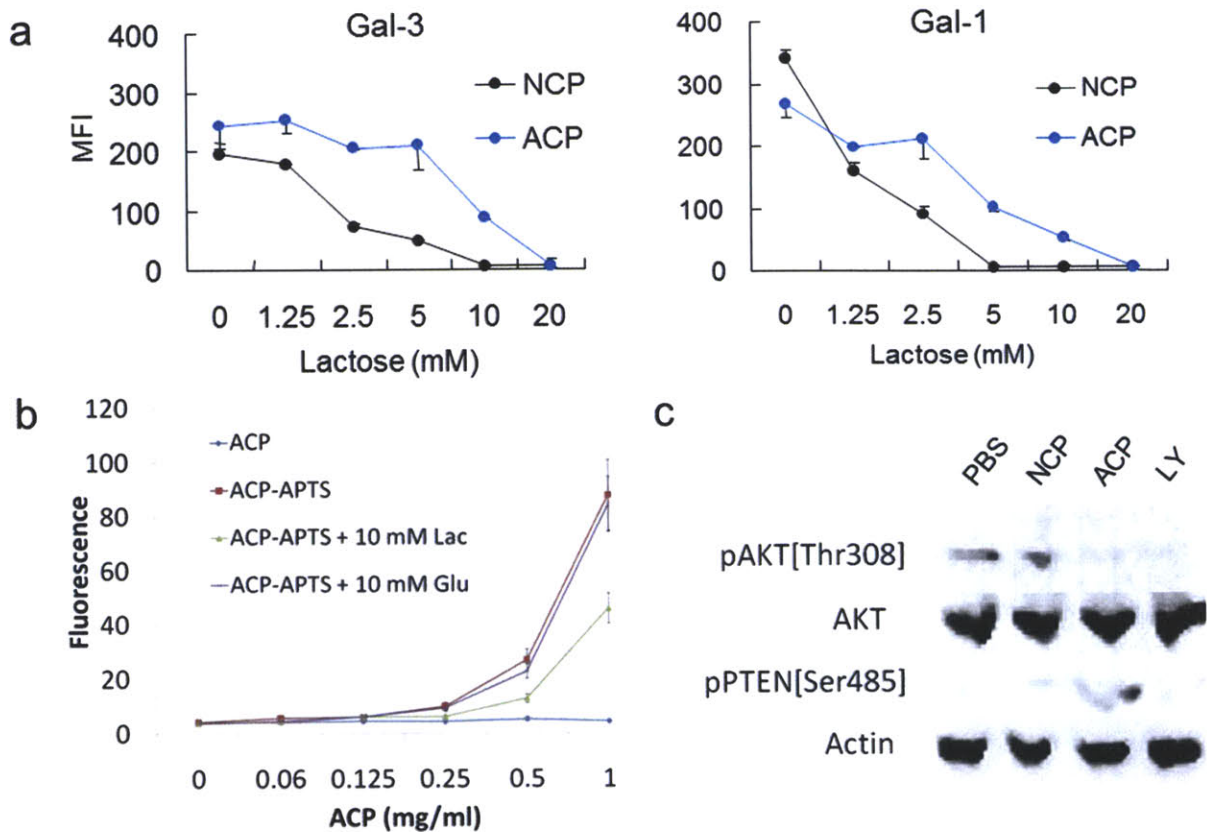


Figure 2.5 Role of galectins in ACP anti-tumor activity. (a) Quantification of the interaction of fluorescently labeled Gal-1 and Gal-3 with NCP and ACP adsorbed to polystyrene beads by flow cytometry. MFI results are presented as means and coefficients of variance produced by Quanta Analysis™ software. (b) Quantification of the interaction of B16F10 cells and APTS-labeled ACP at designated concentrations by flow cytometry. Competitive inhibition is demonstrated in the presence of 10 mM lactose. (c) B16F10 expression of AKT, pAKT(Thr308), pPTEN(Ser380), and actin after treatment with PBS, NCP, ACP, and LY294002 (LY), as measured by western blot. NCP or ACP treatment is at 1 mg/mL.

2.3.3. Galectin-1 and galectin-3 preferentially bind to ACP

Gal-3 is the proposed mediator of pectin activity [15, 16, 32], however recent evidence has shown that modified pectins may still have anti-tumor activity against cell lines absent in Gal-3 expression [10]. In light of this report, we also investigated whether galectin-1 (Gal-1) contributed to pectin anticancer activity. Gal-1, like Gal-3, is expressed by many tumors and is implicated as participating in a regulatory role of tumor progression [34]. In order to investigate the ability of ACP to bind to these galectins, ACP and NCP were passively adsorbed onto polymer microparticles and probed using fluorescently labeled recombinant Gal-3 and Gal-1. Flow cytometric analysis of

fluorescence intensity established binding of both Gal-3 and Gal-1 to ACP (**Figure 2.5a**). Competitive inhibition by lactose demonstrated that ACP binding occurs at the galectin carbohydrate recognition domains (CRDs) and that the relative specific binding interaction of both galectins is greater for ACP than for NCP. These findings indicate that modifying pectin to generate ACP creates or exposes CRD-specific binding structures for both Gal-3 and Gal-1. To explore the functional consequence of this galectin binding, we quantified the interaction of B16F10 cells with fluorescently labeled ACP *in vitro* in the presence or absence of lactose. Competitive inhibition by lactose partially inhibited the interaction of ACP with B16F10 cells (**Figure 2.5b**), supporting a role for galectins in the anticancer mechanism of ACP.

2.3.4. Galectins modulate ACP activity through AKT signaling

An intracellular mechanism of action for anticancer pectins has yet to be established in solid tumors. The involvement of the AKT pathway has been linked to pectin treatment of myeloma [35], and this pathway is a central modulator of tumor processes including invasion, survival, and metabolism [36]. Recent evidence has also supported the involvement of both Gal-1 and Gal-3 in modulating this pathway [37-39]. To investigate a link between the anti-tumor effect of ACP against B16F10 melanoma and intracellular AKT signaling, we treated B16F10 cells *in vitro* with ACP and quantified AKT protein phosphorylation. Treatment with both ACP and the phosphoinositide 3-kinase (PI3K) inhibitor LY294002 reduced AKT phosphorylation at the Thr308 residue, while no change to AKT phosphorylation was observed after treatment with NCP relative to PBS control (**Figures 2.5c** and **2.6a**). We next investigated whether AKT dephosphorylation is mediated by the interaction of ACP with galectins. B16F10 cells were treated with ACP in combination with antibodies to either Gal-1 or Gal-3. Antibodies to both galectins partially reversed the ACP-induced reduction of AKT phosphorylation (**Figure 2.6a**), supporting that both galectins are involved in modulating ACP's effect on AKT signaling.

2.3.5. Tumor PTEN is necessary for ACP-induced signaling

We further investigated the mechanism of ACP-induced AKT dephosphorylation by examining the involvement of PI3K and PTEN in this pathway. PI3K and PTEN are two opposing

regulators of AKT phosphorylation: PI3K phosphorylates PIP2 to PIP3 to phosphorylate AKT while PTEN reverses this process to dephosphorylate AKT [40, 41]. B16F10 cells treated with ACP showed increased phosphorylation of PTEN at Ser385 with no change to PI3K phosphorylation (Figures 2.5c and 2.6b). In contrast, the control inhibitor LY294002 reduced phosphorylation of PI3K (Figure 2.6b) but did not affect phosphorylation of PTEN (Figure 2.6a). In order to determine whether functional PTEN is necessary for ACP activity, a knockdown of B16F10 PTEN was achieved using siRNA (Figure 2.6b). Knockdown of PTEN eliminated ACP's reduction of AKT phosphorylation, though the effect of LY294002 was unchanged (Figure 2.6b). These results collectively demonstrate that functional PTEN is necessary for AKT dephosphorylation after ACP treatment and that PI3K is not a mediator of ACP activity.

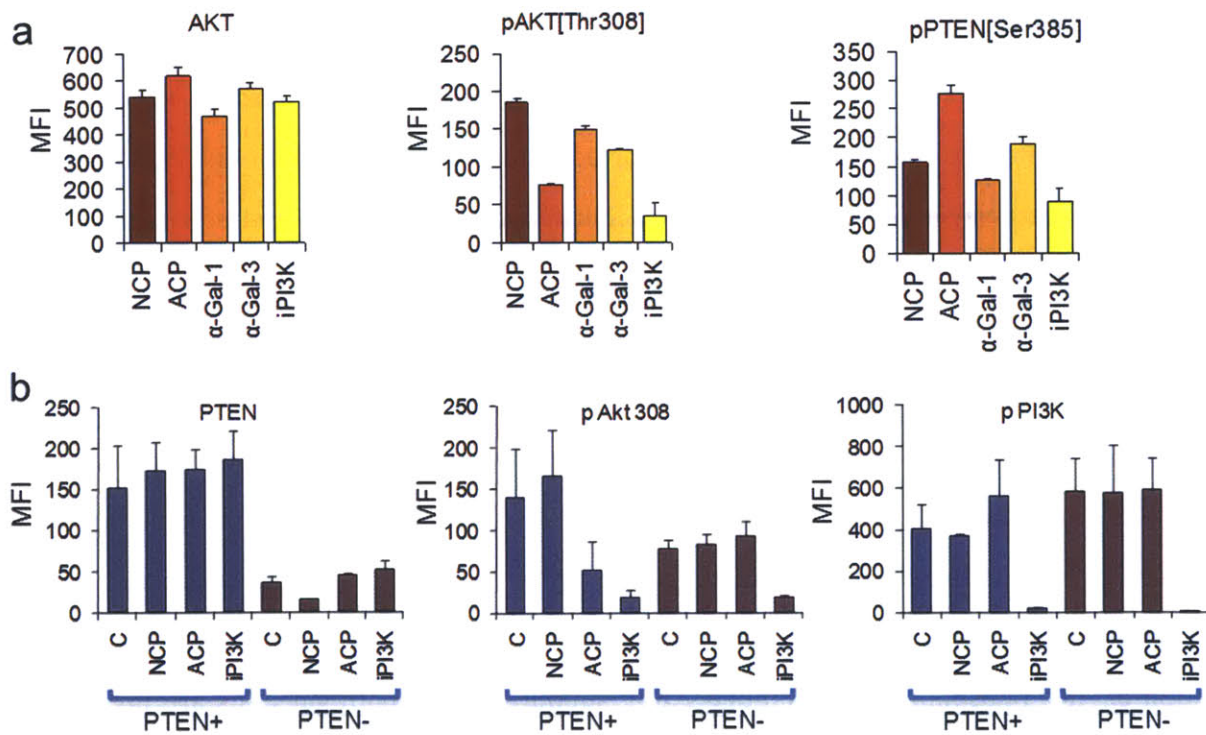


Figure 2.6 Pathway analysis of ACP anti-tumor activity. (a) Quantification of B16F10 AKT and PTEN phosphorylation by flow cytometry after treatment of cells with ACP or NCP and co-treatment with Gal-1/-3 antibodies. (b) B16F10 phosphoprotein levels after siRNA knockdown of PTEN expression followed by treatment with NCP, ACP, iPI3K (LY294002) or PBS control, as measured by flow cytometry. MFI results are presented as means and coefficients of variance produced by Quanta Analysis™ software.

2.4. Discussion

Modified citrus pectins currently offer promise as a solution to the ongoing search for non-toxic, inexpensive and effective clinical therapies. Modified pectins have demonstrated anti-tumor and/or anti-metastatic efficacy in a range of animal models while demonstrating low systemic toxicity [5-7, 16]. The identity of the bioactive pectin fragments and their mechanism of action remain cryptic however. Treatment of pectin to expose galactose and arabinose-containing structures within the neutral branched regions of pectin has been directly connected with increased pectin interaction with Gal-3, a known regulator of tumor progression [15, 32]. A tumor apoptosis-inducing fragment within pectin has also recently been shown to contain an essential ester linkage other than a carboxymethylester, though a specific structure was not identified [10]. Since modified pectin formulations are often ubiquitously fragmented, little additional information has been reported regarding the identity of the bioactive fragments or the optimal modification procedure to generate these fragments. In this study, we isolated a new anti-tumor modified pectin fraction, termed ACP, enriched for proposed bioactive constituents. The GalA-rich pectin backbone was fragmented and demethylated using heat and alkali treatment to liberate the neutral branched regions of pectin implicated in galectin binding. A commonly employed acid-treatment step was omitted to preserve the structural integrity of the neutral branches and to protect any unidentified bioactive linkages within these regions. Size exclusion chromatography increased the solubility of our formulation and avoided the need for additional pectin fragmentation.

Pectin's mechanism of action is also still an active area of investigation. Early studies identified a mechanism for anticancer pectins in Gal-3-mediated processes including cell adhesion, aggregation, and migration [7, 16]. There are conflicting reports regarding whether modified pectins directly inhibit tumor cell viability *in vitro*. While several studies have demonstrated that modified pectins induce tumor cell apoptosis [10, 15], others demonstrate a lack of direct tumor cytotoxicity [4] and still others do not report on this finding [5, 7, 16]. Indirect mechanisms of anti-tumor activity have also been documented for different modified pectins including an anti-angiogenic function [7] as well as the ability to stimulate the host immune system [4]. An additional

complication for the identification of a consensus mechanism of activity is the use of different modified pectin formulations across studies. Many studies employ pre-processed pectin powders heterogeneous in citrus source [5-7, 16] and still others use pectins isolated from non-citrus sources altogether [4, 15]. The diversity of direct and indirect anti-tumor mechanisms and the evidence that different modified pectin formulations demonstrate distinct functional activities *in vitro* indicate the likelihood of a complex interaction of multiple mechanisms dependent upon key and as yet unknown differences in pectin fine structure. To generate a structurally reproducible anticancer pectin formulation for comparison across studies, we generated ACP from NCP directly from the citrus source of lemon fruit.

Anticancer pectins have previously been proposed to regulate tumor progression through binding and modulation of Gal-3 signaling. Gal-3 has established roles in physiological processes related to tumor progression including tumor signaling, inflammation, and immunity [17, 18]. A recent study demonstrated for the first time that at least certain anti-tumor pectin formulations are effective against cell lines that do not express Gal-3 [10], supporting the role for additional mediators of pectin activity. Gal-1 is an additional galectin with established roles in regulating tumor progression and may have the untested binding affinity for structures present within the pectin matrix [34, 42]. We demonstrate here that Gal-1 and Gal-3 bind to ACP and that galectins are involved in mediating direct ACP-tumor cell interaction as well as modulating tumor signaling. This study is the first to our knowledge to demonstrate the involvement of Gal-1 in mediating anticancer pectin activity.

We also describe here key constituents in the first pectin-induced anti-tumor signaling cascade reported in solid tumors. The AKT pathway directs numerous intracellular processes, and the phosphorylation state of AKT is a central regulator of tumor survival and progression [36]. We demonstrate that ACP treatment inhibits the phosphorylation of tumor AKT similarly to treatment with the PI3K inhibitor LY294002. Intriguingly, we also demonstrate that the effect of AKT on this pathway is dependent upon functional tumor PTEN expression and, unlike LY294002, is independent of the classical PI3K-mediated drug pathway.

In conclusion, we present here a new integrated methodology for generating and characterizing the modified pectin formulation ACP using activation and isolation conditions that enrich for the formation of soluble, galectin-binding pectin structures. We demonstrate the first structure-function link that Gal-1 and Gal-3 interaction with bioactive structures enriched within ACP promotes an anticancer intracellular signaling cascade mediated by the dephosphorylation of AKT. This activity is dependent upon the presence of functional PTEN, and suggests the use of ACP for treatment of PTEN-expressing tumors. ACP's ready availability and low toxicity would further support the use of this agent in combination therapy regimes with traditional chemotherapy agents. It is our hope that the link provided here between pectin structure, mechanism, and therapeutic outcome will assist in bringing anticancer pectins closer to widespread clinical use.

Attributions The work described in this chapter is the result from multiple investigators' efforts. David Eavarone contributed efforts with pectin preparation, *in vivo* experiments, cell viability experiments, western blotting, adhesion experiments, and flow cytometry (including signaling and knock-down experiments). Tom Haller contributed efforts with pectin preparation, structural characterization (CE, NMR, MS), and cloning of galectins. Ido Bachelet assisted with western blotting, galectin interaction experiments, and cell signaling experiments. Karunya Srinivasan assisted with pectin preparation, CE and MS. I participated in these studies by assisting with pectin preparation, CE, *in vivo* experiments, chemoinvasion studies, western blotting, adhesion experiments, and MS.

2.5. References

1. Caffall, K.H. and D. Mohnen, *The structure, function, and biosynthesis of plant cell wall pectic polysaccharides*. Carbohydr Res, 2009. **344**(14): p. 1879-900.
2. Mohnen, D., *Pectin structure and biosynthesis*. Curr Opin Plant Biol, 2008. **11**(3): p. 266-77.
3. Liu, H.Y., et al., *Inhibitory effect of modified citrus pectin on liver metastases in a mouse colon cancer model*. World J Gastroenterol, 2008. **14**(48): p. 7386-91.
4. Han, S.B., et al., *Pectic polysaccharide isolated from Angelica gigas Nakai inhibits melanoma cell metastasis and growth by directly preventing cell adhesion and activating host immune functions*. Cancer Lett, 2006. **243**(2): p. 264-73.
5. Platt, D. and A. Raz, *Modulation of the lung colonization of B16-F1 melanoma cells by citrus pectin*. J Natl Cancer Inst, 1992. **84**(6): p. 438-42.
6. Pienta, K.J., et al., *Inhibition of spontaneous metastasis in a rat prostate cancer model by oral administration of modified citrus pectin*. J Natl Cancer Inst, 1995. **87**(5): p. 348-53.
7. Nangia-Makker, P., et al., *Inhibition of human cancer cell growth and metastasis in nude mice by oral intake of modified citrus pectin*. J Natl Cancer Inst, 2002. **94**(24): p. 1854-62.
8. Guess, B.W., et al., *Modified citrus pectin (MCP) increases the prostate-specific antigen doubling time in men with prostate cancer: a phase II pilot study*. Prostate Cancer Prostatic Dis, 2003. **6**(4): p. 301-4.
9. Chauhan, D., et al., *A novel carbohydrate-based therapeutic GCS-100 overcomes bortezomib resistance and enhances dexamethasone-induced apoptosis in multiple myeloma cells*. Cancer Res, 2005. **65**(18): p. 8350-8.
10. Jackson, C.L., et al., *Pectin induces apoptosis in human prostate cancer cells: correlation of apoptotic function with pectin structure*. Glycobiology, 2007. **17**(8): p. 805-19.
11. Voragen, A.G.J., Pilnik, W., Thibault, J.-F., Axelos, M.A.V. and Renard, C.M.C.G., *Pectins*, in *Food Polysaccharides and Their Applications*, A.M. Stephen, Editor. 1995, Marcel Dekker: New York. p. 287-339.
12. Thibault, J.-F., Renard, C.M.G.C, Axelos, M., Roger, P., and Crepeau, M.J., *Studies on the length of homogalaturonic regions in pectins by acid-hydrolysis*. Carbohydr Res, 1993. **238**: p. 271-286.
13. Renard, C.M.G.C. and J.-F. Thibault, *Degradation of pectins in alkaline condition: kinetics of demethylation*. Carbohydr Res, 1996. **286**: p. 139-150.
14. Kravtchenko, T.P., et al., *Improvement of the selective depolymerization of pectic substances by chemical b-elimination in aqueous solution*. Carbohydrate Polymers, 1992. **19**: p. 237-242.
15. Sathisha, U.V., et al., *Inhibition of galectin-3 mediated cellular interactions by pectic polysaccharides from dietary sources*. Glycoconj J, 2007. **24**(8): p. 497-507.
16. Inohara, H. and A. Raz, *Effects of natural complex carbohydrate (citrus pectin) on murine melanoma cell properties related to galectin-3 functions*. Glycoconj J, 1994. **11**(6): p. 527-32.
17. Nakahara, S., N. Oka, and A. Raz, *On the role of galectin-3 in cancer apoptosis*. Apoptosis, 2005. **10**(2): p. 267-75.
18. Takenaka, Y., T. Fukumori, and A. Raz, *Galectin-3 and metastasis*. Glycoconj J, 2004. **19**(7-9): p. 543-9.
19. Springate CF, C.T., Belt R, Redfern C, Stuart K, *Phase II study of GBC-590 in patients with relapsing or refractory colorectal cancer*. Am Soc Clin Oncol, 2001. **20**: p. 2226a.
20. Azemar, M., et al., *Clinical Benefit in Patients with Advanced Solid Tumors Treated with Modified Citrus Pectin: A Prospective Pilot Study*. Clinical Medicine Insights: Oncology, 2007. **1**(CMO-1-Azémar-et-al): p. 73.

21. Cotter, F., et al., *Single-agent activity of GCS-100, a first-in-class galectin-3 antagonist, in elderly patients with relapsed chronic lymphocytic leukemia*. J Clin Oncol, 2009. **27**(15s): p. abst 7006.
22. Cotter, F., et al. *Caspase activation as a surrogate biomarker for treating chronic lymphocytic leukemia with GCS-100, a novel carbohydrate, in a phase II trial*. in 2008 Molecular Markers. 2008.
23. La Jolla Pharmaceutical Company. *GCS-100 Technology*. 2012 [cited 2012 July 22]; Available from: <http://www.ljpc.com/technology-gcs100technology.html>.
24. Fishman, M.L., et al., *Characterization of pectin, flash-extracted from orange albedo by microwave heating, under pressure*. Carbohydr Res, 2000. **323**(1-4): p. 126-38.
25. Garna, H., et al., *New method for a two-step hydrolysis and chromatographic analysis of pectin neutral sugar chains*. J Agric Food Chem, 2004. **52**(15): p. 4652-9.
26. Frayse, N., et al., *Capillary electrophoresis as a simple and sensitive method to study polysaccharides of Sinorhizobium sp. NGR234*. Electrophoresis, 2003. **24**(19-20): p. 3364-70.
27. Bedouet, L., B. Courtois, and J. Courtois, *Rapid quantification of O-acetyl and O-methyl residues in pectin extracts*. Carbohydr Res, 2003. **338**(4): p. 379-83.
28. Rosenbohm, C., et al., *Chemically methylated and reduced pectins: preparation, characterisation by 1H NMR spectroscopy, enzymatic degradation, and gelling properties*. Carbohydr Res, 2003. **338**(7): p. 637-49.
29. Albin, A., et al., *A rapid in vitro assay for quantitating the invasive potential of tumor cells*. Cancer Res, 1987. **47**(12): p. 3239-45.
30. Irish, J.M., et al., *Single cell profiling of potentiated phospho-protein networks in cancer cells*. Cell, 2004. **118**(2): p. 217-28.
31. Krutzik, P.O. and G.P. Nolan, *Fluorescent cell barcoding in flow cytometry allows high-throughput drug screening and signaling profiling*. Nat Methods, 2006. **3**(5): p. 361-8.
32. Gunning, A.P., R.J. Bongaerts, and V.J. Morris, *Recognition of galactan components of pectin by galectin-3*. Faseb J, 2008.
33. Rolin, C., *Commercial Pectin Preparations*, in *Pectins and their Manipulation*, G.B. Seymour, Knox, J.P., Editor. 2002, CRC Press LLC: Boca Raton.
34. Camby, I., et al., *Galectin-1: a small protein with major functions*. Glycobiology, 2006. **16**(11): p. 137R-157R.
35. Streetly, M.J., et al., *GCS-100, a novel galectin-3 antagonist, modulates MCL-1, NOXA, and cell cycle to induce myeloma cell death*. Blood, 2010. **115**(19): p. 3939-48.
36. Hennessy, B.T., et al., *Exploiting the PI3K/AKT pathway for cancer drug discovery*. Nat Rev Drug Discov, 2005. **4**(12): p. 988-1004.
37. Oka, N., et al., *Galectin-3 inhibits tumor necrosis factor-related apoptosis-inducing ligand-induced apoptosis by activating Akt in human bladder carcinoma cells*. Cancer Res, 2005. **65**(17): p. 7546-53.
38. Abroun, S., et al., *Galectin-1 supports the survival of CD45RA(-) primary myeloma cells in vitro*. Br J Haematol, 2008. **142**(5): p. 754-65.
39. Lin, C.I., et al., *Galectin-3 regulates apoptosis and doxorubicin chemoresistance in papillary thyroid cancer cells*. Biochem Biophys Res Commun, 2009. **379**(2): p. 626-31.
40. Gonzalez, J. and J. de Groot, *Combination therapy for malignant glioma based on PTEN status*. Expert Rev Anticancer Ther, 2008. **8**(11): p. 1767-79.
41. Yin, Y. and W.H. Shen, *PTEN: a new guardian of the genome*. Oncogene, 2008. **27**(41): p. 5443-53.
42. Thijssen, V.L., et al., *Galectin-1 is essential in tumor angiogenesis and is a target for antiangiogenesis therapy*. Proc Natl Acad Sci U S A, 2006. **103**(43): p. 15975-80.

3. Identification of a contaminant in heparin by structure-function characterization

The following work was published in a series of papers, as follows:

1. Guerrini M, Beccati D, Shriver Z, Naggi A, Viswanathan K, Bisio A, Capila I, Lansing JC, Guglieri S, Fraser B, Al-Hakim A, Gunay NS, Zhang Z, Robinson L, Buhse L, Nasr M, Woodcock J, Langer R, Venkataraman G, Linhardt RJ, Casu B, Torri G, Sasisekharan R. *Oversulfated chondroitin sulfate is a contaminant in heparin associated with adverse clinical events*. Nat Biotechnol, 2008 Jun;26(6):669-75. Reproduced with kind permission from Nature Publishing Group.
2. Kishimoto TK, Viswanathan K, Ganguly T, Elankumaran S, Smith S, Pelzer K, Lansing JC, Sriranganathan N, Zhao G, Galcheva-Gargova Z, Al-Hakim A, Bailey GS, Fraser B, Roy S, Rogers-Cotrone T, Buhse L, Whary M, Fox J, Nasr M, Dal Pan GJ, Shriver Z, Langer RS, Venkataraman G, Austen KF, Woodcock J, Sasisekharan R. *Contaminated heparin associated with adverse clinical events and activation of the contact system*. N Engl J Med. 2008 Jun 5;358(23):2457-67. Reproduced with kind permission from Massachusetts Medical Society, Copyright Massachusetts Medical Society.
3. Blossom DB, Kallen AJ, Patel PR, Elward A, Robinson L, Gao G, Langer R, Perkins KM, Jaeger JL, Kurkjian KM, Jones M, Schillie SF, Shehab N, Ketterer D, Venkataraman G, Kishimoto TK, Shriver Z, McMahon AW, Austen KF, Kozlowski S, Srinivasan A, Turabelidze G, Gould CV, Arduino MJ, Sasisekharan R. *Outbreak of adverse reactions associated with contaminated heparin*. N Engl J Med. 2008 Dec 18;359(25):2674-84. Reproduced with kind permission from Massachusetts Medical Society, Copyright Massachusetts Medical Society.

Oversulfated chondroitin sulfate is a contaminant in heparin associated with adverse clinical events

Marco Guerrini^{1,7}, Daniela Beccati^{2,7}, Zachary Shriver^{2,3,7}, Annamaria Naggi¹, Karthik Viswanathan³, Antonella Bisio¹, Ishan Capila², Jonathan C Lansing², Sara Guglieri¹, Blair Fraser⁴, Ali Al-Hakim⁴, Nur Sibel Gunay², Zhenqing Zhang⁵, Luke Robinson³, Lucinda Buhse⁴, Moheb Nasr⁴, Janet Woodcock⁴, Robert Langer^{3,6}, Ganesh Venkataraman^{2,3}, Robert J Linhardt⁵, Benito Casu¹, Giangiacomo Torri¹ & Ram Sasisekharan³

Recently, certain lots of heparin have been associated with an acute, rapid onset of serious side effects indicative of an allergic-type reaction. To identify potential causes for this sudden rise in side effects, we examined lots of heparin that correlated with adverse events using orthogonal high-resolution analytical techniques. Through detailed structural analysis, the contaminant was found to contain a disaccharide repeat unit of glucuronic acid linked $\beta 1 \rightarrow 3$ to a β -*N*-acetylgalactosamine. The disaccharide unit has an unusual sulfation pattern and is sulfated at the 2-*O* and 3-*O* positions of the glucuronic acid as well as at the 4-*O* and 6-*O* positions of the galactosamine. Given the nature of this contaminant, traditional screening tests cannot differentiate between affected and unaffected lots. Our analysis suggests effective screening methods that can be used to determine whether or not heparin lots contain the contaminant reported here.

Heparin, a complex glycosaminoglycan polysaccharide, is widely used as an anticoagulant in a number of settings, including kidney dialysis and acute coronary syndromes^{1–3}. The most serious adverse event associated with heparin, aside from a potential bleeding risk, is thrombocytopenia. Recently there has been a marked increase in serious adverse events associated with heparin therapy, with hundreds of individuals affected^{4–7}. Although heparin therapy is generally well tolerated, recently patients presented—within several minutes after intravenous infusion of unfractionated heparin—with angioedema, hypotension, swelling of the larynx and related symptoms, which in some cases ended in death. Because heparin is a drug commonly used in the clinic, occurrence of these adverse events resulted in a crisis in the United States. Germany and other nations in the European Union have observed similar phenomena, turning this health problem into an international issue^{4,5}. The rapid onset of these symptoms suggests an anaphylactic response, but the exact etiology is currently unknown. Given the clinical history of heparin, this spike in adverse events suggests the potential contamination of heparin. However, standard testing of heparin lots for typical biological contaminants, including protein, lipids and DNA (which, if present, may elicit such side effects), indicated that there is no difference in these regards between lots that elicit adverse events and those that do not⁴. Despite extensive analysis, no obvious differences were found with respect to other potential contaminants, including lead, dioxins and other molecular

entities⁸. Definitive identification of how these heparin lots differ from the clinically approved heparin thus becomes imperative⁹.

To understand the structure or structures of the contaminant(s) present within specific lots of heparin, we sought to identify these contaminants. This exercise required the use of multiple orthogonal techniques, including multidimensional NMR, to overcome the challenges inherent in the analysis of complex polysaccharides, including heparin, which in and of itself comprises a complex mixture of glycosaminoglycan chains. In doing so, we were able to determine definitively the structure of the contaminant, isolate it and confirm its structural identity by comparison to a chemically synthesized standard.

RESULTS

NMR shows unusual *N*-acetyl signals not seen in heparin

For this study, we examined lots that were associated with adverse clinical reactions (designated S1–S6) as well as four control lots of heparin not associated with adverse events (designated C1–C4). Initial analysis of S1–S6 by one-dimensional NMR indicated that all of these samples produced an unusual series of *N*-acetyl signals (Fig. 1a, Supplementary Figs. 1 and 2 online). For example, particularly evident in the proton spectrum of S1 is the signal at 2.16 p.p.m. corresponding to an *N*-acetyl group different from that of heparin (2.04 p.p.m.). This *N*-acetyl signal is also distinct from that of

¹Istituto di Ricerche Chimiche e Biochimiche “G. Ronzoni,” Città Studi, via Giuseppe, Colombo 81, 20133 Milan, Italy. ²Momenta Pharmaceuticals, Inc., 675 West Kendall Street, Cambridge, Massachusetts 02142, USA. ³Department of Biological Engineering, Harvard-MIT Division of Health Sciences & Technology, Koch Institute for Integrative Cancer Research, Massachusetts Institute of Technology, 77 Massachusetts Ave., Cambridge, Massachusetts 02139, USA. ⁴Center for Drug Evaluation and Research, US Food and Drug Administration, 10903 New Hampshire Ave., Silver Spring, Maryland 20993-0002, USA. ⁵Center for Biotechnology and Interdisciplinary Studies, Rensselaer Polytechnic Institute, Troy, New York 12180, USA. ⁶Department of Chemical Engineering, Massachusetts Institute of Technology, 77 Massachusetts Ave., Cambridge, Massachusetts 02139, USA. ⁷These authors contributed equally to this work. Correspondence should be addressed to R. S. (rams@mit.edu).

Received 21 March; accepted 18 April; published online 23 April 2008; doi:10.1038/nbt1407

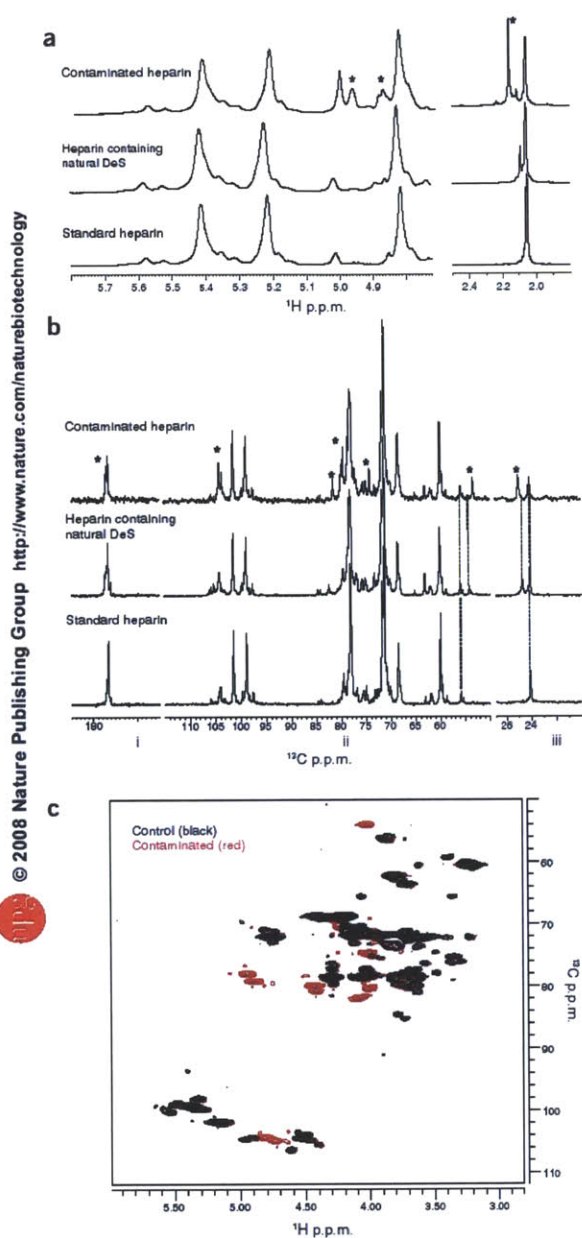


Figure 1 NMR analysis of contaminated heparin. (a) Comparison of anomeric and acetyl regions of the proton spectra of standard heparin, heparin containing natural dermatan sulfate (DeS) and contaminated heparin. (b) Comparison of carbonyl (i), sugar (ii) and *N*-acetyl regions (iii) of the carbon spectra of standard heparin, heparin containing natural dermatan sulfate, and contaminated heparin. Signals due to the contaminant are highlighted by asterisks. (c) HSQC spectrum of the contaminated sample S1 overlaid on control sample C1.

dermatan sulfate, a known impurity in heparin samples (2.08 p.p.m.)¹⁰. To complement and extend the proton analysis, carbon (100 MHz) NMR spectroscopy was performed. Comparison of the carbon spectra of S1 and C1 indicates the presence of several additional signals not normally associated with heparin structural signatures (Fig. 1b). The acetyl signal at 25.6 p.p.m. together with the signal at 53.5 p.p.m. are indicative of the presence of an *O*-substituted *N*-acetylgalactosamine residue of unknown structure, but again distinct from the *N*-acetylgalactosamine contained within dermatan sulfate, with corresponding signals at 24.8 p.p.m. and 54.1 p.p.m., respectively. Other signals are visible in the ring and anomeric regions of the carbohydrate moiety. The latter signals (103–105 p.p.m.) agree with a beta configuration of glycosidic linkages for the contaminant.

To further identify the number and type of any major contaminants, we collected multidimensional heteronuclear single quantum coherence (HSQC) spectra on S1 and C1 to separate the observed signals in two dimensions—the carbon and proton signals. Ten major signals observed in sample S1 were not seen in C1. These same signals were observed in samples S2–S6 but not in samples C2–C4 (Supplementary Figs. 3 and 4 online). In addition, these results and those from other two-dimensional experiments, including total correlation spectroscopy (TOCSY), correlation spectroscopy (COSY) and rotating-frame nuclear Overhauser effect spectroscopy (ROSEY), were also consistent with the basic findings outlined above, namely that the principal contaminant consists of a polymeric repeat of *N*-acetylgalactosamine linked to glucuronic acid exclusively through beta linkages.

Identification of an impurity and a contaminant in heparin

Much of the analysis outlined above focused on sample S1, as it possessed signals in the *N*-acetyl region at 2.04 p.p.m. (arising from heparin) and at 2.16 (arising from the unknown contaminant). In addition to this unusual signal at ~2.16 p.p.m., some samples (S2–S6 and C2–C4) possessed an additional *N*-acetyl peak (Supplementary Fig. 5b online), which had a chemical shift of 2.08 p.p.m., indicating the presence of another species that is distinct from the contaminant. Given the observed chemical shifts, this species is most likely dermatan sulfate, a known natural impurity of heparin^{10,11}. To confirm the identity of this species, we performed a two-dimensional (2D) ^1H - ^{13}C HSQC experiment on C2 (Supplementary Fig. 5d) and compared the results to those obtained on C1, a sample that did not show this additional signal. The chemical shifts observed in C2 but not in C1 are similar to those reported in the literature¹⁰, and this observation suggests that the additional peaks in the HSQC of C2 can be assigned to dermatan sulfate. This assignment was confirmed by comparison to ^1H and HSQC data obtained on a standard of dermatan sulfate (Supplementary Fig. 5a,c). Through an analysis similar to that completed on sample C2, we confirmed the presence of dermatan sulfate in those samples presenting a proton NMR signal at 2.08 p.p.m. Therefore, samples S2–S6, but not sample S1, contained both dermatan sulfate (an impurity typically found in heparin) and the unusual contaminant.

Finally, to confirm the findings from the NMR analysis of the samples, we conducted enzymatic digestion of S1–S6 and C1–C4 with either a combination of heparinases or heparinases plus $\Delta 4,5$ glycuronidase and 2-*O* sulfatase followed by separation and analysis by high-performance liquid chromatography (HPLC). Digestion with the heparinases reduces heparin to its component di-, tri- and tetrasaccharides and imparts a $\Delta 4,5$ bond that can be monitored at 232 nm; completed in conjunction with treatment with glycuronidase and sulfatase, this digest permits the identification of minor heparin

species, including those disaccharides containing a modified galacturonic acid^{12,13}. Thus, concomitant use of a matrix of enzymes, especially in conjunction with liquid chromatography–tandem mass spectrometry analysis, allows for the complete separation, identification and quantification of heparin components in the mixture¹⁴. We find that the total areas under the curve, calculated by integration of all heparin di-, tri- and tetrasaccharides observed in the HPLC and summation of the resulting areas, of digested S1–S6 are substantially less than those of the control samples, indicating that the major contaminant is not substantially digested by the heparinases (Table 1). Furthermore, the difference in the area under the curve is correlated with the amount of contaminant present within the sample; samples with larger amounts of contaminant (as measured by proton NMR) had a lower area under the curve as measured by HPLC. Finally, the relative quantities of the individual heparin components are similar between the controls and suspect samples, with only minor differences.

To identify the unknown compound present in the contaminated heparin samples, we attempted to isolate the contaminant using a variety of methods. Given the overall properties of the contaminant, elucidated through NMR, capillary electrophoresis and HPLC analysis, we reasoned that this material could be differentially precipitated upon addition of an organic solvent. Partial purification of the contaminant was indeed achieved through the addition of increasing amounts of ethanol to an aqueous solution of S1. Similarly, because the contaminant contains *N*-acetylhexosamine (and not *N*-sulfohexosamine), it was also purified by degradation of heparin by nitrous acid and isolation of the remaining components.

Isolation of the contaminant allowed definitive identification

After isolation, the proton spectrum of the isolated contaminant reveals a residual heparin content of ~10–30% (depending on the isolation method used) as determined by one-dimensional NMR (data not shown). We carried out additional, detailed NMR studies on this isolated sample. To facilitate an understanding of the experiments and their interpretation, the disaccharide repeat structures of heparin, chondroitin sulfate, dermatan sulfate and heparin, together with positional nomenclature, are presented in Figure 2. In the carbon spectrum, at neutral pH values, one apparent signal arises at 177.6 p.p.m, characteristic of carbonyl groups. Acidification of a solution of the product from pH 6.5 to pH 4 (Fig. 3a) reveals two distinct carbonyl signals consistent with the carbonyl group of an *N*-acetyl function and the protonated form of carboxylic acid, respectively.

Table 1 Total area under the curve for heparinase digests of S1–S6 and C1–C4

Sample	Total area
C1	2.52×10^7
C2	2.70×10^7
C3	2.33×10^7
C4	2.39×10^7
S1	1.74×10^7
S2	9.50×10^6
S3	1.94×10^7
S4	1.59×10^7
S5	1.91×10^7
S6	1.96×10^7

Similar shifts were not observed for any other signals except C-5 of uronic acid (U5), for which this carbon's chemical shift is sensitive to the ionization state of the carboxylic acid as well as the identity of the counterion present (Fig. 3b). To further characterize the isolated sample, we used homonuclear (COSY and TOCSY, data not shown) and heteronuclear (HSQC, HSQC-TOCSY and heteronuclear multiple bond correlation (HMBC)) 2D-NMR spectroscopy (Fig. 3c,d). These analyses indicated the presence of two types of residues. Chemical shift patterns were in agreement with one type of monosaccharide being a 4,6-*O*-sulfo-*N*-acetylgalactosamine and the other being a 2,3-*O*-sulfolglucuronic acid. In addition to confirming the assignments of the sugar moieties, the HMBC spectrum demonstrated the correlation across the glycosidic linkages, indicating the presence of a β -1,4 linkage between galactosamine and glucuronic acid and a β -1,3 linkage between the glucuronic acid and the galactosamine. Confirmatory evidence of this structure was provided by the long-range correlations of H1 of the galactosamine and H5 of glucuronic acid with two different carbonyl groups (177.5 and 177.8 p.p.m) owing to the *N*-acetyl of galactosamine and the carboxylic group of glucuronic acid.

Synthetic oversulfated chondroitin matches contaminant

The identification of the contaminant as an oversulfated chondroitin sulfate containing a tetrasulfated disaccharide unit consisting of glucuronic acid linked to *N*-acetylgalactosamine was surprising, as this is an unusual structure. To ensure the accuracy of this assignment, we prepared a standard by oversulfation of chondroitin sulfate using well-established chemistry. We analyzed this

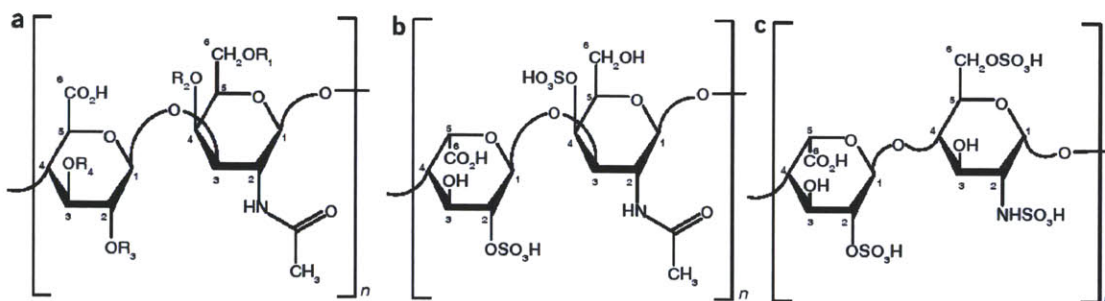


Figure 2 Chemical structures of major repeat units. (a–c) Schematic of major disaccharide repeat units of chondroitin sulfate (a), dermatan sulfate (b) and heparin (c). The carbon atoms are numbered for each monosaccharide of the disaccharide repeat. For chondroitin sulfate, R1–R4 can be either sulfated or unsubstituted.

ARTICLES

standard by 2D NMR and carefully compared the HSQC spectra to both the literature¹⁵ and the HSQC spectrum obtained for the isolated contaminant. Comparison of the HSQC spectrum of the synthesized standard with that of the isolated contaminant (Fig. 4) confirmed that the major contaminant consists of per-*O*-sulfated chondroitin sulfate, with all of the hydroxyl groups of both the uronic acid and galactosamine residues bearing sulfate substituents.

Furthermore, the proton chemical shifts of the contaminant (Table 2) are in agreement with those assigned to fully sulfated chondroitin (degree of sulfation = 4)¹⁵. In addition, mass spectrometry completed after enzymatic digestion of a chemically desulfated¹⁶ version of the contaminant was consistent with the proposed structure (Fig. 5). The final derived structure of the major contaminant present in heparin is shown in Figure 2a, with R₁, R₂, R₃ and R₄ all sulfated.

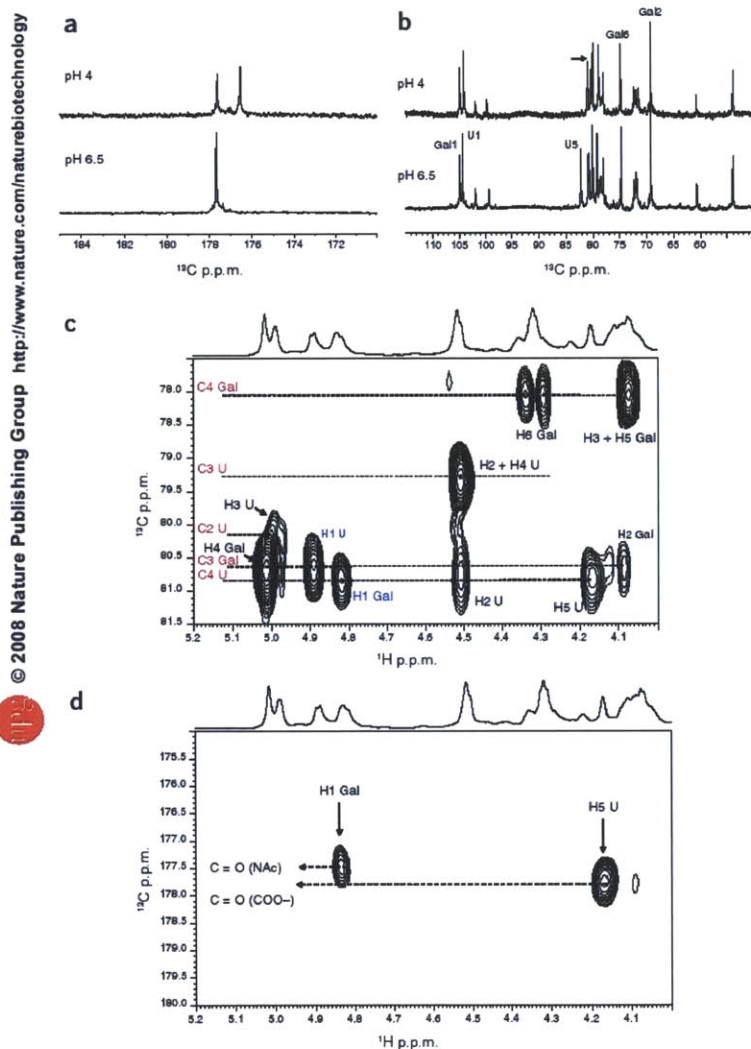


Figure 3 Detailed NMR structural analysis of the contaminant. (a) Carbonyl region of the carbon spectrum of the contaminant measured at pH 6.5 and 4. (b) Sugar region of the carbon spectrum of the contaminant measured at pH 6.5 and 4. The arrow points to the shift in the C5 of glucuronic acid (U5) upon pH adjustment. (c) A portion of the 600-MHz HMBC spectrum of the contaminant. Intramolecular two- and three-bond proton-carbon correlations are shown in black; interglycosidic proton-carbon correlations are indicated in blue; carbon connectivity shown in red. (d) Portion of the 600-MHz HMBC spectrum of the contaminant. Long-range correlation between the H1 of *N*-acetylgalactosamine (Gal) with the C=O of the acetyl group and H5 of glucuronic acid (U) with the carboxylic group are shown.

DISCUSSION

Several factors required the use of multiple approaches to ensure an accurate structural determination of the oversulfated chondroitin contaminant. First, heparin is a chemically complex polydisperse mixture of saccharides, making careful interpretation of results necessary to avoid misinterpretation. Detailed analysis is especially important when addressing the multiple isomeric possibilities within the chains of a complex mixture, and it necessitates the use of orthogonal techniques, including an enzyme matrix and multidimensional NMR. Second, oversulfated materials, such as the chondroitins, are resistant to enzymatic digestion techniques and copurify with heparin, rendering their isolation challenging^{15,17}.

These complexities manifest themselves in a number of ways: for example, structurally distinct species may have overlapping signals and properties, thereby 'masking' them within a single analysis. A nonintegrated approach can therefore potentially lead to false conclusions, especially when attempting to differentiate between heparin, dermatan sulfate and oversulfated chondroitin sulfate in any given sample. In this study, we present a set of experimental techniques that discriminate between dermatan sulfate (a known impurity of heparin) and oversulfated chondroitin sulfate.

The structure of the contaminant, which contains a tetrasulfated disaccharide repeat, is highly unusual. First, the presence of a 3-*O*-sulfated glucuronic acid is rare, only observed in specific contexts within certain organisms¹⁸. In addition, a tetrasulfated disaccharide repeat unit has not been isolated to date from animal tissues. Consequently, it is highly unlikely that the contaminant reported here is produced naturally. Finally, chemically synthesized tetrasulfated disaccharide repeat units of chondroitin sulfate are known to exhibit a high degree of anti-factor IIa activity¹⁵, which could explain how contaminated heparin would pass an activity screen, such as a whole-blood coagulation test. Further investigation is warranted to understand how this contaminant was introduced.

With respect to the potential biological ramifications of this finding, it is possible that the presence of an oversulfated chondroitin sulfate within heparin preparations

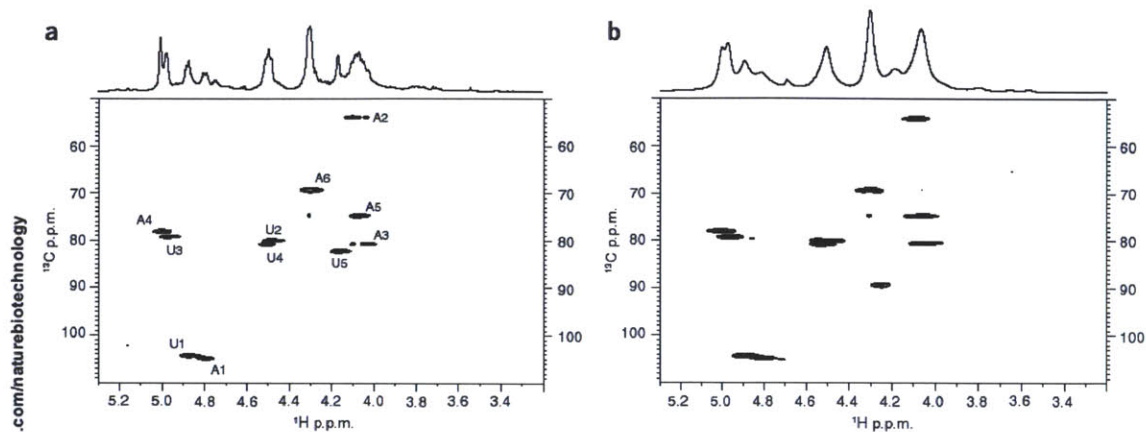


Figure 4 Structural assignment of the contaminant by NMR using isolated and synthetic materials. (a) ^1H -NMR and HSQC spectra of the isolated contaminant. Signals for 4,6-*O*-sulfo-*N*-acetylgalactosamine (A) and of 2,3-*O*-sulfo-glucuronic acid (U) are labeled. (b) ^1H -NMR and HSQC spectra of the chemically synthesized oversulfated chondroitin.

can provoke increased side effects. In the case of chondroitins, chondroitin sulfates A and C are expressed by human cells and are generally nonimmunogenic. Highly sulfated polysaccharides, however, such as oversulfated chondroitins, have been shown to be potent mediators of the immune response^{19–22}. Indeed, complications associated with administration of highly sulfated chondroitins have been observed in humans. Arteparon, an oversulfated chondroitin that is structurally identical to the contaminant²³ (Fig. 2), injected intramuscularly in humans²⁴, was marketed for the treatment of degenerative joint disease in Europe. It was demonstrated that this product can induce an allergic-type response²⁵. Because of patient deaths, most likely due to thromboembolic complications, the product was rapidly withdrawn from the European market²⁶. The structural determination of the

contaminant described here enables further investigation into the biological roles and potential pharmacological effects of oversulfated chondroitins, present within heparin preparations, in the recently reported adverse events.

Taken together, our orthogonal analytical experiments provide strong support for the structure we have assigned to the contaminant. This study also provides a set of screening methods that could be used to monitor the heparin supply and ensure the absence of oversulfated chondroitin sulfate contamination. For example, using the structural information presented here, it is now possible to (i) design reference standards that ensure accuracy, quantification and specificity of analysis for a given analytical method and (ii) devise an experimental protocol to clearly define the nature and extent, if any,

Table 2 Chemical shifts observed for contaminant by two independent laboratories and comparison to literature data on oversulfated chondroitin sulfate

Monosaccharide	Lab 1 ^a		Lab 2 ^b		¹ H (literature) ^c , fully <i>O</i> -sulfonated CS
	¹ H (observed)	¹³ C (observed)	¹ H (observed)	¹³ C (observed)	
4,6- <i>O</i> -Sulfo- <i>N</i> -acetylgalactosamine					
H1/C1	4.77	105.0	4.79	104.8	4.86
H2/C2	4.06	54.0	4.10	54.0	4.10
H3/C3	4.05	80.7	4.03	80.7	4.10
H4/C4	4.98	78.0	5.00	78.0	5.02
H5/C5	4.05	74.8	4.07	74.7	4.06
H6,6'/C6	4.28	69.3	4.30	69.2	4.29
<i>N</i> -Acetyl	2.12 ^d	25.6	2.16 ^e	25.6	2.16
2,3- <i>O</i> -Sulfo-glucuronic acid					
H1/C1	4.87	104.5	4.87	104.3	4.97
H2/C2	4.47	80.0	4.49	80.0	4.53
H3/C3	4.95	79.3	4.98	79.2	4.94
H4/C4	4.46	80.9	4.51	80.8	4.55
H5/C5	4.12	82.0	4.17	82.2	4.20

^aChemical shifts are measured at 303 K and referenced to external 2,2-dimethyl-2-silapentane-5-sulfonate sodium salt (DSS). ^bChemical shifts are measured at 308 K and referenced to external sodium trimethylsilylpropionate (TSP) (which resonates 0.12 p.p.m. upfield of DSS²⁹). ^cMeasured at 303 K and referenced to TSP (ref. 15). CS, chondroitin sulfate. ^dAdditional minor signals observed at 2.20 and 2.07 p.p.m. ^eAdditional minor signals observed at 2.23 and 2.11 p.p.m.

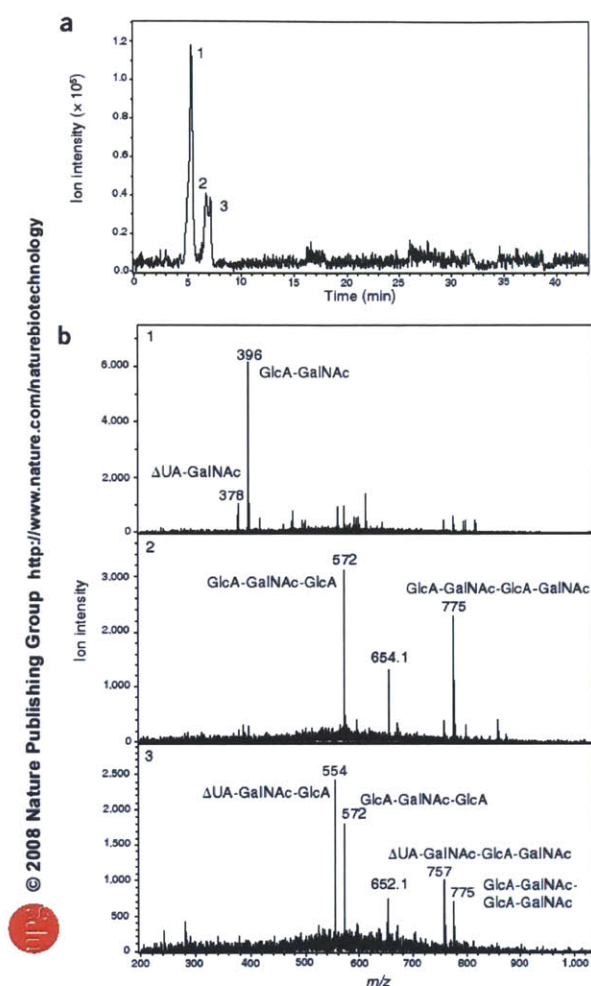


Figure 5 Liquid chromatography–mass spectrometry (LC-MS) analysis of the contaminant. (a) Total ion chromatogram with detection of three peaks (1–3). (b) Specific ions and associated structures observed in each peak. After desulfation, the contaminant was digested with chondroitinase ABC and analyzed by LC-MS. The presence of saturated and unsaturated oligosaccharides indicates that the backbone of the impurity could be digested with chondroitinase ABC and suggests that the backbone is a glucuronic acid–*N*-acetylgalactosamine repeat (UA-GalNAc).

of contamination in a given lot of heparin. Finally, the ramifications of these findings extend beyond scientific considerations and include clinical and health policy issues.

METHODS

Materials. Chondroitin sulfate type A from whale cartilage, pyridine–sulfur trioxide complex, tributylamine, dry *N,N*-dimethylformamide, pyridine, methanol, dimethylsulfoxide, NaNO₂, NaBH₄, 2,2-dimethyl-2-silapentane-5-sulfonate sodium salt and sodium trimethylsilylpropionate were purchased from Sigma-Aldrich. Tetrabutylammonium chloride was purchased from Fluka. 99.9% D₂O

and 99.96% D₂O were obtained from Cambridge Isotope Laboratories. The following ten lots of unfractionated heparin were tested: S1, S2, S3, S4, S5, S6, C1, C2, C3 and C4. All heparin samples were supplied by the FDA.

NMR analysis. Samples for ¹H-NMR or 2D NMR analysis were dissolved in 0.7 ml of D₂O (99.9%) and were either freeze-dried repeatedly to remove exchangeable protons or directly measured without any treatment to preserve potential volatile components. The thoroughly dried samples were dissolved in 0.7 ml of D₂O (99.96%). Before spectrum acquisition, samples were sonicated for 60 s to remove air bubbles. Spectra were obtained at 303 K or 308 K using a 600-MHz Varian VNMR5 spectrometer or a 600-MHz Bruker Avance 600 spectrometer, both equipped with a 5-mm triple-resonance inverse cryoprobe. Monodimensional ¹H spectra were obtained with presaturation of residual HOD, for 32–128 scans. DQF-COSY and 2D-TOCSY spectra were acquired using 32 scans per series of 2,048 × 512 data points. HSQC and HSQC-TOCSY spectra were recorded with carbon decoupling during acquisition with 320 increments for 12–64 scans. The polarization transfer delay was set with a ¹J_{C-H} coupling value of 155 Hz. HMBC spectrum was recorded with 320 increments of 64 scans for each, without carbon decoupling and with twofold low-pass J-filter to suppress one-bond correlations²⁷. The delay for evolution of long-range couplings was set with a *J*_{LC} of 8 Hz. Samples for ¹³C-NMR analysis were dissolved in D₂O (99.9%) at 40 mg/ml and analysis was performed at 303 K with a 400-MHz Bruker spectrometer equipped with a multinuclear probe.

Composition analysis by ion-pair RPHPLC. Samples were constituted in capillary electrophoresis–grade water and digested under two different conditions. The first digest used an enzyme cocktail of heparinases I (500 mIU), II (400 mIU) and III (500 mIU) at 30 °C, for 16 h. A portion of this digest was further treated with 2-O-sulfatase (1,000 mIU) and Δ4,5-glycuronidase (2,000 mIU) for 6 h at 30 °C to obtain the second digest. Each digest was passed through a Ni²⁺ spin column (Qiagen) and analyzed by ion-pair RPHPLC similar to as previously described¹⁴. Elution was monitored by UV detection at 232 nm.

Isolation of major contaminant. Absolute ethanol was added to sample S1 (300 mg), dissolved in 1.5 ml of water until a white precipitate appeared (ethanol 23%, vol/vol). Precipitated material was separated by centrifugation for 5 min at 5,000 r.p.m. (~4,000g) on a Labofuge 200 (Heraeus). In addition to the above, sample S1 was treated with nitrous acid²⁸. A solution of the sample (500 mg) was dissolved in 20 ml of H₂O and cooled at 4 °C. Also at 4 °C, 140 mg of NaNO₂ dissolved in 1 ml of water was added to the sample and the pH was adjusted to 1.7 with 0.1 M HCl. The solution was stirred at 4 °C for 20 min; an additional 100 mg NaNO₂ was added and the solution stirred for another 20 min. The solution pH was then adjusted to 7 with NaOH and the resulting reaction was brought to room temperature. Solid NaBH₄ (200 mg) was added in several portions with stirring. After 2 h, the pH was adjusted to 4 with 0.1 M HCl and the solution was neutralized with 0.1 M NaOH. The product, obtained by precipitation with four volumes of methanol, was recovered by centrifugation, dissolved in water and freeze-dried.

Chemical sulfonation of chondroitin sulfate. Fully sulfated chondroitin sulfate was prepared from chondroitin sulfate, as described¹³. Chondroitin sulfate (108 mg) was converted into its tributylamine salt and dissolved in dry *N,N*-dimethylformamide (1 ml). After addition of 159 mg of pyridine–sulfur trioxide complex, the solution was heated for 1 h at 40 °C. The reaction was interrupted by addition of 2 ml of water and the product was precipitated at 4 °C by addition of 35 ml of an ethanol solution saturated with sodium acetate. The product recovered by centrifugation was dissolved in water, dialyzed at room temperature and recovered by freeze-drying.

Note: Supplementary information is available on the Nature Biotechnology website.

ACKNOWLEDGMENTS

The authors would like to thank Sucharita Roy for work on the chemical synthesis of oversulfated chondroitin sulfate standards, Scott Bailey for assistance in the analysis of selected samples by one- and two-dimensional NMR and Laura Citterio for work in various separation and analytical steps. We also thank James Anderson, Josh Sorafine and Andre Jones for design of composition experiments and HPLC analysis of the heparinase-digested samples. Finally, we thank Ada Ziolkowski for help with manuscript preparation. This work was supported in

part by US National Institute of General Medical Sciences grants GM57073 (R.S.) and GM38060 (R.J.L.).

COMPETING INTERESTS STATEMENT

The authors declare competing financial interests: details accompany the full-text HTML version of the paper at <http://www.nature.com/naturebiotechnology/>.

Published online at <http://www.nature.com/naturebiotechnology/>

Reprints and permissions information is available online at <http://npg.nature.com/reprintsandpermissions/>

1. Capilla, I. & Linhardt, R.J. Heparin-protein interactions. *Angew. Chem. Int. Edn. Engl.* **41**, 391–412 (2002).
2. Lepor, N.E. Anticoagulation for acute coronary syndromes: from heparin to direct thrombin inhibitors. *Rev. Cardiovasc. Med.* **8** (suppl. 3), S9–S17 (2007).
3. Fischer, K.G. Essentials of anticoagulation in hemodialysis. *Hemodial. Int.* **11**, 178–189 (2007).
4. Contaminant detected in heparin material of specified origin in the USA and in Germany; serious adverse events reported; recall measures initiated. World Health Organization Alert No. 118 (7 March 2008). <http://www.who.int/medicines/publications/drugalerts/Alert_118_Heparin.pdf>
5. Notice of Recall from Rotexmedica to Bfarm (German Regulatory Authorities). Rotexmedica/Bfarm Notice (7 March 2008). <<http://www.akd.ae.de/20/40/Archiv/2008/20080310.pdf>>
6. Acute allergic-type reactions among patients undergoing hemodialysis—multiple states, 2007–2008. *Morbidity Mortal. Wkly Rept.* **57** (1 February 2008).
7. 2008 Heparin Recall Information. Baxter Investigation Updates (5.14.19 March 2008). <<http://www.baxter.com/products/biopharmaceuticals/heparin.html>>
8. Baxter provides update on investigation. Baxter Investigation Update (14 March 2008). <http://www.baxter.com/products/biopharmaceuticals/downloads/heparin_03-14-08.pdf>
9. Communication. Information on heparin sodium injection. US Food and Drug Administration. <<http://www.fda.gov/cder/drug/infopage/heparin/default.htm>>
10. Holme, K.R. & Perlin, A.S. Nuclear magnetic resonance spectra of heparin in admixture with dermatan sulfate and other glycosaminoglycans. 2-D spectra of the chondroitin sulfates. *Carbohydr. Res.* **186**, 301–312 (1989).
11. Guerrini, M., Bisio, A. & Torri, G. Combined quantitative ^1H and ^{13}C nuclear magnetic resonance spectroscopy for characterization of heparin preparations. *Semin. Thromb. Hemost.* **27**, 473–482 (2001).
12. Myette, J.R. *et al.* Molecular cloning of the heparin/heparan sulfate delta 4,5 unsaturated glycuronidase from *Flavobacterium heparinum*, its recombinant expression in *Escherichia coli*, and biochemical determination of its unique substrate specificity. *Biochemistry* **41**, 7424–7434 (2002).
13. Myette, J.R. *et al.* The heparin/heparan sulfate 2-O-sulfatase from *Flavobacterium heparinum*. Molecular cloning, recombinant expression, and biochemical characterization. *J. Biol. Chem.* **278**, 12157–12166 (2003).
14. Kuberan, B. *et al.* Analysis of heparan sulfate oligosaccharides with ion pair-reverse phase capillary high performance liquid chromatography-microelectrospray ionization time-of-flight mass spectrometry. *J. Am. Chem. Soc.* **124**, 8707–8718 (2002).
15. Maruyama, T., Tolda, T., Imanari, T., Yu, G. & Linhardt, R.J. Conformational changes and anticoagulant activity of chondroitin sulfate following its O-sulfonation. *Carbohydr. Res.* **306**, 35–43 (1998).
16. Solvolytic desulfation of glycosaminoglycan sulfates with dimethyl sulfoxide containing water or methanol. Nagasawa, K., Inoue, Y. & Kamata, T. *Carbohydr. Res.* **58**, 47–55 (1977).
17. Linhardt, R.J. Analysis of glycosaminoglycans with polysaccharide lyases. in *Current Protocols in Molecular Biology* (eds. Ausubel, F.A. *et al.*) **17**, 13B.1–17B.13.16 (Wiley, New York, 1994).
18. Kinoshita, A. *et al.* Novel tetrasaccharides isolated from squid cartilage chondroitin sulfate E contain unusual sulfated disaccharide units GlcA(3-O-sulfate) β 1-3GalNAc(6-O-sulfate) or GlcA(3-O-sulfate) β 1-3GalNAc. *J. Biol. Chem.* **272**, 19656–19665 (1997).
19. Hadding, U. *et al.* Ability of the T cell-replacing polyanion dextran sulfate to trigger the alternate pathway of complement activation. *Eur. J. Immunol.* **3**, 527–529 (1973).
20. Kang, O.H. *et al.* Suppressive effect of non-anaphylactogenic anti-IgE antibody on the development of dextran sulfate sodium-induced colitis. *Int. J. Mol. Med.* **18**, 893–899 (2006).
21. Siebeck, M. *et al.* Dextran sulfate activates contact system and mediates arterial hypotension via B2 kinin receptors. *J. Appl. Physiol.* **77**, 2675–2680 (1994).
22. Hojima, Y., Cochrane, C.G., Wiggins, H.C., Austen, K.F. & Steven, R.L. In vitro activation of the contact (Hageman factor) system of plasma by heparin and chondroitin sulfate E. *Blood* **63**, 1453–1459 (1984).
23. Naggi, A. *et al.* Sulfamino-galactosaminoglycans, a new class of semi-synthetic polysaccharides. In *Biomedical and Biotechnological Advances in Industrial Polysaccharides* (eds. Crescenzi, V., Dea, I.C.M. & Paoletti, S.) 101–108 (Gordon & Breach Science, New York, 1989).
24. Slegmenth, W. & Radl, I. Comparison of glycosaminoglycan polysulfate (Arteparon) and physiological saline solution in arthrosis of the large joints. Results of a multicenter double-blind study. *Z. Rheumatol.* **42**, 223–228 (1983).
25. Greinacher, A., Michels, I., Schäfer, M., Kiefel, V. & Mueller-Eckhardt, C. Heparin-associated thrombocytopenia in a patient treated with polysulphated chondroitin sulphate: evidence for immunological crossreactivity between heparin and polysulphated glycosaminoglycan. *Br. J. Haematol.* **81**, 252–254 (1992).
26. Weimann, G. *et al.* Glucosamine sulfate does not crossreact with the antibodies of patients with heparin-induced thrombocytopenia. *Eur. J. Haematol.* **66**, 195–199 (2001).
27. Cicero, O., Barbato, G. & Bazzo, R. Sensitivity enhancement of a two-dimensional experiment for the measurement of heteronuclear long-range coupling constants, by a new scheme of coherence selection by gradients. *J. Magn. Reson.* **148**, 209–213 (2001).
28. Cifonelli, J.C. Reaction of heparitin sulfate with nitrous acid. *Carbohydr. Res.* **8**, 233–242 (1968).
29. Wishart, D.S. *et al.* ^1H , ^{13}C and ^{15}N chemical shift referencing in biomolecular NMR. *J. Biomol. NMR* **6**, 135–140 (1995).



ORIGINAL ARTICLE

Contaminated Heparin Associated with Adverse Clinical Events and Activation of the Contact System

Takashi Kei Kishimoto, Ph.D., Karthik Viswanathan, Ph.D., Tanmoy Ganguly, Ph.D., Subbiah Elankumaran, Ph.D., Sean Smith, B.S., Kevin Pelzer, Ph.D., Jonathan C. Lansing, Ph.D., Nammalwar Sriranganathan, Ph.D., Ganlin Zhao, M.D., Zoya Galcheva-Gargova, Ph.D., Ali Al-Hakim, Ph.D., Gregory Scott Bailey, B.S., Blair Fraser, Ph.D., Sucharita Roy, Ph.D., Thomas Rogers-Cotrone, M.S., Lucinda Buhse, Ph.D., Mark Whary, Ph.D., James Fox, Ph.D., Moheb Nasr, Ph.D., Gerald J. Dal Pan, M.D., Zachary Shriver, Ph.D., Robert S. Langer, Sc.D., Ganesh Venkataraman, Ph.D., K. Frank Austen, M.D., Janet Woodcock, M.D., and Ram Sasisekharan, Ph.D.

ABSTRACT

BACKGROUND

There is an urgent need to determine whether oversulfated chondroitin sulfate (OSCS), a compound contaminating heparin supplies worldwide, is the cause of the severe anaphylactoid reactions that have occurred after intravenous heparin administration in the United States and Germany.

METHODS

Heparin procured from the Food and Drug Administration, consisting of suspect lots of heparin associated with the clinical events as well as control lots of heparin, were screened in a blinded fashion both for the presence of OSCS and for any biologic activity that could potentially link the contaminant to the observed clinical adverse events. *In vitro* assays for the activation of the contact system and the complement cascade were performed. In addition, the ability of OSCS to recapitulate key clinical manifestations *in vivo* was tested in swine.

RESULTS

The OSCS found in contaminated lots of unfractionated heparin, as well as a synthetically generated OSCS reference standard, directly activated the kinin-kallikrein pathway in human plasma, which can lead to the generation of bradykinin, a potent vasoactive mediator. In addition, OSCS induced generation of C3a and C5a, potent anaphylatoxins derived from complement proteins. Activation of these two pathways was unexpectedly linked and dependent on fluid-phase activation of factor XII. Screening of plasma samples from various species indicated that swine and humans are sensitive to the effects of OSCS in a similar manner. OSCS-containing heparin and synthetically derived OSCS induced hypotension associated with kallikrein activation when administered by intravenous infusion in swine.

CONCLUSIONS

Our results provide a scientific rationale for a potential biologic link between the presence of OSCS in suspect lots of heparin and the observed clinical adverse events. An assay to assess the amidolytic activity of kallikrein can supplement analytic tests to protect the heparin supply chain by screening for OSCS and other highly sulfated polysaccharide contaminants of heparin that can activate the contact system.

From Momenta Pharmaceuticals (T.K.K., T.G., S.S., J.C.L., G.Z., Z.G.-G., G.S.B., S.R., Z.S., G.V.), the Harvard-Massachusetts Institute of Technology Division of Health Sciences and Technology, Koch Institute for Integrative Cancer Research (K.V., Z.S., R.S.L., G.V., R.S.), and the Massachusetts Institute of Technology (M.W., J.F.) — all in Cambridge, MA; Virginia-Maryland College of Veterinary Medicine, Virginia Polytechnic Institute and State University, Blacksburg (S.E., K.P., N.S., T.R.-C.); the Center for Drug Evaluation and Research, Food and Drug Administration, Silver Spring, MD (A.A.-H., B.F., L.B., M.N., G.J.D.P., J.W.); and Brigham and Women's Hospital and Harvard Medical School, Boston (K.F.A.). Address reprint requests to Dr. Sasisekharan at the Department of Biological Engineering, Harvard-MIT Division of Health Sciences and Technology, Koch Institute for Integrative Cancer Research, Massachusetts Institute of Technology, 77 Massachusetts Ave., 16-561, Cambridge, MA 02139, or at rams@mit.edu.

This article (10.1056/NEJMoa0803200) was published at www.nejm.org on April 23, 2008.

N Engl J Med 2008;358:2457-67.

Copyright © 2008 Massachusetts Medical Society.

IN JANUARY 2008, HEALTH AUTHORITIES IN the United States began receiving reports of clusters of acute hypersensitivity reactions in patients undergoing dialysis that had been occurring since November 2007. Symptoms included hypotension, facial swelling, tachycardia, urticaria, and nausea. Although initial investigations focused on dialysis equipment, an investigation by the Centers for Disease Control and Prevention identified the receipt of heparin sodium for injection (1000 U per milliliter, in 10-ml and 30-ml multidose vials), manufactured by Baxter Healthcare, as a common feature of the cases.¹ This finding led Baxter Healthcare to recall, on January 17, 2008, nine lots of heparin sodium for injection. As of April 13, 2008, there were 81 reports of death that involved at least one sign or symptom of an allergic reaction or hypotension in patients receiving heparin since January 1, 2007. However, the fact that allergic symptoms or hypotension were reported does not mean that these were the cause of death in all cases.

After this initial recall, there were continuing reports of allergic-type reactions, including some deaths, after injection of bolus heparin not only in patients undergoing dialysis but also in patients in other clinical settings, such as those undergoing cardiac procedures. On February 28, 2008, Baxter Healthcare recalled all remaining lots and doses of its multidose and single-dose vials of heparin sodium for injection and HEP-LOCK heparin flush products. Since that recall, monitoring by the Food and Drug Administration (FDA) has indicated that, in March 2008, the number of deaths reported in association with heparin usage had returned to baseline levels.²

However, on March 6, a heparin recall was announced in Germany because of a cluster of reactions in patients undergoing dialysis that were linked to a different manufacturer's heparin. On the same day, the FDA posted descriptions of analytic methods on its Web site and recommended that all manufacturers and regulatory authorities screen for a contaminant in heparin.³ This screening revealed widespread contamination of the heparin supply in at least 12 countries.

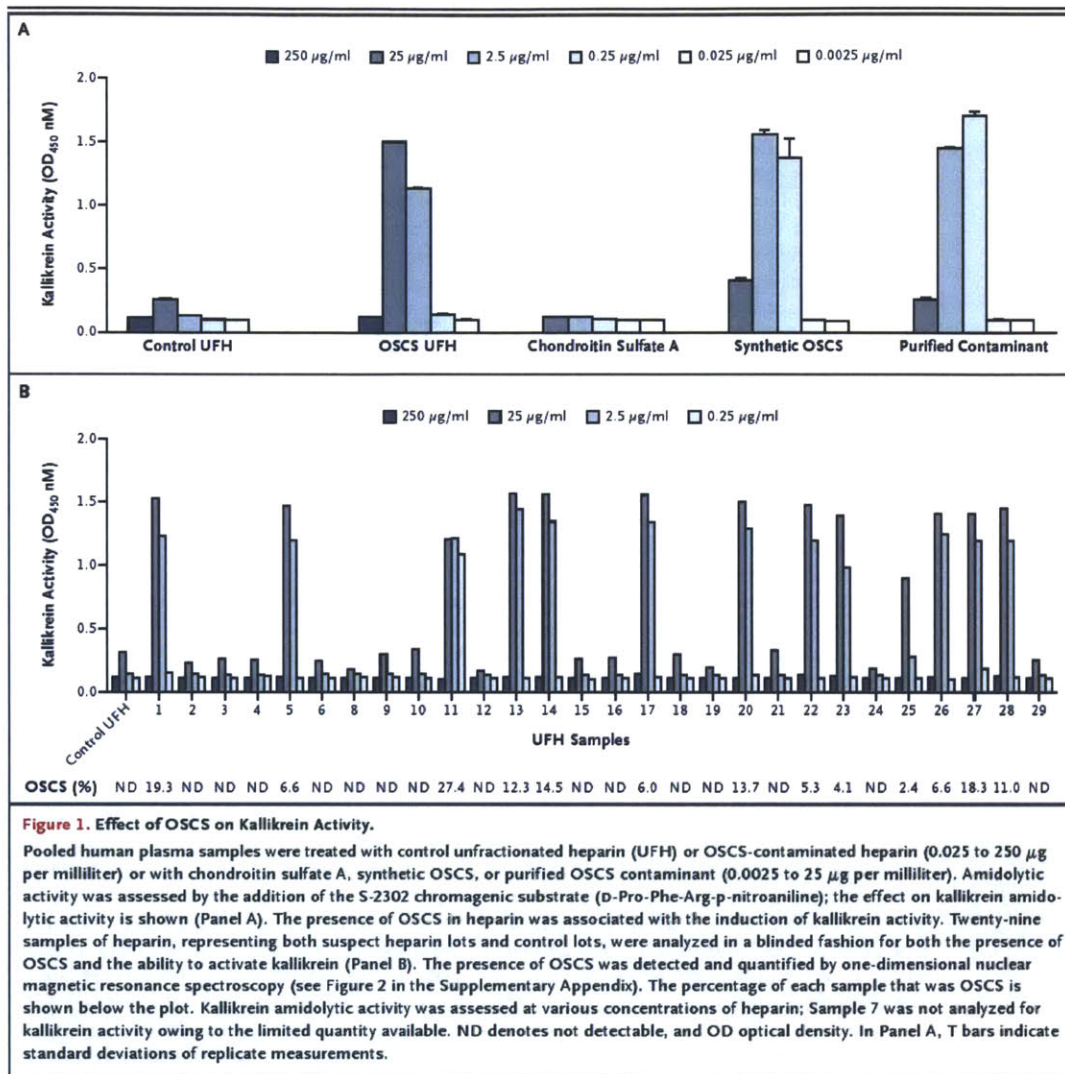
The contaminant was recently identified as an unusual oversulfated form of chondroitin sulfate (OSCS) representing up to approximately 30% wt/wt in suspect lots of heparin; no other contaminants were observed.⁴ In addition, dermatan sulfate, a known impurity of heparin, was found in selected samples. Both heparin and chondroi-

tin sulfate are members of the glycosaminoglycan family of complex polysaccharides; heparin contains a disaccharide repeat unit of glucuronic-iduronic acid linked to glucosamine, and chondroitin sulfate contains a disaccharide repeat unit of glucuronic acid linked to galactosamine. Analysis of the contaminant unexpectedly revealed an unusual type of sulfation not found in any natural sources of chondroitin sulfate and indicated that OSCS, containing four sulfates per disaccharide unit, is structurally similar to heparin (see the Supplementary Appendix, available with the full text of this article at www.nejm.org).

However, the biologic link between the presence of the OSCS in heparin and the adverse clinical events remained to be established. Highly charged polyanionic polymers are known to modulate various enzymatic cascades in plasma, affecting coagulation, fibrinolysis, inflammation, and vasculature function.^{5,6} Bradykinin, a potent vasoactive peptide mediator, is generated through the activation of the contact system of coagulation, which is initiated upon contact of factor XII with a negatively charged surface in the presence of prekallikrein and high-molecular-weight kininogen. Highly sulfated polysaccharides have been shown to serve as a negatively charged surface that can initiate fluid-phase activation of the contact system.^{5,7} However, initial attempts to recapitulate the adverse responses in experimental models were unsuccessful.⁸ Without a definitive link between the contaminant and the clinical reactions, concerns remain that the screening tests currently in place may not be adequate to prevent further cases. We therefore set out to identify a biologic basis for a link between OSCS and allergic-type reactions.

CASE REPORT

A representative case involved a 63-year-old woman with a complex medical history, including end-stage renal disease treated with the use of hemodialysis for 7 years, who received heparin intravenously during hemodialysis (5000-U loading dose and 500 U per hour during the procedure) three times weekly. In mid-January 2008, the development of "low blood pressure" was reported, along with nausea and dyspnea, during dialysis. She was treated with normal saline and oxygen (2 liters per minute), and the rates of ultrafiltration and blood flow were slowed. She recovered after 30 minutes, and dialysis was contin-



ued. Two days later, she again received intravenous heparin (5000-U loading dose and 500 U per hour) from the same lots of heparin from the same manufacturer (Baxter Healthcare). Immediately after dialysis was initiated, the patient had an anaphylactoid reaction, with a sudden drop in blood pressure (to 65/34 mm Hg), dyspnea, nausea, vomiting, and constitutional symptoms. She was treated with a bolus of normal saline and oxygen (2 liters per minute). Hemodialysis was continued for another hour. The patient continued to feel ill, was admitted to the hospital, and was discharged

2 days later, after recovery. Further dialysis was performed with the use of heparin from another manufacturer.

METHODS

TEST SAMPLES

Twenty-nine clinical lots of heparin, including 13 associated with clinical adverse events, were procured from the FDA and coded as unknown samples 1 through 29. A laboratory lot of heparin was included as a control. For all analytic and biologic

tests, samples were dosed on a weight basis; specific activity of heparin is typically approximately 180 U per milligram. OSCS was purified to homogeneity from a lot of heparin that was known to be contaminated, as previously described.⁴ Briefly, OSCS-contaminated heparin was subjected to anion-exchange chromatography followed by alcohol precipitation to isolate the contaminant.⁴ The identity of the contaminant was confirmed by means of multiple orthogonal techniques, including multidimensional nuclear magnetic resonance (NMR), enzymatic digestion followed by high-performance liquid chromatography, and liquid chromatography–mass spectrometry.⁴ After identification of the contaminant as OSCS, a synthetic standard was generated through chemical sulfonation of chondroitin sulfate A and was exhaustively characterized to ensure authenticity, as previously described.⁴ The synthetic OSCS was used in spiking experiments to qualify the analytic procedures (especially one-dimensional proton NMR, described below) to determine limits of detection and to establish accurate quantification.⁴ The limit of detection for this assay was determined to be 0.3% on a weight basis for both dermatan sulfate and OSCS.

ANALYTIC METHODS

To ensure accurate identification and quantification of any contaminants and impurities, the 29 coded test samples were subjected to orthogonal analytic techniques. Proton NMR, anion-exchange chromatography, and capillary electrophoresis were used to screen the samples for the presence of OSCS, dermatan sulfate, and other nonheparin components. The levels of OSCS and dermatan sulfate were quantified with the use of a 600-MHz NMR instrument to ensure peak resolution. The details of quantification, as well as a representative spectrum, are given in Figure 1 and Table 1 in the Supplementary Appendix. For samples with unusual patterns, the identity of contaminants or impurities, including OSCS, was confirmed by means of detailed characterization, including the use of multidimensional NMR.⁴

AMIDOLYTIC ACTIVITY OF KALLIKREIN

Pooled human plasma or factor XII–depleted plasma (American Diagnostica) was treated with various concentrations of coded test samples of heparin, chondroitin sulfate A, or synthetic OSCS for 5 minutes at 37°C. The amidolytic activity of kal-

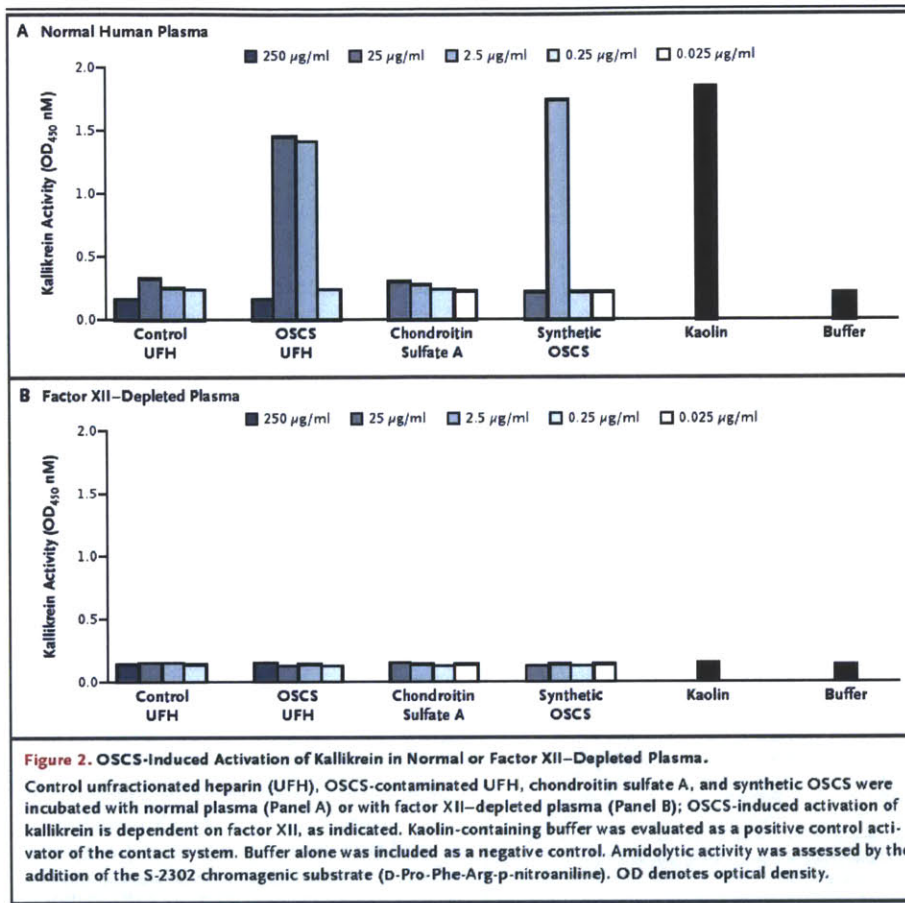
likrein (with a small contribution of factor XII)⁹ was assessed by adding the S-2302 chromagenic substrate (D-Pro-Phe-Arg-p-nitroaniline [pNA]) for 30 minutes at 37°C, followed by spectrophotometric measurement of the absorbance at 450 nM.

GENERATION OF C3a AND C5a

Pooled human EDTA plasma or factor XII–depleted plasma (American Diagnostica) was treated with various concentrations of OSCS-contaminated heparin, control heparin, chondroitin sulfate A, or synthetic OSCS for 30 minutes at 37°C. C3a and C5a activation products of the complement cascade were assayed by means of a sandwich enzyme-linked immunosorbent assay (ELISA), as specified in the manufacturer's instructions (Becton Dickinson and Integrated Biotech Laboratories for C3a and C5a, respectively).

IN VIVO STUDIES

The swine were handled and treated in compliance with the Public Health Service Policy on Humane Care and Use of Laboratory Animals and the federal Animal Welfare Act. The experimental procedures were performed according to the Institutional Animal Care and Use Committee–approved protocol of the Virginia Polytechnic Institute and State University, Blacksburg. Domestic Yorkshire crossbred swine were of either sex (Virginia Polytechnic Institute and State University) and ranged in weight from 10 to 25 kg. They were initially anesthetized with an intravenous injection of 6 mg of tiletamine hydrochloride per kilogram of body weight and 2.2 mg of xylazine per kilogram, and then a single-lumen silicone catheter was implanted in the left jugular vein of each animal. Adequate anesthesia was maintained throughout the procedure with the administration of supplemental tiletamine. After a 5-minute stabilization period, each pig received an intravenous bolus infusion of 5 mg of the test substance per kilogram (three to six pigs per test substance). All the pigs were continuously monitored for vital signs with the use of an oscillometric blood pressure monitor (Cardell 9401/9403, CAS Medical Systems) for systolic, diastolic, and mean arterial blood pressures, pulse oximetry for pulse and respiratory rates, and a rectal probe for body temperature. At the end of the 60-minute observation period, the animals were euthanized with the use of an intravenous infusion of Fatal Plus

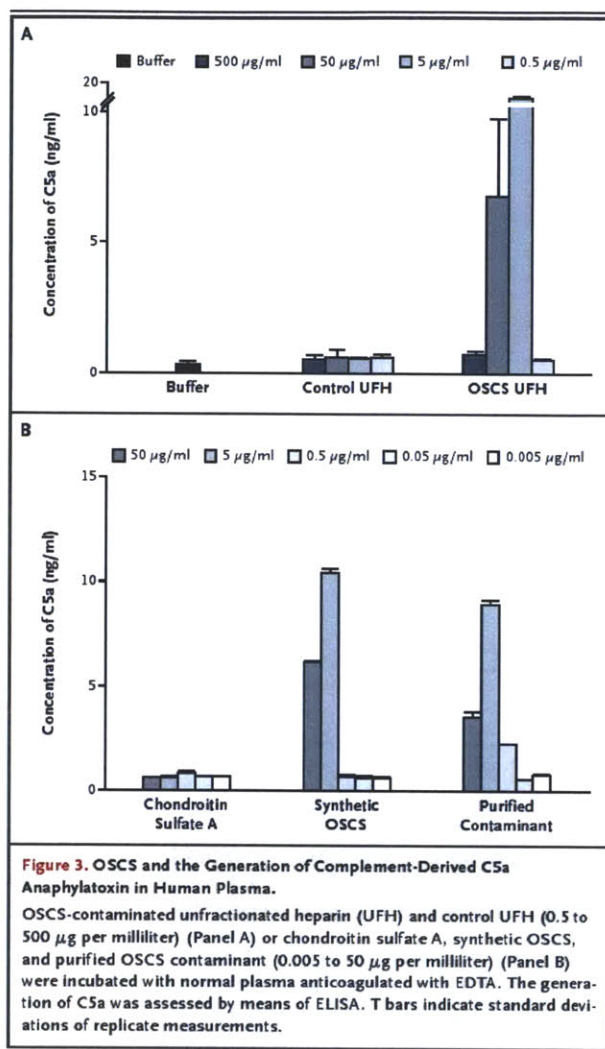


(Vortech Pharmaceuticals) at a dose of 0.22 ml per kilogram. Blood samples were collected at baseline and at 5, 10, 20, 40, and 60 minutes and were kept in 5 mM EDTA. Plasma was isolated after centrifugation at 4°C and flash-frozen on dry ice. Frozen samples were thawed at 4°C and assayed for amidolytic activity of kallikrein with the addition of the S-2302 chromagenic substrate (D-Pro-Phe-Arg-pNA), as described above.

RESULTS

Given the association of activation of the contact system with negatively charged polysaccharides, we sought to elucidate whether an *in vitro* biologic response could be correlated with the identity or levels of contaminant within heparin lots. To this end,

we examined the ability of a sample of OSCS-contaminated heparin, containing 19.3% wt/wt OSCS (Table 1 in the Supplementary Appendix), to activate kallikrein amidolytic activity in human plasma (Fig. 1A). The contaminated heparin showed a bell-shaped dose response, which is typical of glycosaminoglycan-mediated responses.^{5,10} At 2.5 and 25 µg per milliliter, robust activation of kallikrein was found with the contaminated heparin sample but not with a control sample of uncontaminated heparin. These concentrations are in the range of a clinically efficacious concentration of heparin of approximately 1 to 5 µg per milliliter, based on a specific activity of about 180 U per milligram. High concentrations of the OSCS-contaminated heparin (250 µg per milliliter) induced little or no amidolytic activity of kallikrein, suggesting that at this



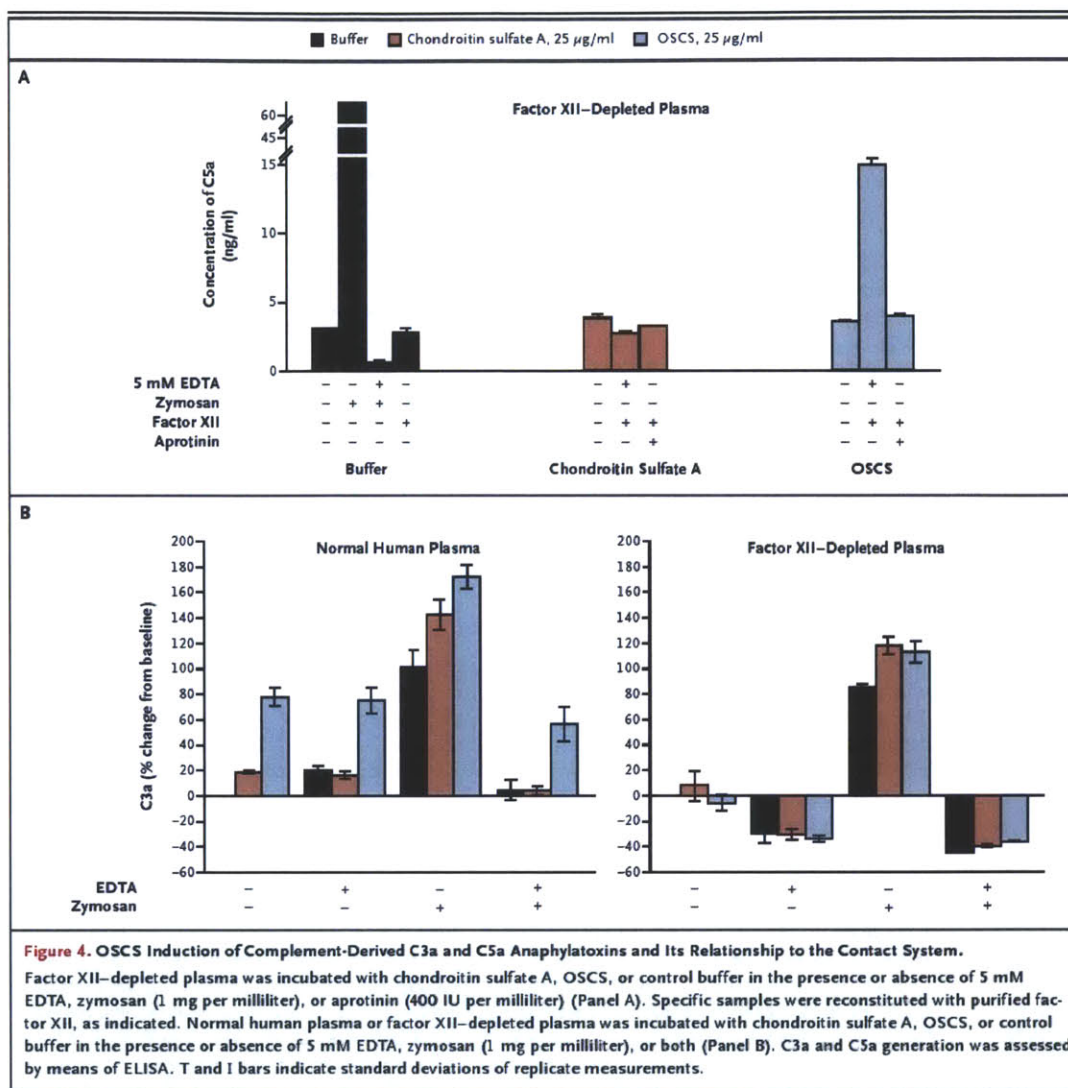
concentration, heparin may inhibit or cause depletion of factor XII, as previously described.^{7,11,12} This high concentration of heparin also prevented activation of the contact system in response to kalin, a potent activator (data not shown).

To further verify that the contaminant was responsible for the activation of the contact system, OSCS was purified to homogeneity by means of anion-exchange chromatography followed by alcohol precipitation. In addition, an OSCS standard was created through chemical sulfonation of chondroitin sulfate A, to form OSCS.⁴ The purified contaminant and the OSCS standard were

identical, as judged by several orthogonal analytic techniques, including two-dimensional NMR.⁴ Both the purified contaminant and the synthetic OSCS showed robust activation of kallikrein activity at 0.25 µg and 2.5 µg per milliliter (Fig. 1A). The peak activity of the purified contaminant and the synthetic OSCS standard were observed at a level that was approximately an order of magnitude lower than that found for the contaminated heparin sample. This is consistent with the observation that the OSCS constituted approximately 20% of the contaminated sample. Chondroitin sulfate A showed no induction of amidolytic activity.

These results are in good agreement with the observations of Hojima et al.,⁵ who demonstrated that oversulfated chondroitin, but not chondroitin A, B, or C, can activate the kinin pathway. Heparin also activated the contact system in an in vitro model system involving purified protein components^{5,13} but did not in plasma,¹³ suggesting that negative-regulatory factors present in plasma may prevent activation of the contact system by heparin. One such mechanism is the fact that heparin is known to enhance antithrombin III-mediated inhibition of factor XII. Our results indicate that OSCS, in contrast to heparin but similar to dextran sulfate,¹³ can activate the contact system in plasma.

The 29 heparin samples procured from the FDA, consisting of both suspect heparin lots associated with clinical events as well as control heparin lots, were screened in a blinded fashion for both the presence of OSCS and the ability to activate the contact system (Fig. 1B). There was complete correspondence between the presence of detectable amounts of OSCS by one-dimensional proton NMR and the ability of a sample to induce robust amidolytic activity of kallikrein (Fig. 1B). The biologic activity was generally characterized as an all-or-none response, with all 13 samples containing detectable levels of OSCS having a positive response at 25 µg or 2.5 µg per milliliter. Sample 11, which contained the highest level of contaminant (27.4%), also showed activity at 0.25 µg per milliliter, whereas Sample 25, which contained the lowest level of contaminant (2.4%), showed only modest activity at 2.5 µg per milliliter. In contrast, there was no association between the level of inducible kallikrein activity and the level of dermatan sulfate (Fig. 2 in the Supplementary Appendix), an impurity found in many heparin preparations.



Direct activation of the contact system by the contaminated heparin and the synthetic OSCS standard was confirmed through the use of human plasma depleted of factor XII, the upstream activator of prekallikrein¹⁴ (Fig. 2). The contaminated heparin, the synthetically derived OSCS, and the positive control (the kaolin-containing reagent) all failed to induce the amidolytic activity of kallikrein in factor XII-deficient plasma.

We next examined the ability of contaminated heparin to generate C3a and C5a, potent anaphylato-

toxins derived from complement proteins. Exposure of human plasma to the contaminated heparin, but not to control heparin, induced the production of C5a (Fig. 3). OSCS-induced C5a generation showed a bell-shaped dose response similar to that found for kallikrein activation. Peak C5a activity was observed at 50 μg and 5 μg per milliliter of heparin containing 19.3% OSCS. At 500 μg per milliliter, significant generation of C5a was not observed. Similar results were obtained with the purified OSCS isolated from contami-

nated heparin and the synthetic OSCS standard, but not with chondroitin sulfate A.

Surprisingly, the generation of C5a by OSCS-contaminated heparin was more robust in the presence of EDTA, a Ca²⁺- and Mg²⁺-chelating agent, than in the absence of EDTA. The classic and alternative pathways of complement activation are known to be dependent upon Ca²⁺ and Mg²⁺, respectively. As expected, EDTA blocked C3a and C5a generation in response to zymosan, a potent activator of the alternative pathway (Fig. 4). These results suggested the possibility that OSCS induces the generation of C3a and C5a in a manner that bypasses the C3 and C5 convertases. To determine whether the generation of C3a and C5a was linked to the activation of the contact system, we next examined C3a and C5a generation in factor XII–depleted plasma (Fig. 4). As expected, zymosan induced the generation of C3a and C5a in factor XII–depleted plasma, and this activity was inhibited by EDTA. In contrast, neither C3a nor C5a was generated in factor XII–depleted plasma activated with OSCS, suggesting that OSCS bypasses the normal pathways for complement activation in a manner that is dependent on contact activation through factor XII. The generation of C5a could be restored by reconstituting the factor XII–depleted plasma with purified factor XII (Fig. 4A). This finding is further supported by the observation that C5a generation induced by OSCS-contaminated heparin can be inhibited by aprotinin, a protease inhibitor of kallikrein but not of factor XIIa (Fig. 4A). Crosstalk between the contact system and the complement cascade has been suggested previously.^{15–18} For example, factor XII has been shown to activate the classical pathway by activating C1.¹⁵ It has also been proposed to substitute for factor D in activating the alternative pathway.¹⁶ However, in these cases, activation of the complement cascade still occurs through divalent cation–dependent pathways. Kallikrein has been shown to act directly on C5 to generate C5a-like biologic activity.¹⁷ Both kallikrein and factor XII can activate the plasminogen pathway leading to the activation of plasmin, which has also been implicated in complement activation.¹⁸ Preliminary data suggest that OSCS is unable to induce C5a generation in plasminogen-depleted plasma (data not shown).

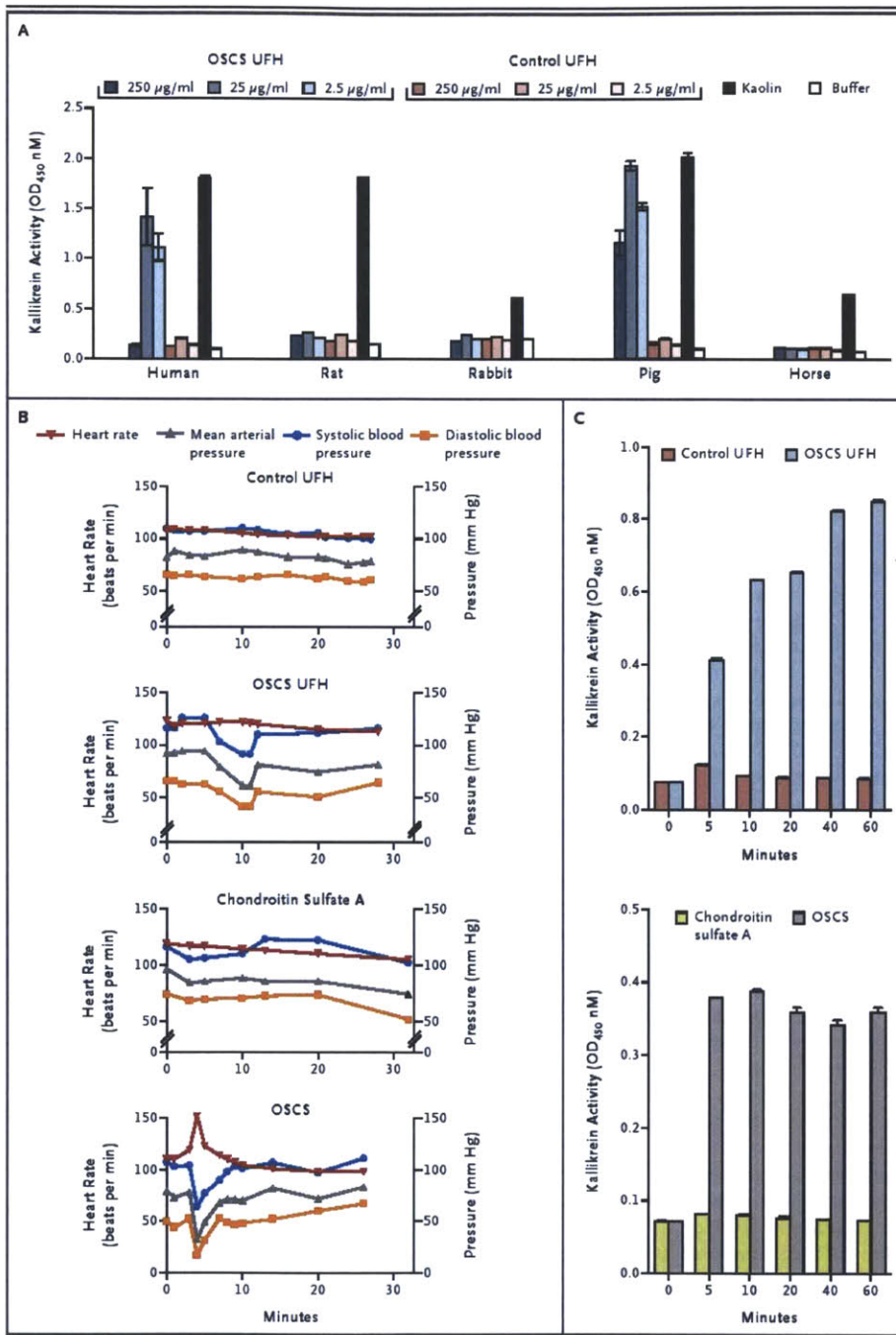
To identify an appropriate species for in vivo testing of OSCS, a panel of plasma samples were

Figure 5 (facing page). In Vitro and In Vivo Activity of OSCS.

Human, rat, rabbit, pig, and horse plasma samples were incubated with various concentrations of OSCS-contaminated unfractionated heparin (UFH) or control UFH (Panel A). Kaolin-containing buffer was tested as a positive control. Buffer alone was included as a negative control. Kallikrein amidolytic activity was assessed by the addition of the S-2302 chromogenic substrate; OSCS induces hypotension and kallikrein activity in swine (Panels B and C). Anesthetized Yorkshire cross-bred pigs (three to six pigs per group) were treated with a single intravenous bolus (5 mg per kilogram) of control UFH, OSCS-contaminated UFH, chondroitin sulfate A, or synthetic OSCS. Representative data for the heart rate, the mean arterial pressure, the systolic blood pressure, and the diastolic blood pressure are shown (Panel B). EDTA-anticoagulated plasma was collected at baseline and at 5, 10, 20, 40, and 60 minutes after infusion of test samples (Panel C). OD denotes optical density. In Panels A and C, T and I bars indicate standard deviations of replicate measurements.

screened for amidolytic activity in response to OSCS-contaminated heparin (Fig. 5A). Only swine plasma supported robust amidolytic activity of kallikrein in response to kaolin and OSCS-contaminated heparin but not control heparin. In contrast, rabbit, horse, and rat plasma showed moderate-to-robust amidolytic activity in response to kaolin but not to OSCS-contaminated heparin. These findings are consistent with a report that initial attempts to provoke an allergic response with suspect lots of heparin were unsuccessful.⁸ Similarly, we found that rabbits treated with 5 mg of intravenous OSCS-contaminated heparin per kilogram showed no change in temperature, blood pressure, or heart rate as compared with rabbits treated with control heparin (data not shown). Wiggins¹⁹ demonstrated previously that dextran sulfate can induce hypotension in rabbits, but only at a high dose (20 mg per kilogram) and in a manner independent of complement or kinin activation. In contrast, moderate doses of dextran sulfate (5 mg per kilogram) induced a robust hypotensive response in pigs that was dependent on activation of the contact system.²⁰

To test the in vivo activity of OSCS, pigs were treated with a single intravenous dose (5 mg per kilogram) of OSCS-contaminated heparin, control heparin, synthetic OSCS, or chondroitin sulfate A and were monitored for 60 minutes. Animals treated with control heparin and those treated with OSCS-contaminated heparin showed similar anti-Xa activity during the entire 60-minute



observation period (activity at 5 minutes, approximately 3 to 4 IU per milliliter) (Fig. 4 in the Supplementary Appendix). Animals treated with chondroitin sulfate A or synthetic OSCS showed no anti-Xa activity. These results suggest that any anticoagulant activity of OSCS is mediated through a non-antithrombin III-dependent mechanism. Two of six animals treated with OSCS-contaminated heparin had at least a 30% drop in blood pressure over the first 30 minutes after infusion (Fig. 5B). One animal remained in a hypotensive state for more than 15 minutes. In contrast, none of the four animals treated with control heparin showed any substantive changes in blood pressure. The adverse events were more severe in pigs treated with the synthetic OSCS, a result consistent with the greater exposure to OSCS in animals treated with pure OSCS as compared with contaminated heparin containing approximately 20 to 30% OSCS. All three pigs treated with synthetic OSCS showed a profound drop in blood pressure (maximal decrease, 45 to 59%) and a concurrent increase in heart rate within minutes after infusion. One animal had difficulty breathing and became cyanotic after a precipitous drop in blood pressure. The heart rate of a second animal increased from 114 beats per minute to 196 beats per minute within 4 minutes after the infusion of OSCS. The third pig showed a transient but pronounced spike in heart rate with a corresponding drop in blood pressure (Fig. 5B). In contrast, none of the three pigs treated with chondroitin sulfate A showed any significant changes in blood pressure or heart rate within the first 30 minutes after drug infusion. Thus, intravenous infusion of OSCS is capable of recapitulating the hallmark cardiovascular features of the reaction in swine. The changes in physiological parameters were mirrored by rapid induction of the amidolytic activity of kallikrein (Fig. 5C). Kallikrein activity remained high throughout the observation period, even after the vital functions returned to normal, suggesting depletion of high-molecular-weight kininogen and inactivation of bradykinin by kininases *in vivo*, as previously shown with dextran sulfate.²⁰ Induction of kallikrein activity was evident in all animals that received OSCS-contaminated heparin, even when no substantive changes in blood pressure were observed. These findings suggest that activation of kallikrein does not always manifest as clinical symptoms, perhaps because of individual varia-

tion in control mechanisms that regulate bradykinin activity. Nonetheless, these results also suggest that swine may be an appropriate species in which to assess the potential consequences of OSCS contaminant in cardiovascular and dialysis models as well as in heparin-coated devices.

DISCUSSION

The recent reports of allergic-type serious adverse events in patients receiving heparin and the subsequent detection of widespread contamination have caused intense international concern about the safety of this essential drug. Urgent problems included an immediate and unknown risk to patients' lives, a threat to the supply of a widely used, essential drug, and the need for international cooperation in managing the integrity of a global supply chain. This crisis necessitated an urgent need to both understand the basis for these clinical events and to prevent future occurrences. The development of an analytic assay for OSCS, coupled with the rapid response of manufacturers and regulatory authorities around the world, has undoubtedly limited the harm. However, in the absence of a biologic link between the OSCS contaminant and the adverse events, the adequacy of screening heparin lots to prevent a recurrence is a concern.

Determining whether a link exists between the presence of OSCS and a biologic response required the convergence of two distinct analyses. First, there was a requirement to develop analytic techniques of sufficient sensitivity and specificity to ensure accurate identification and quantification of contaminants or impurities that are present within heparin. Second, there was a requirement to develop a sensitive, clinically appropriate biologic test to determine at what levels, if any, the OSCS would have relevant biologic activity.

With regard to the analytic techniques, a tiered approach was required to ensure effective translation to biologic characteristics. Screening methods were developed to rapidly identify whether heparin lots were contaminated or impure. Then, methods were further developed to enable quantification of the contamination levels. Finally, more sophisticated techniques, such as multidimensional NMR, enabled complete characterization of the contaminant or impurity. This tiered approach was necessitated by the fact that heparin is a polydisperse mixture of glycosaminoglycan chains; orthogonal

techniques were therefore required to ensure capture of the other nonheparin components.

Here, we demonstrate that the OSCS present in suspect heparin lots, as well as a synthetic OSCS standard, can directly activate the contact system and induce the generation of C3a and C5a anaphylatoxins *in vitro*. Moreover, OSCS activates kallikrein *in vivo* and can induce a profound hypotensive response in pigs, thus providing a potential biologic link between the contaminant and the anaphylactoid reactions seen in affected patients. The finding that hypotension did not develop in all animals treated with OSCS-contaminated heparin, even at a relatively high dose, is consistent with the observation that the majority of patients who received contaminated heparin did not experience an adverse event. However, it is important to note that all animals treated with OSCS-contaminated heparin showed evidence of kallikrein activation *in vivo*, even in the absence of clinical signs. Patients undergoing dialysis who are also receiving heparin therapy are already at high risk for hypotension because of their exposure to the dialysis membrane, which can also activate the contact system, and their treatment with angiotensin-converting-enzyme inhibitors, which inhibit bradykinin degra-

tion. Exposure to OSCS-contaminated heparin may further increase the risk and could potentially trigger an adverse event. Finally, these findings also suggest that a simple *in vitro* bioassay could complement the previously described analytic tests⁴ to help protect the global supply chain of heparin, by allowing the screening of heparin lots for the presence not only of OSCS but also of other polysulfated contaminants that may have unintended pharmacologic consequences.

Supported by grants from the National Institute of General Medical Sciences and the National Heart and Lung Institute (GM57073 and HL080278-01, respectively, to Dr. Sasisekharan).

Drs. Kishimoto, Ganguly, Lansing, Zhao, Galcheva-Gargova, Roy, Shriver, and Venkataraman, Mr. Smith, and Mr. Baily report being employees of Momenta Pharmaceuticals and holding equity in the company, which has technology on the analysis and characterization of complex mixtures, including heparin. Drs. Sasisekharan and Langer report receiving consulting fees from Scientific Protein Labs and Momenta Pharmaceuticals and holding equity in Momenta Pharmaceuticals. Dr. Austen reports receiving consulting fees from Momenta Pharmaceuticals. No other potential conflict of interest relevant to this article was reported.

We thank Dr. Allen P. Kaplan for helpful discussions; Pete Jobst, Animal Resource Manager, and Andrea Aman, Animal Care Technician, at the Virginia-Maryland College of Veterinary Medicine for their excellent technical help during the *in vivo* experiments; and Ms. Alison Long, Mr. Chris Honan, Dr. Cedric Hubeau, Mr. Erick Moy, and the staff of the Massachusetts Institute of Technology Division of Comparative Medicine for help with the animal studies.

REFERENCES

1. Acute allergic-type reactions among patients undergoing hemodialysis — multiple states, 2007–2008. *MMWR Morb Mortal Wkly Rep* 2008;57:124-5.
2. Information on adverse event reports and heparin. Rockville, MD: Food and Drug Administration, 2008. (Accessed May 12, 2008, at http://www.fda.gov/cder/drug/infopage/heparin/adverse_events.htm.)
3. Information on heparin sodium injection. Rockville, MD: Food and Drug Administration, 2008. (Accessed May 12, 2008, at <http://www.fda.gov/cder/drug/infopage/heparin/default.htm#screening>.)
4. Guerrini M, Beccati D, Shriver Z, et al. Oversulfated chondroitin sulfate is a major contaminant in heparin associated with adverse clinical events. *Nat Biotechnol* (in press).
5. Hojima Y, Cochrane CG, Wiggins RC, Austen KF, Stevens RL. *In vitro* activation of the contact (Hageman factor) system of plasma by heparin and chondroitin sulfate E. *Blood* 1984;63:1453-9.
6. Henry SP, Ciclas PC, Leeds J, et al. Activation of the alternative pathway of complement by a phosphorothioate oligonucleotide: potential mechanism of action. *J Pharmacol Exp Ther* 1997;281:810-6.
7. Silverberg M, Diehl SV. The autoactivation of factor XII (Hageman factor) induced by low-Mr heparin and dextran sulfate: the effect of the Mr of the activating polyanion. *Biochem J* 1987;248:715-20.
8. Baxter provides update on the heparin investigation. Deerfield, IL: Baxter, March 19, 2008. (Accessed May 12, 2008, at http://www.baxter.com/products/biopharmaceuticals/downloads/heparin_03-19-08.pdf.)
9. Silverberg M, Dunn JT, Garen L, Kaplan AP. Autoactivation of human Hageman factor: demonstration utilizing a synthetic substrate. *J Biol Chem* 1980;255:7281-6.
10. Verhamme IM, Bock PE, Jackson CM. The preferred pathway of glycosaminoglycan-accelerated inactivation of thrombin by heparin cofactor II. *J Biol Chem* 2004;279:9785-95.
11. Stead N, Kaplan AP, Rosenberg RD. Inhibition of activated factor XII by antithrombin-heparin cofactor. *J Biol Chem* 1976;251:6481-8.
12. Olson ST, Sheffer R, Francis AM. High molecular weight kininogen potentiates the heparin-accelerated inhibition of plasma kallikrein by antithrombin: role for antithrombin in the regulation of kallikrein. *Biochemistry* 1993;32:12136-47.
13. Pixley RA, Cassello A, De La Cadena RA, Kaufman N, Colman RW. Effect of heparin on the activation of factor XII and the contact system in plasma. *Thromb Haemost* 1991;66:540-7.
14. Kaplan AP, Austen KF. A prealbumin activator of prekallikrein. II. Derivation of activators of prekallikrein from active Hageman factor by digestion with plasmin. *J Exp Med* 1971;133:696-712.
15. Ghebrehiwet B, Silverberg M, Kaplan AP. Activation of the classical pathway of complement by Hageman factor fragment. *J Exp Med* 1981;153:665-76.
16. DiScipio RG. The activation of the alternative pathway C3 convertase by human plasma kallikrein. *Immunology* 1982;45:587-95.
17. Wiggins RC, Ciclas PC, Henson PM. Chemotactic activity generated from the fifth component of complement by plasma kallikrein of the rabbit. *J Exp Med* 1981;153:1391-404.
18. Schaiff WT, Eisenberg PR. Direct induction of complement activation by pharmacologic activation of plasminogen. *Coron Artery Dis* 1997;8:9-18.
19. Wiggins RC. A different cleavage site for high molecular weight kininogen *in vivo* following intravenous injection of dextran sulfate in the rabbit. *Circ Res* 1986;58:595-604.
20. Siebeck M, Cheronis JC, Fink E, et al. Dextran sulfate activates contact system and mediates arterial hypotension via B2 kinin receptors. *J Appl Physiol* 1994;77:2675-80.

Copyright © 2008 Massachusetts Medical Society.

ORIGINAL ARTICLE

Outbreak of Adverse Reactions Associated with Contaminated Heparin

David B. Blossom, M.D., Alexander J. Kallen, M.D., M.P.H., Priti R. Patel, M.D., M.P.H., Alexis Elward, M.D., M.P.H., Luke Robinson, B.S., Ganpan Gao, Ph.D., Robert Langer, Sc.D., Kiran M. Perkins, M.D., Jennifer L. Jaeger, M.D., Katie M. Kurkjian, D.V.M., M.P.H., Marilyn Jones, R.N., M.P.H., Sarah F. Schillie, M.D., M.P.H., Nadine Shehab, Pharm.D., Daniel Ketterer, M.D., Ganesh Venkataraman, Ph.D., Takashi Kei Kishimoto, Ph.D., Zachary Shriver, Ph.D., Ann W. McMahon, M.D., K. Frank Austen, M.D., Steven Kozłowski, M.D., Arjun Srinivasan, M.D., George Turabelidze, M.D., Ph.D., Carolyn V. Gould, M.D., Matthew J. Arduino, Dr.P.H., and Ram Sasisekharan, Ph.D.

ABSTRACT

BACKGROUND

From the Epidemic Intelligence Service Program (D.B.B., A.J.K., J.L.J., K.M.K., S.F.S.), the Office of Workforce and Career Development (D.B.B., A.J.K., K.M.P., J.L.J., K.M.K., S.F.S., D.K.), and the Division of Healthcare Quality Promotion (D.B.B., A.J.K., P.R.P., S.F.S., N.S., A.S., C.V.G., M.J.A.), Centers for Disease Control and Prevention, Atlanta; St. Louis Children's Hospital (A.E.), BJC Healthcare (M.J.), and the Missouri Department of Health and Senior Services (G.T.) — all in St. Louis; the Departments of Biological Engineering (L.R., G.G., R.L., R.S.) and Chemical Engineering (R.L.), the Harvard-MIT Division of Health Sciences and Technology (R.L., R.S.), and the Koch Institute for Integrative Cancer Research (L.R., G.G., R.L., R.S.), Massachusetts Institute of Technology; and Momenta Pharmaceuticals (G.V., T.K.K., Z.S.) — both in Cambridge, MA; the Center for Drug Evaluation and Research, Food and Drug Administration, Silver Spring, MD (A.W.M., S.K.); and Brigham and Women's Hospital and Harvard Medical School, Boston (K.F.A.). Address reprint requests to Dr. Patel at the Centers for Disease Control and Prevention, 1600 Clifton Rd., MS-A31, Atlanta, GA 30333, or at ppatel@cdc.gov.

In January 2008, the Centers for Disease Control and Prevention began a nationwide investigation of severe adverse reactions that were first detected in a single hemodialysis facility. Preliminary findings suggested that heparin was a possible cause of the reactions.

METHODS

Information on clinical manifestations and on exposure was collected for patients who had signs and symptoms that were consistent with an allergic-type reaction after November 1, 2007. Twenty-one dialysis facilities that reported reactions and 23 facilities that reported no reactions were included in a case-control study to identify facility-level risk factors. Unopened heparin vials from facilities that reported reactions were tested for contaminants.

RESULTS

A total of 152 adverse reactions associated with heparin were identified in 113 patients from 13 states from November 19, 2007, through January 31, 2008. The use of heparin manufactured by Baxter Healthcare was the factor most strongly associated with reactions (present in 100.0% of case facilities vs. 4.3% of control facilities, $P < 0.001$). Vials of heparin manufactured by Baxter from facilities that reported reactions contained a contaminant identified as oversulfated chondroitin sulfate (OSCS). Adverse reactions to the OSCS-contaminated heparin were often characterized by hypotension, nausea, and shortness of breath occurring within 30 minutes after administration. Of 130 reactions for which information on the heparin lot was available, 128 (98.5%) occurred in a facility that had OSCS-contaminated heparin on the premises. Of 54 reactions for which the lot number of administered heparin was known, 52 (96.3%) occurred after the administration of OSCS-contaminated heparin.

CONCLUSIONS

Heparin contaminated with OSCS was epidemiologically linked to adverse reactions in this nationwide outbreak. The reported clinical features of many of the cases further support the conclusion that contamination of heparin with OSCS was the cause of the outbreak.

This article (10.1056/NEJMoa0806450) was published at www.nejm.org on December 3, 2008.

N Engl J Med 2008;359:2674-84.
Copyright © 2008 Massachusetts Medical Society.

UNFRACTIONATED HEPARIN IS AN ANTI-coagulant medication that is used to prevent or treat thromboembolic disorders. Heparin is also commonly used to prevent clotting of extracorporeal blood during hemodialysis and cardiac surgery, as well as to maintain the patency of intravenous devices. Chemically, heparin is a heterogeneous mixture of sulfated polysaccharides; its main anticoagulant activity is mediated through activation of antithrombin. Commercially available heparin is derived from animal tissues; only porcine-derived heparin is approved for the U.S. market. Although heparin-induced thrombocytopenia is a well-described immune-mediated phenomenon among patients receiving heparin, immediate hypersensitivity reactions (e.g., exanthemas, bronchospasm, angioedema, and anaphylaxis) that are directly attributable to heparin have rarely been reported.^{1,2}

On January 7, 2008, the Missouri Department of Health and Senior Services notified the Centers for Disease Control and Prevention (CDC) about a cluster of allergic-type reactions among patients undergoing hemodialysis at a pediatric hospital.³ Symptoms occurred within minutes after the initiation of a dialysis session, and manifestations included facial edema, tachycardia, hypotension, urticaria, and nausea. The CDC's national case-finding effort identified, in multiple states, additional clusters of similar reactions among patients undergoing hemodialysis, and subsequently among patients undergoing photopheresis or treatment for cardiac conditions. A common feature that preceded many of the reactions was the receipt of heparin produced by Baxter Healthcare. On January 17, 2008, nine lots of vials of heparin manufactured by Baxter were voluntarily recalled.⁴ A more extensive recall of heparin products manufactured by Baxter occurred on February 28, 2008.⁵

In March 2008, the Food and Drug Administration (FDA) announced that a "heparin-like" compound had been identified as a contaminant in the active pharmaceutical ingredient used in heparin manufactured by Baxter. This contaminant was identified as oversulfated chondroitin sulfate (OSCS),⁶ and the ability of OSCS in the active pharmaceutical ingredient to activate the contact and complement systems was shown.⁷ In this report, we describe the CDC epidemiologic investigation that was undertaken to establish the cause of the allergic-type reactions among patients undergoing dialysis, provide a clinical description of the reactions that occurred after the adminis-

tration of heparin, and report on laboratory tests for the presence of OSCS in finished-product heparin vials that were related to these reactions.

METHODS

EPIDEMIOLOGIC INVESTIGATION OF REACTIONS AMONG PATIENTS UNDERGOING DIALYSIS

Case Finding

After being notified about the Missouri cluster, the CDC began active case finding. Inquiries about allergic-type reactions were circulated by various methods, including the use of e-mail distribution lists targeting providers in the field of nephrology and the CDC's Epidemic Information Exchange. We used a standard form to collect information about the adverse events, as well as information about the demographic and clinical characteristics of the patients who had reactions and exposures of those patients to medication and medical devices. Since the original cluster and the majority of reactions that were reported subsequently occurred among patients undergoing dialysis, our initial case definition was restricted to reactions associated with dialysis. For this aspect of the investigation, we characterized a definite case as the sudden onset of angioedema (i.e., facial edema) or urticaria in a patient within 1 hour after the initiation of a hemodialysis session that occurred after November 1, 2007. A probable case was characterized by the development, within the same period after initiation of hemodialysis, of hypotension, loss of consciousness, or signs and symptoms from at least two of the following categories: sensation of burning, warmth, or flushing; numbness or tingling; difficulty swallowing; shortness of breath, audible wheezing, or chest tightness; tachycardia; and nausea, vomiting, or diarrhea.

Facility-Based Case-Control Study

Because a clustering of cases was noted in specific dialysis facilities, and patients within a facility had relatively uniform exposures to medical products, we conducted a case-control study to identify risk factors, using the facility as the unit of analysis. Dialysis facilities that completed a case-report form for at least one definite or probable case (21 facilities in 11 states) were considered to be case facilities and were compared with control facilities that reported no such reactions (23 facilities in 9 states). Control facilities were identified with the use of the Centers for Medicare and Medicaid Services Dialysis Facility Compare Web site.⁸ These

Table 1. Characteristics of Facilities Evaluated in a Facility-Based Case–Control Study.

Characteristic	Facilities with at Least One Case of Adverse Reaction (N = 21)	Facilities with No Case of Adverse Reaction (N = 23)	P Value
	no. (%)		
Manufacturer of heparin used			
Baxter Healthcare	21 (100.0)	1 (4.3)	<0.001
APP Pharmaceuticals	2 (9.5)	20 (87.0)	<0.001
Other	0	2 (8.7)	0.49
Manufacturer of dialysis machines used			
Gambro	16 (76.2)	7 (30.4)	0.03
Fresenius Medical Care	9 (42.9)	13 (56.5)	0.55
B. Braun	1 (4.8)	3 (13.0)	0.61
Other	1 (4.8)	0	0.48
Manufacturer of dialyzers used			
Gambro	10 (47.6)	8 (34.8)	0.54
Fresenius Medical Care	9 (42.9)	14 (60.9)	0.37
Other	7 (33.3)	6 (26.1)	0.75
Reused dialyzers	15 (71.4)	9 (39.1)	0.04
Saline priming solution delivered to patient*	11 (52.4)	13 (56.5)	0.76
Patient census >70 patients	10 (47.6)	12 (52.2)	1.00

* Saline solution is used to clear the tubing and dialyzer of air and residual disinfectant. In some instances, some of the priming solution that has passed through the circuit is delivered to the patient.

facilities were selected randomly among the pooled dialysis facilities in the 11 states in which case facilities were located. Owing to the pooling of potential controls, two states with case facilities were not represented among the control facilities. A representative of each case and control facility was contacted by telephone and surveyed between January 28, 2008, and February 8, 2008. Oral consent was obtained, and a clinical manager was asked to identify the medical products and supplies that had been used at the facility in the period after December 15, 2007, including heparin products and dialysis equipment (e.g., machines, tubing, and dialyzers), and to describe the facility's practices with respect to dialyzer reuse and reprocessing. Proportions were compared with the use of Fisher's exact test and Stata software, version 9.0 (Stata). All reported P values are two-sided.

ASSESSMENT OF REACTIONS, HEPARIN PRODUCTS, AND EXPOSURE TO CONTAMINATED LOTS

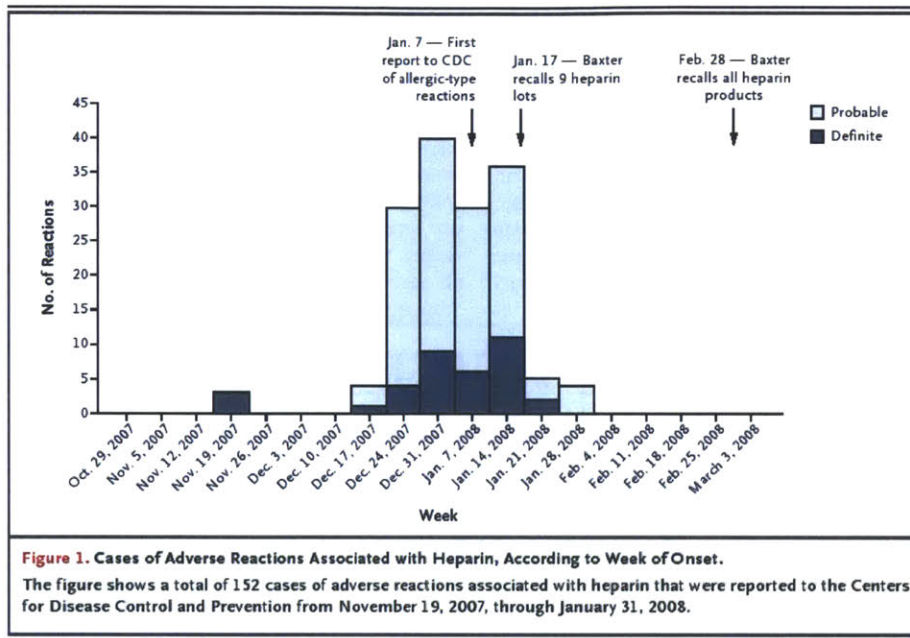
Clinical Description of Heparin Reactions

After preliminary findings suggested that heparin was strongly associated with cases and simi-

lar reactions were reported among patients who were not undergoing hemodialysis, we expanded our case definition to include reactions in a broader population of patients. For the purposes of describing heparin reactions in this broader population, a probable or definite adverse reaction associated with heparin met the same clinical and temporal criteria as those in the case definition for patients undergoing dialysis but was defined as occurring within 1 hour after the administration of heparin (rather than within 1 hour after the initiation of a hemodialysis session).

Analytic and In Vitro Evaluation of Heparin Products

Unopened finished-product vials of heparin were solicited from health care facilities that reported cases. Heparin vials received by the CDC were categorized by lot number; 10 lots of heparin manufactured by Baxter Healthcare were tested. Samples from each unique lot number and three controls were tested for the presence of OSCS and were assessed for their effect on the amidolytic activity of kallikrein in human plasma as a measure of the



activation of the kinin-kallikrein pathway. The quantification of OSCS levels and the measurement of amidolytic activity were performed with the use of previously described methods.^{6,7}

Exposure to Contaminated Heparin Lots

Although the specific lot number of heparin that had been administered in each case patient was requested, most facilities did not routinely record this information. Instead, many facilities reported likely exposures on the basis of the heparin lots that were present in the facility at the time of the reaction. Exposure to heparin lots contaminated with OSCS was described in the following manner. A known exposure to an OSCS-contaminated lot was defined as either documented receipt by a patient of heparin from a lot that tested positive for OSCS or exposure of a patient to one of several heparin lots in the facility, all of which tested positive for OSCS.

RESULTS

DIALYSIS CASES

A total of 131 adverse events met our initial case definition. Of these cases, 128 (97.7%) occurred after the administration of heparin; in 122 of those

cases (95.3%), the heparin that was used was manufactured by Baxter Healthcare. The only other factors identified in more than 50% of the cases were the use of acid concentrate manufactured by Minntech (59.5%), the use of dialysis machines (53.8%) and dialyzers (53.5%) manufactured by Gambro, and the practice of reusing hemodialyzers (52.0%).

FACILITY-BASED CASE-CONTROL STUDY

Twenty-one case facilities in 11 states had been identified by late January 2008 and were included in the study. The mean number of cases at case facilities was 4.2 (range, 1 to 11). Fifty-two facilities were contacted to obtain 23 control facilities in nine states. Of the 29 facilities that were contacted but not included as controls, 16 refused to participate, 7 did not respond, 5 reported a possible allergic-type reaction, and 1 was not a dialysis facility.

In univariate analysis, the use of Gambro dialysis machines and the administration of Baxter heparin were significantly associated with the presence of adverse reactions at the facility (Table 1). The factor with the strongest association was the use of Baxter heparin, which was reported by all case facilities and only one control facility (100.0% vs. 4.3%, $P < 0.001$).

ADVERSE REACTIONS ASSOCIATED WITH HEPARIN

A total of 152 heparin reactions that met our case definition were identified from November 19, 2007, through January 31, 2008 (Fig. 1), among the 194 events that were reported to the CDC. The 152 cases occurred in 113 patients from 13 states and included 130 reactions in 100 patients undergoing hemodialysis, 8 reactions in 6 patients undergoing treatment for cardiac conditions, and 14 reactions in 7 patients undergoing photopheresis. The average age of the 113 case patients was 53 years; 57 (50.4%) of the case patients were women.

Table 2 shows the clinical characteristics of the 152 heparin reactions in 113 case patients. The mean time to a reaction after exposure to heparin was 5.1 minutes among patients undergoing hemodialysis. The most common manifestations were hypotension (50.0%), nausea (48.7%), and shortness of breath (37.5%). Thirty-six reactions (23.7%) involved facial swelling. Although urticaria was reported in several of the cases in the initial cluster, this feature was infrequent (3.3%) among all cases. Fever (0.7%), chills (1.3%), wheezing (0%), and difficulty swallowing (0%) were also rare

Table 2. Clinical Characteristics of the 152 Adverse Reactions after Administration of Heparin.*

Characteristic	All Reactions (N = 152)	Probable Reactions (N = 116)	Definite Reactions (N = 36)
Time from administration of heparin to reaction — min			
During hemodialysis	5.1±9.1	5.3±10.0	4.5±6.2
During treatment for cardiac conditions	14±17.2	15.9±17.7	1±0
During photopheresis†	30±13.1	30±13.1	—
Manifestation — no. (%)			
Facial edema			
Any	36 (23.7)	0	36 (100)
Lips	23 (15.1)	0	23 (63.9)
Eyelids	17 (11.2)	0	17 (47.2)
Throat	12 (7.9)	0	12 (33.3)
Tongue	11 (7.2)	0	11 (30.6)
Mouth	10 (6.6)	0	10 (27.8)
Urticaria			
Any	5 (3.3)	0	5 (13.9)
Low blood pressure			
Systolic pressure <80 mm Hg	17 (11.2)	14 (12.1)	3 (8.3)
Nausea			
Any	74 (48.7)	56 (48.3)	18 (50.0)
Shortness of breath			
Any	57 (37.5)	38 (32.8)	19 (52.8)
Vomiting			
Any	37 (24.3)	27 (23.3)	10 (27.8)
Tingling			
Any	36 (23.7)	28 (24.1)	8 (22.2)
Flushing			
Any	35 (23.0)	31 (26.7)	4 (11.1)
Tachycardia			
Any	33 (21.7)	29 (25.0)	4 (11.1)
Diaphoresis			
Any	23 (15.1)	23 (19.8)	0
Abdominal pain			
Any	17 (11.2)	12 (10.3)	5 (13.9)
Diarrhea			
Any	8 (5.3)	7 (6.0)	1 (2.8)
Loss of consciousness			
Any	6 (3.9)	6 (5.2)	0
Chills			
Any	2 (1.3)	2 (1.7)	0
Fever			
Any	1 (0.7)	1 (0.9)	0
Difficulty swallowing			
Any	0	0	0
Wheezing			
Any	0	0	0

Table 2. (Continued.)

Characteristic	All Reactions (N = 152)	Probable Reactions (N = 116)	Definite Reactions (N = 36)
Follow-up care — no./total no. (%)			
Blood cultures obtained [‡]	32/144 (22.2)	26/109 (23.9)	6/35 (17.1)
Evaluation in an emergency department [§]	22/144 (15.3)	9/109 (8.3)	13/35 (37.1)
Hospitalization [§]	13/144 (9.0)	5/109 (4.6)	8/35 (22.9)
Use of intravenous heparin — no. (%)	149 (98.0)	115 (99.1)	34 (94.4)
Brand of heparin — no. (%)			
Baxter Healthcare	141 (92.8)	110 (94.8)	31 (86.1)
APP Pharmaceuticals	6 (3.9)	4 (3.4)	2 (5.6)
Baxter or APP	2 (1.3)	1 (0.9)	1 (2.8)
Not reported	3 (2.0)	1 (0.9)	2 (5.6)

* Plus-minus values are means \pm SD.

[†] Although heparin is administered at the beginning of photophoresis, the patient is not exposed to it until later in the process.

[‡] The total numbers exclude eight reactions (one definite and seven probable) owing to missing data.

[§] The total numbers exclude the eight reactions (one definite and seven probable) that occurred in patients undergoing treatment for cardiac conditions because these patients were hospitalized at the time of the adverse reactions.

or absent. In 15.3% of the cases, the reaction required further evaluation in the emergency department, and in 9.0% of the cases, required hospitalization. A total of 149 reactions (98.0%) occurred after intravenous administration of heparin. The other three involved exposure to heparin through other means (e.g., a dialysis circuit primed with heparin). The brand of heparin most commonly used (in 92.8% of the cases) was manufactured by Baxter Healthcare.

None of the 113 patients with adverse reactions that met our case definition died immediately after the reaction. Three deaths among patients undergoing treatment for cardiac conditions were reported to the CDC, but the reactions in these patients did not meet our case definition because they occurred between 8 and 11 hours after administration of the heparin.

ANALYTIC AND IN VITRO FINDINGS

The samples tested included 10 different lot numbers of heparin vials collected from facilities and 3 control samples (Fig. 2). Of the lots collected from facilities, Lots A through G and Lot J represent eight of the nine lots of Baxter heparin that were recalled on January 17, 2008. A high level of activation of kallikrein was observed with samples from Lots A through D and F through J at concentrations of 2.5 and 25 μ g per milliliter. These concentrations are in the range of a clinically efficacious con-

centration of heparin of approximately 1 to 5 μ g per milliliter, based on a specific activity of approximately 180 U per milligram. There was little activation of kallikrein from heparin samples that did not contain OSCS, including the control samples and Lot E.

EXPOSURE TO CONTAMINATED HEPARIN LOTS

Information on the lot of Baxter heparin was reported for 130 of the 152 heparin reactions. In 128 of the 130 (98.5%), OSCS-contaminated heparin was present in the facility; in 106 of the 130 (81.5%), facility records indicated that only OSCS-contaminated heparin could have been received by the patient (either because all heparin lots present in the facility tested positive for OSCS or because the single lot received by the patient was known and tested positive). Furthermore, of 54 heparin reactions for which the specific lot number of administered heparin was known, 52 (96.3%) resulted from an OSCS-contaminated lot.

The 106 reactions for which there was known exposure to OSCS-contaminated heparin occurred in 77 case patients. Of these case patients, 40 (51.9%) had a reported allergy to medication, most commonly to antibiotics. Six patients (7.8%) had a reported food allergy. An angiotensin-converting-enzyme (ACE) inhibitor was prescribed for 20 of these case patients (26.0%) at the time of the reaction.

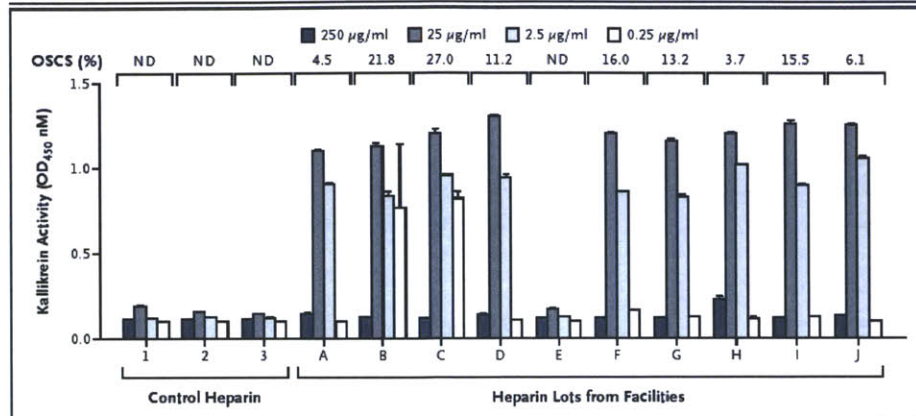


Figure 2. Association of Oversulfated Chondroitin Sulfate (OSCS) in Unfractionated Heparin with Induction of Kallikrein Activity.
 Thirteen samples of heparin, including one sample of non-clinical-grade heparin (control heparin 1), representing both suspect heparin lots and control lots, were analyzed in a blinded fashion for both the presence of OSCS and the ability to activate kallikrein. The presence of OSCS was detected and quantified as described elsewhere.⁶ The amidolytic activity of kallikrein was assessed at various concentrations of heparin, as indicated. Lots A through D and F through J contained OSCS. Samples from Lot E, as well as controls 1 through 3, contained no detectable OSCS. Lots A through G and Lot J were recalled on January 17, 2008. T bars indicate standard deviations of replicate measurements. ND denotes not detected.

Table 3 shows the clinical characteristics of the heparin reactions in case patients who were known to have received OSCS-contaminated heparin (106 reactions) and heparin that contained more than 20% OSCS (18 reactions). Low blood pressure was documented in 58.5% of the reactions; a systolic pressure lower than 80 mm Hg, however, was reported for only 9.4% of the reactions. Other common symptoms in case patients included nausea (46.2% of reactions), vomiting (28.3%), shortness of breath (25.5%), flushing (25.5%), tingling (24.5%), and tachycardia (24.5%). Facial swelling was associated with 17 reactions (16.0%). The 18 reactions involving heparin contaminated with more than 20% OSCS showed similar manifestations, although nausea was more frequent in this subgroup of cases (occurring in 72.2% of reactions), as was shortness of breath (38.9%).

DISCUSSION

We describe findings from a national investigation of adverse reactions among patients who received heparin and characterize 152 cases that occurred between November 19, 2007, and January 31, 2008. Our initial evaluation of reactions among patients undergoing hemodialysis sug-

gested that heparin was a potential cause, and a facility-based case-control study confirmed a strong epidemiologic association between the receipt of heparin produced by Baxter Healthcare and reactions. Reports to the CDC of heparin reactions declined after the initial Baxter recall of nine lots of heparin vials on January 17, 2008 (Fig. 1). By February 28, 2008, when all Baxter heparin products had been recalled, the CDC was no longer receiving reports of cases. Our findings confirm the presence of OSCS in finished-product vials of heparin manufactured by Baxter Healthcare that were used by facilities that reported cases, as well as the ability of these vials to induce kallikrein activation, and provide evidence that the vast majority of the patients with reactions had been exposed to heparin vials contaminated with OSCS.

Kishimoto et al.⁷ previously demonstrated kallikrein activation from OSCS in the active pharmaceutical ingredient of contaminated heparin. Since finished-product vials may contain heparin from more than one lot of the active pharmaceutical ingredient, the vials tested in this investigation best represent the heparin product that case patients received. We found similar biologic activity among multiple vials of heparin that were known to result in adverse reactions, and the clinical picture described among the outbreak cases nation-

Table 3. Clinical Characteristics of the 106 Adverse Reactions in Patients Confirmed to Have Received Heparin Contaminated with OSCS and with >20% OSCS.*

Characteristic	Reaction with OSCS-Contaminated Heparin (N = 106)	Reaction with Heparin Contaminated with >20% OSCS (N = 18)
Case status — no. (%)		
Probable	89 (84.0)	16 (88.9)
Definite	17 (16.0)	2 (11.1)
Patient population — no. (%)		
Dialysis	85 (80.2)	18 (100)
Cardiac	7 (6.6)	0
Photopheresis†	14 (13.2)	0
Time from administration of heparin to reaction — min		
During dialysis	4.8±9.0	3.7±1.7
During treatment for cardiac conditions	15.9±17.7	—
During photopheresis	30±13.2	—
Manifestations — no. (%)		
Facial edema		
Any	17 (16.0)	2 (11.1)
Eyelids	11 (10.4)	0
Lips	11 (10.4)	1 (5.6)
Tongue	5 (4.7)	1 (5.6)
Mouth	5 (4.7)	2 (11.1)
Throat	3 (2.8)	1 (5.6)
Urticaria	2 (1.9)	0
Low blood pressure	62 (58.5)	10 (55.6)
Systolic pressure <80 mm Hg	10 (9.4)	0
Nausea	49 (46.2)	12 (66.7)
Vomiting	30 (28.3)	4 (22.2)
Shortness of breath	27 (25.5)	7 (38.9)
Flushing	27 (25.5)	4 (22.2)
Tachycardia	26 (24.5)	0
Tingling	26 (24.5)	7 (38.9)
Diaphoresis	17 (16.0)	5 (27.8)
Loss of consciousness	4 (3.8)	0
Difficulty swallowing	0	0

* Forty-six reactions are not included: 2 were in patients who did not receive OSCS-contaminated heparin, and 22 were in patients who may have received OSCS-contaminated heparin but for whom receipt could not be confirmed; for the remaining 22 reactions, we did not receive lot information and were thus unable to make a determination. Plus-minus values are means ±SD. OSCS denotes oversulfated chondroitin sulfate.

† Although heparin is administered at the beginning of photopheresis, the patient is not exposed to it until later in the process.

ally is consistent with the biologic mediators previously identified in response to OSCS.

The adverse reactions that were reported to the CDC encompassed a constellation of signs and

symptoms, initially among patients undergoing hemodialysis. Some manifestations were overt (e.g., facial edema), others were more subtle (e.g., flushing), and many were not uncommon for pa-

tients undergoing hemodialysis or treatment for cardiac conditions (e.g., hypotension and dyspnea). Our initial case definition was intentionally broad to accommodate the many presentations and potential sources of allergic-type reactions in the absence of a clear cause or mechanism.

Similar adverse reactions have been documented among patients undergoing dialysis and have, in the past, been attributed to many causes, including dialyzer membranes, water impurities, residual disinfectants, and medications such as ACE inhibitors.⁹⁻¹¹ A systemic inflammatory response has also been described in the setting of cardiopulmonary bypass and has been attributed to activation of the contact system resulting from interaction of blood with the artificial surfaces of the bypass circuit and other mechanisms that activate the kinin-kallikrein pathway, complement system, and other systems.¹²

Heparin alone rarely causes the symptoms, such as angioedema, that were observed in this investigation.¹³ Heparin has antiinflammatory properties, and the use of heparin-coated devices is thought to decrease the risk of an inflammatory response.¹⁴⁻¹⁷ Although there have been occasional adverse reactions associated with heparin that have been attributed to animal proteins or allergens,² most adverse events reported in association with heparin products have been the result of either intrinsic or extrinsic microbial contamination.¹⁸⁻²⁰

Various clinical manifestations were observed in patients with adverse reactions who received OSCS-contaminated heparin. Although hypotension was the most common, a large proportion of case patients had nausea, shortness of breath, vomiting, tingling, flushing, and diaphoresis. Urticaria was not a prominent feature among the case patients. This finding is consistent with reactions that are not mediated by mast cells and supports the role of bradykinin and other mediators instead.²¹ In addition, there was no substantial difference between reactions that occurred as a result of heparin contaminated with OSCS and those that occurred as a result of heparin contaminated with a high concentration of OSCS (>20%). This finding may be consistent with data showing that at clinical concentrations of heparin (2.5 and 25 μg per milliliter), the level of kallikrein activation is similar, regardless of the concentration of OSCS. Furthermore, the relatively infrequent need for case patients to be evaluated in the emergency department or hospitalized supports the notion

that the clinical manifestations of these adverse reactions were mostly transient.

Twenty-six percent of case patients were taking an ACE inhibitor when they received OSCS-contaminated heparin and had the reaction. ACE inhibitors cause an accumulation of bradykinin and, thus, might be expected to predispose patients to a reaction or to worsen the reaction. The prevalence of ACE-inhibitor use among patients who received OSCS-contaminated heparin at these facilities but did not have reactions is unknown. In two studies of patients undergoing hemodialysis, the prevalence of ACE-inhibitor use was 24% and 51%,^{22,23} suggesting that the prevalence among case patients in this investigation was not greater than expected.

On the basis of available evidence, an allergic mechanism seems to be an unlikely cause of these reactions. Thus, it is interesting that a preexisting allergy to medication was identified among 51.9% of case patients, although it is possible that these reports of a history of intolerance to medication did not truly indicate allergic phenomena, and the prevalence of preexisting allergies among patients who did not have a reaction is unknown.

It should be recognized that the cases described in this report do not represent the entire outbreak. As of May 31, 2008, the FDA Adverse Event Reporting System had received reports of more deaths after heparin administration (238 deaths) than we had reports of cases.²⁴ No determination of a causal association between these deaths and heparin administration has been reported, and many deaths occurred among patients with severe underlying or life-threatening conditions.

We could not calculate attack rates because we did not know the total number of patients in the United States who received heparin during this period. We suspect that OSCS-contaminated heparin was used more broadly than in only those facilities that reported cases. According to national sales distribution data from the IMS National Sales Perspectives (IMS Health), approximately 7,163,700 single-dose and 3,339,400 multidose vials of Baxter heparin were sold by the manufacturer to distributors in the United States during the period from November 2007 through January 2008 (data abstracted by the FDA from IMS Health: IMS National Sales Perspectives: Retail and Non-Retail. Nov '07-Jan. '08. Extracted September 4, 2008). These data do not provide a direct estimate of use, but they do provide a national

estimate of the number of vials sold by the manufacturer into retail and nonretail channels of distribution. The lack of reports from other facilities may represent underreporting or underrecognition of reactions, evidence of intermittent contamination, patterns of distribution and use, or other factors.

There were several challenges to this investigation. First, health care facilities rarely recorded lot numbers of the heparin that was administered to patients. In many cases, we could determine only the heparin lots that a patient might have received. Second, our case descriptions are limited by the accuracy of information provided by health care personnel at reporting facilities. However, the fact that health care personnel reported reactions with the use of standard case-report forms probably increased the overall quality of the clinical information we obtained, as compared with information obtained by other methods. Finally, it was difficult to build precise case definitions owing to inherent uncertainties in this investigation. We attempted to reduce misclassification by establishing limits with respect to the time of onset and the symptoms that were required to be classified as a case, but some true cases may have been misclassified as noncases.

This report of a nationwide outbreak attributed to a newly discovered contaminant in heparin products contributes to our understanding of the epidemiology and biology of the adverse reactions that occurred. It also underscores the importance of a public health mechanism to address serious noninfectious adverse events in health care settings, the pivotal role of clinicians who recognize and report clusters of unusual events to public health authorities, and the need for ongoing col-

laboration among public health agencies, clinicians, basic-science researchers, and industry to prevent future safety threats associated with medications.

The CDC investigation had no external funding. The laboratory analysis was supported in part by grants from the National Institutes of Health (GM57073 and HL080279, to Dr. Sasisekharan).

Dr. Venkataraman reports being an employee of Momenta Pharmaceuticals and holding equity in the company, which performs the analysis and characterization of complex mixtures, including heparin, and being an inventor on patent applications for Momenta Pharmaceuticals; Dr. Kishimoto, being an employee of, holding equity in, and being an inventor on patent applications for Momenta Pharmaceuticals; Dr. Langer, receiving consulting fees from Momenta Pharmaceuticals and Scientific Protein, having equity in Momenta Pharmaceuticals, and serving on a paid board of Momenta Pharmaceuticals; Dr. Shriver, being an employee of Momenta Pharmaceuticals and holding equity in the company; Dr. Sasisekharan, holding equity in Momenta Pharmaceuticals and receiving consulting fees or serving on a paid board of Momenta Pharmaceuticals and Scientific Protein Labs; Dr. Austen, receiving consulting fees from Momenta Pharmaceuticals; Dr. Elward, receiving consulting fees or serving on a paid advisory board for Trinity and receiving grant support from SAGE Products; and Dr. Schillie, holding equity in Pfizer, Lilly, Monsanto, Walgreens, General Electric, and Abbott. No other potential conflict of interest relevant to this article was reported.

The findings and conclusions in this report are those of the authors and do not necessarily represent the views of the Centers for Disease Control and Prevention. Use of trade names and commercial sources is for identification only and does not imply endorsement by the U.S. Department of Health and Human Services.

We thank the many health care professionals at facilities at which adverse events occurred for reporting to public health authorities and for sending heparin vials for laboratory testing; the state epidemiologists and representatives of the End Stage Renal Disease Network for their assistance in facilitating contact between facilities with adverse events and the CDC; Laura Governale (IMS Health), Gary Warns (Gambro), and Bill Singley (Mintech) for the timely information they provided; and representatives of the FDA for their close collaboration, especially in the early stages of this outbreak investigation, in particular, Karen Deasy and Tarun Mallick, who served as important links between the FDA and the CDC and furthered our collective efforts.

REFERENCES

- Bircher AJ, Harr T, Hohenstein L, Tsakiris DA. Hypersensitivity reactions to anticoagulant drugs: diagnosis and management options. *Allergy* 2006;61:1432-40.
- Bottio T, Pittarello G, Bonato R, Fagiolo U, Gerosa G. Life-threatening anaphylactic shock caused by porcine heparin intravenous infusion during mitral valve repair. *J Thorac Cardiovasc Surg* 2003;126:1194-5.
- Acute allergic-type reactions among patients undergoing hemodialysis — multiple states, 2007–2008. *MMWR Morb Mortal Wkly Rep* 2008;57:124-5.
- Recall — firm press release: Baxter issues urgent nationwide voluntary recall of heparin 1,000 units/ml 10 and 30ml multi-dose vials. Rockville, MD: Food and Drug Administration, 2008. (Accessed November 24, 2008, at http://www.fda.gov/oc/po/firmrecalls/baxter01_08.html.)
- Recall — firm press release: Baxter to proceed with recall of remaining heparin sodium vial products. Rockville, MD: Food and Drug Administration, 2008. (Accessed November 24, 2008, at http://www.fda.gov/oc/po/firmrecalls/baxter02_08.html.)
- Guerrini M, Beccati D, Shriver Z, et al. Oversulfated chondroitin sulfate is a contaminant in heparin associated with adverse clinical events. *Nat Biotechnol* 2008; 26:669-75.
- Kishimoto TK, Viswanathan K, Gan- guly T, et al. Contaminated heparin associated with adverse clinical events and activation of the contact system. *N Engl J Med* 2008;358:2457-67.
- Information on Dialysis Facility Compare. Baltimore: Centers for Medicare & Medicaid Services, 2008. (Accessed November 24, 2008, at <http://www.medicare.gov/Dialysis/Include/DataSection/Questions/SearchCriteria.asp?version=default&browser=IE%7C6%7CWInXP&language=English&defaultstatus=0&pagelist=Home>.)
- Arduino MJ. CDC investigations of noninfectious outbreaks of adverse events in hemodialysis facilities, 1979-1999. *Semin Dial* 2000;13:86-91.

10. Ebo DG, Bosmans JL, Couttenye MM, Stevens WJ. Haemodialysis-associated anaphylactic and anaphylactoid reactions. *Allergy* 2006;61:211-20.
11. Pegues DA, Beck-Sague CM, Woollen SW, et al. Anaphylactoid reactions associated with reuse of hollow-fiber hemodialyzers and ACE inhibitors. *Kidney Int* 1992;42:1232-7.
12. Zakkar M, Taylor K, Hornick PL. Immune system and inflammatory responses to cardiopulmonary bypass. In: Gravlee GP, Davis RF, Stammers AH, Ungerleider RM, eds. *Cardiopulmonary bypass: principles and practice*. 3rd ed. Philadelphia: Lippincott Williams & Wilkins, 2007:321-7.
13. Berkun Y, Haviv YS, Schwartz LB, Shalit M. Heparin-induced recurrent anaphylaxis. *Clin Exp Allergy* 2004;34:1916-8.
14. Walenga JM. Non-anticoagulant effects of unfractionated and low-molecular weight heparins. *Clin Adv Hematol Oncol* 2007;5:759-60.
15. Ludwig RJ, Alban S, Boehncke WH. Structural requirements of heparin and related molecules to exert a multitude of anti-inflammatory activities. *Mini Rev Med Chem* 2006;6:1009-23.
16. Maharaj C, Laffey JG. New strategies to control the inflammatory response in cardiac surgery. *Curr Opin Anaesthesiol* 2004;17:35-48.
17. Wan S, LeClerc JL, Antoine M, DeSmet JM, Yim AP, Vincent JL. Heparin-coated circuits reduce myocardial injury in heart or heart-lung transplantation: a prospective, randomized study. *Ann Thorac Surg* 1999;68:1230-5.
18. *Pseudomonas* bloodstream infections associated with a heparin/saline flush — Missouri, New York, Texas, and Michigan, 2004–2005. *MMWR Morb Mortal Wkly Rep* 2005;54:269-72.
19. Souza Dias MB, Habert AB, Borrasca V, et al. Salvage of long-term central venous catheters during an outbreak of *Pseudomonas putida* and *Stenotrophomonas maltophilia* infections associated with contaminated heparin catheter-lock solution. *Infect Control Hosp Epidemiol* 2008;29:125-30.
20. Vonberg RP, Gastmeier P. Hospital-acquired infections related to contaminated substances. *J Hosp Infect* 2007;65:15-23.
21. Schwartz LB. Heparin comes clean. *N Engl J Med* 2008;358:2505-9.
22. Bishu K, Gricz KM, Chewaka S, Agarwal R. Appropriateness of antihypertensive drug therapy in hemodialysis patients. *Clin J Am Soc Nephrol* 2006;1:820-4.
23. Leyppoldt JK, Cheung AK, Delmez JA, et al. Relationship between volume status and blood pressure during chronic hemodialysis. *Kidney Int* 2002;61:266-75.
24. Information on adverse event reports and heparin. Rockville, MD: Food and Drug Administration, 2008. (Accessed November 24, 2008, at http://www.fda.gov/cder/drug/infopage/heparin/adverse_events.htm.)

Copyright © 2008 Massachusetts Medical Society.

RECEIVE IMMEDIATE NOTIFICATION WHEN
A JOURNAL ARTICLE IS RELEASED EARLY

To be notified when an article is released early on the Web and to receive the table of contents of the *Journal* by e-mail every Wednesday evening, sign up through our Web site at www.nejm.org

3.1. Summary and overall significance

In late 2007 and early 2008, clusters of serious anaphylactoid-type responses were observed in patients undergoing kidney dialysis. In total, more 200 deaths worldwide were linked to the outbreak. The number and severity of reactions in patients coupled with the notion that heparin is an essential drug used in a variety of clinical situations underscored an urgent need to understand the basis of the reactions and prevent future occurrences. Initial investigations by the Centers for Disease Control (CDC) and Food and Drug Administration (FDA) identified a link between adverse reactions and certain batches of heparin manufactured by Baxter Laboratories, which prompted the recall of all heparin manufactured by the company. Efforts to identify the source of adverse reactions eliminated more obvious potential causes, such as viral agents or greater levels of protein impurities in suspect lots. To further investigate and determine the root causes of the reactions, the FDA assembled a multidisciplinary team consisting of members from academia, industry, and the agency.

Heparin is composed of a complex mixture of polysaccharide chains. The similar chemical properties of the constituent chains leads to overlapping properties and signals in analytical techniques and thus challenges the complete structural elucidation of all components in heparin, and in particular, any additional components with similar physicochemical properties. To overcome these challenges, a framework encompassing multiple orthogonal analytical techniques was employed to identify the cause of the reactions. Results from enzymatic digestions, HPLC, MS, and multidimensional NMR converged on the identification of oversulfated chondroitin sulfate (OSCS) as the major contaminant. Importantly, the use of multiple analytical methods which provide complementary structural information enabled identification of the contaminant as OSCS with greater confidence while also ruling out other structurally related constituents, including the natural impurity dermatan sulfate. To further characterize OSCS as the cause of adverse reactions, an investigation into the biological activity of OSCS was performed. The presence of OSCS was shown to induce activation of the contact system, which can lead to a rapid onset of an anaphylactoid response, as well as activation of the complement system anaphylatoxins C3a and

C5a. These *in vitro* findings were corroborated with *in vivo* studies using pig, a relevant animal system to mimic the human response based on *in vitro* screening of plasma from different animal species. Administration of OSCS or OSCS-contaminated heparin to pigs resulted in blood pressure and heart rate changes consistent with activation of the contact system. Lastly, an epidemiological study demonstrated that confirmed and probable cases of anaphylactoid responses in patients significantly correlated with administration of heparin containing OSCS, a finding which further supported the role of OSCS as causing adverse clinical events.

The results of these studies have important implications, both for ensuring the safety of heparin products as well as for the regulation of other drugs and biologics more broadly. First, heparin is an essential drug, widely used in a variety of medical situations. Therefore, identification of the root cause of the outbreak was critical not only to resolve the immediate crisis but also to prevent future occurrences for this essential drug. To ensure accuracy in assigning the cause of the adverse reactions, it was critical to define and characterize the contaminant structurally, biologically and epidemiologically in the context of clinical presentation and symptoms. Multiple lines of evidence across these fields all converged on OSCS as the major contaminant responsible for the observed anaphylactoid reactions, thus reinforcing findings from each area of investigation – structure, activity, and epidemiology of OSCS-contaminated heparin.

Second, the findings of these studies highlight the need for regulatory tests that are specific to the molecular features of drug products, both in terms of structure and activity. Heparin is a complex biological product present as a mixture of related structures. Before the 2007-2008 heparin contamination outbreak, regulatory tests, as outlined in the US and other pharmacopeias, were based on more general structural and activity features of heparin, which described attributes of heparin but lacked much descriptive details of the mixture. Such tests were unable to detect the presence of OSCS due to its similar chemical and activity properties as heparin. Modern analytical techniques, such as those utilized in these studies, provide increased resolution and information content in characterizing structural features of complex drug products. For example in the case of heparin, ¹H-NMR enables distinction between heparin and OSCS, in part, by detecting the fine

differences in *N*-acetyl groups. Thus, incorporation of high-resolution analytical techniques into an overall set of regulatory tests significantly improves the ability to define impurities and contaminants in drug products. In addition to structure-determination assays, activity tests more specific to the biological mechanisms of drug products aid the detection and discernment of impurities and contaminants. In the case of heparin, the required potency test utilized a crude clotting assay with sheep blood, an assay in which many agents, including heparin and OSCS, demonstrate anticoagulant activity. In response to these issues, the US pharmacopeia for heparin has been updated with new tests, including ¹H-NMR, anion-exchange HPLC, and anti-Xa/anti-IIa activity ratio, which characterize more specific molecular and activity features of heparin.

Third, the supply chain for drug products is increasingly globalized and with greater complexity, including that for heparin. Most raw material for pharmaceutical heparin is obtained from pigs in China, and increasingly, the manufacture and production of heparin is also occurring in China. The increasing reliance of the importation of drug products into the US necessitates global regulation strategies to ensure the safety (and efficacy) of drugs, however significant challenges and barriers exist. Harmonization of regulatory standards across the globe is a critical facet towards addressing international supply chain issues. Indeed, in the case of heparin before the contamination outbreak, significant differences existed between regulatory tests implemented and criteria required, perhaps most notably of which was differences in heparin activity. In addition to increased harmonizing of standards, regulatory tests need to be updated for products, particularly those which have long market lives, to ensure assays appropriately monitor impurities and components which are most likely to lead to issues in safety and efficacy in the context of modern manufacture procedures. The potential consequences of not having updated tests in place was seen for heparin; as a drug used for multiple decades, many of the tests in place were outdated and did not provide sufficient molecular characterization to detect many potential impurities, such as OSCS. Collectively, the increased complexity and globalization of pharmaceutical supply chains prompt modified surveillance strategies which incorporate greater harmonization across regulatory bodies as well as vigilant and modernized post-marketing monitoring of drug products.

Lastly, these studies provide a practical lesson towards and insight into the coordination of efforts between the FDA and scientists and physicians from academia and industry to rapidly resolve urgent drug issues. Circumstances surrounding the heparin contamination outbreak, including the immediacy of the reactions and the essentialness of heparin as a medical drug, necessitated an investigation to *rapidly* determine the cause of reactions and hence prevent additional harm. Formation of a multidisciplinary team provided the expertise to thoroughly and expediently characterize suspect versus control lots of heparin, but the speed and success of such a broad-team investigation critically hinged on coordination of people, resources, and results. Indeed, with such a team assembled and appropriately coordinated for the heparin contamination investigation, it was possible to converge on identification of the contaminant and formation of a biological link in less than three months. The scientific and managerial leadership of the heparin contamination may be a useful model for the coordination of efforts to resolve other urgent medical and drug-related issues.

Attributions I would like to acknowledge that these studies were team-based investigations involving many individuals from different academic, industry, and FDA groups. My participation in these studies involved assisting with the development of the kallikrein activity assay and applying the assay to test multiple lots of heparin.

4. Engineering of a broad spectrum neutralizing antibody to dengue virus by structure-guided rational design

4.1. Introduction and motivation

Dengue is the most common vector-borne viral disease in humans, with an estimated 3.6 billion people at risk for infection. Globally, more than 200 million dengue infections occur each year, resulting in approximately 21,000 deaths [1]. The high morbidity associated with dengue leads to significant public health, social, and economic impact on populations and countries where dengue is endemic [2]. Currently, no approved vaccine or specific therapy exists for dengue, leaving a large unmet public health need.

Dengue virus (DV), the causative agent of dengue disease, is a member of the *Flaviviridae* family and exists as a complex of four serotypes (DV1-4). The 50 nm DV particle is composed of a 10.7 kb positive-sense RNA genome, host-derived lipid bilayer, and multiple copies of three viral structural proteins – capsid (C), precursor membrane/membrane (prM/M), and envelope (E) proteins [3]. The surface of a mature DV particle has 180 copies of M and 90 copies of E protein homodimers, which form a compact architecture with the E proteins oriented parallel to the viral membrane, thus giving the mature virus a smooth, spike-less appearance [4]. The arrangement of E proteins on the virion surface yields an icosahedral lattice in which each of the three E protein monomers per icosahedral asymmetric unit has a different chemical environment (**Figure 4.1**) [4]. The E protein is composed of three domains: EDI, EDII, and EDIII (**Figure 4.1**) [5]. EDII displays a conserved fusion loop at its distal end, which is responsible for facilitating fusion with host cell endosomes, and EDIII is thought to be responsible for binding yet-unidentified host cell receptor(s) [6].

Monoclonal antibodies (mAbs) as novel antiviral therapeutics and prophylactics are of growing interest owing to their high biochemical specificity, activity by both direct and indirect

mechanisms (i.e., effector functions), long serum half-life, and decreasing costs of manufacture [7-9]. Development of potent neutralizing mAbs against the DV complex to combat severe disease offers a promising therapeutic and prophylactic strategy, however no mAbs have yet been identified which potently neutralize all four serotypes. The principal target of neutralizing antibodies is the E protein, which shares approximately 70% sequence identity in its amino acid sequence between serotypes, thus leading to substantial antigenic diversity [10]. Cross-reactive neutralizing mAbs to DV have been shown to typically localize to one of two epitopes: the highly conserved EDII fusion loop (fl) or the 'A' β -strand on EDIII (Figure 4.1). Antibodies recognizing the EDII-fl show broad neutralization (i.e., all four serotypes), however their neutralization potency is low due to inaccessibility of this epitope in the mature virion structure [11, 12]. In contrast, EDIII A-strand antibodies tend to show potent neutralizing activity, however with limited breadth, neutralizing only 1-3 serotypes [13-15]. Another significant challenge to the development of a therapeutic mAb for dengue is addressing concerns regarding antibody-dependent enhancement (further discussed in Section 4.4 "Discussion").

The high potency but limited cross-reactivity of EDIII A-strand mAbs

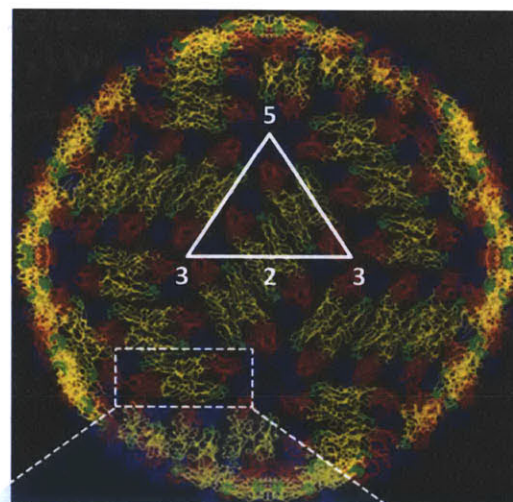


Figure 4.1 Structure of DV and E protein. DV surface structure is composed of 90 dimers of E protein arranged with icosahedral symmetry. Numbers represent the 5-, 3-, and 2-fold axes of symmetry. The E protein is composed of three domains: EDI (red), EDII (yellow), and EDIII (blue). Cross-reactive neutralizing epitopes are marked: EDII fusion loop (green) and EDIII A-strand (magenta).

makes this class of DV mAbs attractive targets for rational engineering towards the development of a potent broad-spectrum therapeutic/prophylactic DV mAb. The A-strand mAb 4E11, originally isolated from a mouse infected with DV1 [16], displays potent to modest neutralizing activity against DV1-3 but weak DV4 neutralizing activity [15]. We reasoned that, using a structure-function-based approach, 4E11 could be rationally re-engineered for increased neutralization activity to DV4 while maintaining DV1-3 activity.

In this chapter, 4E11 is rationally mutated using structure-guided approaches for increased affinity and neutralizing activity to DV4 while preserving neutralizing activity to DV1-3. An integrated structure-function approach is employed in which a structure-based empirical informatics computational methodology is developed to predict affinity-enhancing mutations in 4E11, and functional binding and neutralization assays are applied to characterize the mutations. An engineered mAb is developed and experimentally defined, revealing an activity profile with binding and potent neutralization to all four serotypes.

4.2. Methods

4.2.1. Cells & viruses

Vero (African green monkey kidney) and C6/36 (*Aedes albopictus*) cells were purchased from ATCC. Vero cells were cultured with DMEM/F-12 (50:50) medium (Invitrogen) supplemented with 10% FBS (Invitrogen) in a 37°C humidified 5% CO₂ incubator. C6/36 cells were maintained in EMEM (ATCC) supplemented with 10% FBS in a 28°C humidified 5% CO₂ incubator. Suspension Freestyle 293 cells (Invitrogen) were cultured in Freestyle 293 medium (Invitrogen) in flasks maintained at 135 RPM in a 37°C humidified 8% CO₂ incubator. Dengue viruses TH-S-man (serotype 1), NGC (serotype 2), and H87 (serotype 3), and BC287/97 (serotype 4) were purchased from ATCC or BEI Resources. Viruses were propagated by infection of C6/36 cells (MOI ~0.1) and harvested after 5-8 days. Aliquots were stored at -80°C.

4.2.2. Focus forming assay

Viruses were titered by focus forming assay with Vero cells and expressed as focus-forming units (FFU) per ml. Serial dilutions of virus were incubated for 2 hours with 95% confluent Vero cells in 24-well plates at 37°C, after which one ml of viscous overlay (DMEM/F12 containing 1% Aquacide II [EMD Millipore]) was added to the monolayer. After 4-6 day incubation period at 37°C, the overlay was removed, cells were fixed with formalin, and foci were revealed by sequential incubation with pan-flavivirus 4G2 mouse antibody, HRP-conjugated goat anti-mouse IgG antibody (Santa Cruz Biotechnology), and TrueBlue Peroxidase Substrate (KPL).

4.2.3. Expression and purification of antibodies and EDIII proteins

Chimeric 4E11 (designated '4E11') was generated by DNA synthesis (DNA 2.0) of 4E11 VH and VL regions (GenBank accession numbers AJ131288.1 and AJ131289.1, respectively) and cloned using standard techniques into pcDNA 3.3 plasmid (Invitrogen) containing the constant region of either human IgG1 heavy chain or human kappa light chain. For mouse 4E11 (designated 'm4E11'), the same DNA sequences were cloned into mouse IgG2a heavy chain (pFUSEss-CHIg-mG2a) and mouse kappa light chain (pFUSEss-CLIg-mk) plasmids (InvivoGen). Mutant mAbs were generated by either site-directed mutagenesis (Agilent) or variable region DNA synthesis (DNA 2.0). Antibodies were expressed in Freestyle 293 cells by transient transfection with polyethylenamine (PEI) and purified by protein A chromatography. EDIII DNA sequences (corresponding to E protein amino acid residues 293-400) of strains TH-S-man, NGC, H87, and BC298/97, representing serotypes 1-4, respectively, were synthesized (DNA 2.0) with C-terminal 6X-His tags and cloned into pJExpress414 plasmids. The proteins were expressed in Origami2(DE3) *E. coli* (EMD Millipore), essentially as described [17]. Briefly, overnight cultures of Origami2 cells harboring EDIII-pJExpress414 plasmids were used to inoculate 500 ml cultures, which were then grown at 37°C until OD₆₀₀ reached 0.6. The culture was equilibrated to room temperature for one hour, after which IPTG was added (1 mM, final) to induce expression for 3 hours at room temperature. Bacterial cells were harvested by centrifugation and lysed by sonication. After removal of insoluble material by centrifugation, EDIII from centrifugation supernatant was purified by IMAC using His-Trap columns (GE Healthcare) and stored at 4°C or -20°C for long-term storage.

4.2.4. Indirect ELISA

EDIII in PBS (0.1 $\mu\text{g}/\text{well}$) was adsorbed to Maxisorp 96-well plates (Nunc) at 4°C overnight. Plates were then washed with PBS-T (PBS containing 0.1% Tween-20) and blocked with PBS-T containing 1% BSA for 1 hour. Serial dilutions of antibody were added to wells and incubated for 2 hours, and after washing, bound antibody was revealed by HRP-conjugated rabbit anti-human IgG (Jackson ImmunoResearch) followed by TMB substrate (KPL) addition. The reaction was stopped by 1N sulfuric acid, and OD_{450} was determined using a Molecular Devices spectrophotometric plate reader. Apparent dissociation constant, K'_D , was determined by fitting a standard four-parameter logistic model to the data, with the inflection point being equal to K'_D .

4.2.5. Competition ELISA

The affinities of antibodies to EDIII, in solution at equilibrium, were determined by competition ELISA [18]. In 96-well plates, serial dilutions of EDIII were mixed with antibody at 0.2 nM in PBS-TB (PBS containing 0.01% Tween-20 and 0.01% BSA). The mixtures were incubated overnight to allow equilibrium to be reached. Subsequently, an optimized EDIII indirect ELISA was performed to measure the concentration of unbound or singly bound antibody. The conditions of the ELISA were developed such that antibody concentration is linearly proportional to absorbance and that the equilibrium is not significantly disturbed, conditions important for obtaining accurate results [18]. Maxisorp plates coated with EDIII-DV1 (2.5 ng/well, 4°C overnight) were blocked with PBS-TB containing 1% BSA for 1 hour. After washing wells with PBS-TB, equilibrium antibody-EDIII mixtures were added to the wells and incubated for 20 min. After washing, bound antibody was detected by incubation with diluted HRP-conjugated rabbit anti-human IgG (Jackson ImmunoResearch) for 1 hour, followed by addition of TMB substrate (KPL). The reaction was stopped with 1N sulfuric acid, and OD_{450} was determined. The data were fit, by least squares regression in Excel (Microsoft), to the following model derived from mass action and as described [19], with adjustment to take into account antibody bivalence [20]:

$$A_i = (A_{max} - A_o) \times \frac{\sqrt{u^2 + 4K_D[mAb]_o} - u}{2[mAb]_o} \times \left(\frac{w - \sqrt{w^2 - 4[EDIII]_i[mAb]_o}}{2[mAb]_o} + 1 \right)^{-1} + A_o$$

where

$$u = [EDIII]_i - [mAb]_o + K_D$$

and

$$w = [EDIII]_i + [mAb]_o + K_D$$

and $[mAb]_o$ is the initial antibody concentration, $[EDIII]_i$ is the variable concentration of EDIII, A_i is the OD₄₅₀ at $[EDIII]_i$, A_{max} and A_o are the maximal and minimal OD₄₅₀ (when $[EDIII] = 0$ and $[EDIII] = \infty$, respectively), and K_D is the equilibrium dissociation constant. For data fitting, K_D was the sole floating parameter.

4.2.6. Surface plasmon resonance

Surface plasmon resonance (SPR) experiments were performed with a Biacore 3000 (GE Healthcare) instrument. Briefly, substoichiometrically biotinylated antibody (ligand) was applied to a CAPture Kit chip (GE Healthcare), and EDIII protein flowed as the analyte. Kinetic parameters (k_{on} and k_{off}) were determined by fitting resultant RU curves to a 1:1 binding model using BIAevaluation software (GE Healthcare). Since no binding of WT 4E11 was detected to EDIII-DV4, this interaction was also tested by steady state experimental conditions, which increases sensitivity of detection to $K_D < 0.1$ mM. K_D was determined by the ratio k_{off}/k_{on} .

4.2.7. Focus reduction neutralization test (FRNT)

Neutralizing activity of antibodies was assessed by the focus reduction neutralization test (FRNT). Serially diluted antibody was mixed with an equal volume of diluted virus (30 FFU/well) and incubated for 2 hour at 37°C. The mixtures were then transferred to Vero cell monolayers in

24-well plates. Foci were detected by focus forming assay as described above. Each antibody concentration was run in duplicate. Data are expressed as the relative infectivity:

$$\text{Relative infectivity} = \frac{(\text{Average \# foci at } [mAb]_i)}{(\text{Average \# foci with no mAb})} \times 100$$

A standard four-parameter logistic model was fit to the data by least squares regression in Excel with the slope factor and inflection point as floating parameters. The FRNT₅₀ is equal to the inflection point, which is the concentration of mAb at 50% virus neutralization.

4.2.8. Ala-scanning

To identify paratope hot spots of binding interaction, Ala-scanning of 4E11 CDR loops was performed. Briefly, all residues in 4E11 CDR loops were individually mutated to Ala (or Ala→Gly), expressed, purified, and tested for binding to EDIII-DV1-3 by indirect ELISA, as described above. Energetic hot spots were defined as those in which K'_D increased by >100-fold for at least two serotypes.

4.2.9. Computational methods

Computational docking of 4E11 to EDIII was performed in a series of steps. First, a model of 4E11 was generated using the PIGS server [21]. Docking was performed using ZDOCK (Discovery Studio), and mapped epitope and H3 paratope residues [22, 23] were used to constrain the docking to ensure the poses do not deviate significantly from the native complex. The best ranking model from each run was analyzed further for physicochemical features typical of antibody-antigen interfaces, and the top-ranking model was selected. Prediction of energetic hot spots in different docked models was performed with the KFC2 server [24] using a cutoff of -0.4 confidence score.

For rational design of 4E11 mutations, CDR loop residues were examined one at a time. At a given CDR position, the WT residue was systematically substituted by the remaining amino acids excluding glycine and proline and the CDR contact potential score was evaluated at each instance. Single mutations that lead to a better contact potential score than the wild type mAb were modeled and evaluated. Proline and glycine residues were not modified to avoid alteration in the backbone

conformation. Replacements were modeled, and reevaluated computationally to find mutations that met the following requirements - (1) do not alter phi-psi values, (2) do not bury polar groups and (3) improved H-bonds, salt bridges, van der Waals, and hydrophobic contacts and packing.

4.3. Results

4.3.1. Generation of 4E11-EDIII structural model and design of affinity-enhancing mutations

Rational design of affinity-enhancing mutations for 4E11 required a structural understanding of how 4E11 binds its epitope on EDIII. With no available co-crystal structure of 4E11:EDIII at the inception of this study, an accurate 4E11:EDIII model had to be computationally generated. To generate such a model, a three-step approach was undertaken. A structural model of 4E11 was developed using the PIGS server [21], and this model was then docked computationally to EDIII, leading to five model poses with similarly high scoring values. The generation of false positives by computational docking of protein-protein interactions is a common challenge which contributes to the difficulty of *a priori* prediction of correct protein-protein interaction configurations [25]. In order to remove docking decoys and establish an accurate structural model, the five poses were assessed by their interface features, including number of different types of contacts (i.e., hydrogen bonds, electrostatics, and hydrophobic packing), interface surface area, planarity, and charge distribution. Comparison of interface features of the five posed to statistical averages derived from antibody-antigen co-crystal structures led to the removal of four of the five models as likely false positives. To validate the remaining pose, a comparison was performed between paratope and epitope hot spots computationally predicted [24] from the pose and hot spots experimentally identified. Paratope energetic hot spots were determined by experimental Ala-scanning of each position in all CDR loops of 4E11 with binding assessment by indirect ELISA (see Methods), while epitope energetic hot spots have been previously characterized [22]. Hot spot prediction of the selected pose correctly identified 61% of experimentally determined hot spots,

whereas the remaining poses had hot spot prediction accuracies of <45% (range 28-44%), thus indicating that the selected pose was likely to reflect the true 4E11:EDIII binding configuration.

To design affinity-enhancing, cross-reactive mutations, it was hypothesized that important structural features of antibody-antigen interfaces could be mined from the large collection of available antibody-antigen co-crystal structures (>500) in the Protein Data Bank (PDB). Identified structural features correlating with specificity and intermolecular contacts could be applied to predict mutations in 4E11 which would increase contacts with EDIII-DV4 while not detrimentally affecting EDIII-DV1-3 contacts. A mathematical model was designed in which pairwise interactions between epitope and paratope were mined in a manner that takes into account secondary structure of epitope residues (see Methods). A resultant index which quantifies the propensity for particular epitope amino acids given a neighboring paratope residue was applied to predict paratope mutations which could yield greater contacts with neighboring epitope residues than the WT paratope residue. Each predicted mutation from this set was individually modeled to determine mutations likely to make new H-bonds, salt bridges, van der Waals contacts, and hydrophobic packing with DV4 while not perturbing DV1-3 contacts. This computational analysis resulted in a final set of 87 mutations predicted to increase 4E11 affinity to DV4 while not significantly affecting DV1-3 affinities.

4.3.2. Experimental assessment of DV4 affinity-enhancing mutations

Antibodies harboring the 87 predicted affinity-enhancing mutations, individually, were generated by site-directed mutagenesis and expressed in 293 cells. Affinities of single mutant antibodies were assessed by indirect ELISA with recombinant EDIII proteins, which revealed 10 mutations having increased EDIII-DV4 affinity and approximately unchanged affinity to EDIII-DV1-3 relative to WT 4E11 (**Table 4.1**). Eight of the 10 identified mutations were located in the VL, with 7 being in CDR L2 alone. The physicochemical properties of the positive mutations were mostly charged or polar in nature. Using the 4E11:EDIII-DV4 structural model, the location of these paratope residues were shown to reside at the periphery of the antibody-antigen interface area (**Figure 4.2**). Interestingly, the number and variety of DV4-affinity-enhancing mutations

accommodated at each identified position varied substantially. For example, for VL-N57, a mutation to Ser or Glu, but not Asp, yielded increased EDIII-DV4 affinity, while for VL-E59, mutations to Gln, Asn, Val, Tyr, Trp, Thr, Ser, Ala, and Asp all showed increased EDIII-DV4 affinity but only Gln and Asn did so while not significantly decreasing affinity to EDIII-DV1-3.

Table 4.1 Mutations with increased EDIII-DV4 affinity and similar affinity to EDIII-DV1-3 relative to WT 4E11, as determined by EDIII indirect ELISA.

Chain and CDR	Position	WT residue	Mutation
VH - H2	55	Ala	Glu
VH - H2	55	Ala	Asp
VL - L1	31	Arg	Lys
VL - L2	57	Asn	Glu
VL - L2	57	Asn	Ser
VL - L2	59	Glu	Gln
VL - L2	59	Glu	Asn
VL - L2	60	Ser	Trp
VL - L2	60	Ser	Tyr
VL - L2	60	Ser	Arg

Initial studies to determine quantitative affinity values of mAbs harboring mutations was performed by EDIII indirect ELISA, a method frequently used to assess antibody affinities towards dengue and other flavivirus EDIII proteins [26-30]. Results, however, were found to be inconsistent with affinity measurements by SPR (data not shown). This discrepancy motivated the development of a new affinity measurement method to achieve greater accuracy than the EDIII indirect ELISA and greater throughput than SPR. A competition ELISA method, which enables measurement of affinity constants at equilibrium in solution [18], was optimized for antibodies and DV EDIII (see Materials and Methods section). Qualitative correspondence was found between the affinity-

enhancing mutations identified by indirect ELISA and results obtained by competition ELISA, indicating the indirect EDIII ELISA accurately identified mutations with affinity improvements.

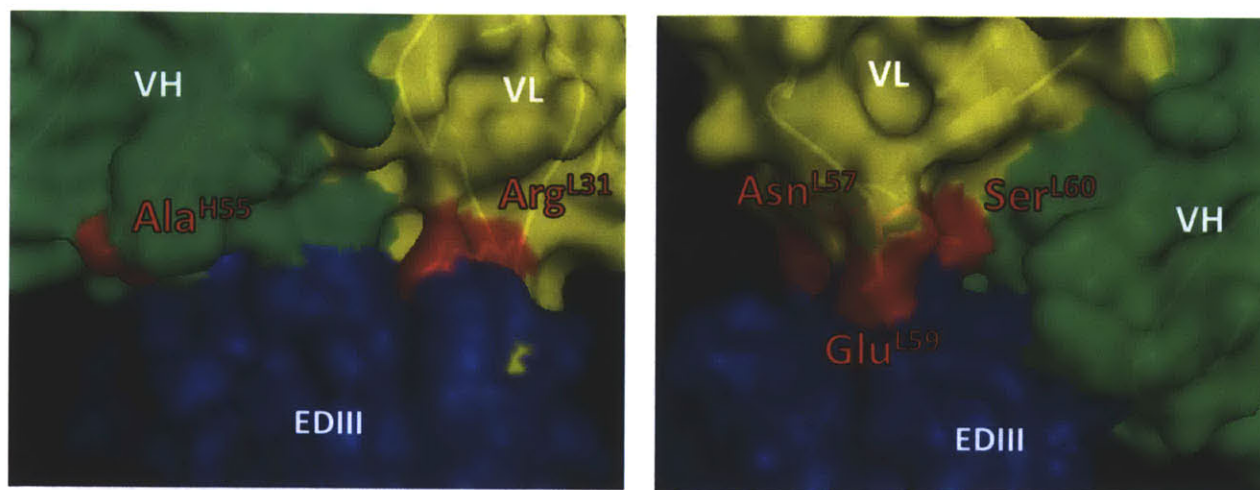


Figure 4.2 Affinity-enhancing mutations localize to the periphery of the 4E11:EDIII-DV4 interface. The positive positions identified in the binding screen are highlighted (red) in a structural model of 4E11:EDIII-DV4 interaction. All positive mutations are located at the periphery of the binding interface. The two panels represent different views of the same model. EDIII, VH, and VL proteins are represented by blue, green, and yellow, respectively. Images generated with PyMOL visualization software.

Competition ELISA results with five single mutant antibodies, representing those mutations which demonstrated the best DV1-4 affinity profiles for each position, are described in **Figure 4.3**. The extent of DV4 affinity enhancement ranges from 1.1-fold (VL-R31K) to 9.2-fold (VH-A55E). Somewhat unexpectedly, two mutations conferred increased affinity to other serotypes; VH-A55E resulted in a 16- and 7-fold affinity increase to EDIII-DV2 and EDIII-DV3, respectively, while VL-N57E demonstrated a 3-fold affinity increase to EDIII-DV2. Only three of the 15 affinities measured to serotypes 1-3 (with the five single mutant antibodies) showed a decrease greater than 2-fold, and only one antibody-EDIII affinity (VL-E59Q for EDIII-DV3) resulted in greater than a 3-fold decrease in affinity. Collectively, these results demonstrate that 4E11 can be re-engineered for increased DV4 affinity while not significantly affecting DV1-3 affinities, and that multiple mutations in 4E11 can confer these activities. The mutations individually, however, resulted modest DV4 affinity gains.

Mutation	CDR	EDIII-DV1 K_D (nM)	EDIII-DV2 K_D (nM)	EDIII-DV3 K_D (nM)	EDIII-DV4 K_D (nM)
4E11 WT	-	0.328	5.20	21.8	40,793
A55E	H2	0.295	0.323	2.95	4442
R31K	L1	0.378	5.35	21.1	37,292
N57E	L2	0.281	1.75	33.9	8408
E59Q	L2	0.772	10.8	102	11,034
S60W	L2	0.284	6.30	23.1	26,351



Figure 4.3 Affinities of single mutant antibodies with increased EDIII-DV4 affinity and similar EDIII-DV1-3 affinities relative to 4E11 WT. Mutations included are those which, for each identified position, demonstrated greatest EDIII-DV4 affinity while approximately maintaining EDIII-DV1-3 affinity. K_D values represent the average of at least two independent experiments.

4.3.3. Affinity and neutralizing activity of engineered mAb 4E-5A

The 10 identified mutations were modeled to assess their steric and contact inter-compatibility in the 4E11:EDIII structural model. From this analysis, a set of mutation combinations was predicted for further increasing DV4 affinity of the engineered mAb. The combination mutants were expressed and tested by competition ELISA. Interestingly, the combination which yielded the greatest affinity to EDIII-DV1-4 was a quintuple mutant, thus a combination of mutations at each of the positions identified. This combination mutant, termed 4E-5A, consisted of VH-A55E, VL-R31K, VL-N57E, VL-N59Q, and VL-S60W mutations. 4E-5A demonstrated affinities of 0.309, 0.246, 16.5, and 91.2 nM for EDIII-DV1-4, respectively, representing a 1.1-, 21.1-, 1.3-, and 447-fold enhancement in affinity for EDIII of serotypes 1-4, respectively (**Table 4.2**). A thermodynamic analysis was performed to assess whether the mutations of 4E-5A, when combined, displayed additive or cooperative effects on affinity to EDIII-DV4 (**Table 4.3**) [31]. The change in free energy of 4E-5A relative to 4E11 ($\Delta\Delta G_{WT \rightarrow 4E-5A} = -3.61$ kcal/mol) was slightly lower than the sum of the change in free energy for the individual mutations ($\Sigma\Delta\Delta G_{ind\ mut} = -3.33$ kcal/mol), however the

difference was within experimental error. Thus, the energetic contributions of the mutations in 4E-5A display additivity, with a possibility of small positive intramolecular cooperativity. A lack of cooperativity (or slight positive cooperativity) indicates the mutations are independent of each other, such that their presence or contacts to EDIII are not significantly affecting other mutations.

Table 4.2 Affinities of 4E11 WT and combined mutant antibody 4E-5A determined by competition ELISA

Antibody	EDIII-DV1		EDIII-DV2		EDIII-DV3		EDIII-DV4	
	K _D (nM) ^a	Relative affinity ^b	K _D (nM)	Relative affinity	K _D (nM)	Relative affinity	K _D (nM)	Relative affinity
4E11 WT	0.328	-	5.2	-	21.8	-	40,793	-
4E-5A	0.309	1.1	0.246	21.1	16.5	1.3	91.2	447.3

^aK_D values represent the average of at least two independent experiments

^bRelative affinity is defined as mutant affinity (K_D) relative to WT affinity (K_D)

Table 4.3 Free energy assessment of individual mutant antibodies and the combination mutant antibody 4E-5A

Antibody	EDIII-DV4 ΔG (kcal/mol) ^a	EDIII-DV4 ΔΔG (kcal/mol) ^b
4E11 WT	-5.98	---
VH-A55E	-7.29	-1.31
VL-R31K	-6.03	-0.05
VL-N57E	-6.92	-0.93
VL-E59Q	-6.76	-0.77
VL-S60W	-6.24	-0.26
4E-5A	-9.59	-3.61

^aFree energy calculated by $\Delta G = RT \ln(K_D)$ at 25°C

^b $\Delta\Delta G = \Delta G_{\text{mutant}} - \Delta G_{\text{WT}}$

To further explore and validate the biophysical properties of 4E-5A, SPR experiments were employed to measure binding affinities and kinetic parameters of 4E11 and 4E-5A (**Table 4.4**). Parameters were obtained for both antibodies with serotypes 1-4 except 4E11 with EDIII-DV4, in which no significant binding was observed (with both kinetic and steady state experiments),

indicating a K_D approximately $>100 \mu\text{M}$ (the lower detection limit of the Biacore instrument). An affinity of 4E11 for EDIII-DV4 equal to lower than $100 \mu\text{M}$ is in approximate agreement with the competition ELISA results, which demonstrated a low affinity of $41 \mu\text{M}$. The remaining K_D results are in good overall quantitative agreement with those obtained by competition ELISA, further validating both sets of data. 4E-5A demonstrated a >877 -fold affinity increase to EDIII-DV4 (assuming a WT $K_D >100 \mu\text{M}$), similar to that obtained by competition ELISA (447-fold). The on-rates for both antibodies were similar across serotypes 1-4 ($\sim 10^6 \text{ M}^{-1}\text{s}^{-1}$), values typical of antibody-antigen interactions. The lack of significant variability in the on-rate is expected, as the association rates for larger molecules such as proteins are typically diffusion-limited [32]. In contrast, the off-rates varied substantially between serotypes for a given antibody as well as between antibodies for the same serotype, particularly for EDIII-DV2. The off-rates range from $5.51 \times 10^{-4} \text{ s}^{-1}$ for 4E11 interaction with EDIII-DV1 to $8.75 \times 10^{-2} \text{ s}^{-1}$ for 4E-5A interaction with EDIII-DV4. The affinity increase associated with 4E-5A to EDIII-DV2 relative to 4E11 is derived from a ~ 10 -fold slower off-rate.

Table 4.4 Kinetic binding parameters and dissociation constant for WT 4E11 and 4E-5A determined by SPR.

mAb	EDIII-DV1			EDIII-DV2			EDIII-DV3			EDIII-DV4		
	k_{on}^{a}	$k_{\text{off}}^{\text{b}}$	K_D (nM) ^c	k_{on}^{a}	$k_{\text{off}}^{\text{b}}$	K_D (nM)	k_{on}^{a}	$k_{\text{off}}^{\text{b}}$	K_D (nM)	k_{on}^{a}	$k_{\text{off}}^{\text{b}}$	K_D (nM)
4E11	1.11	5.51	0.50	1.98	123	6.20	1.34	102	7.58	NB ^d	NB	$>100,000^{\text{e}}$
4E-5A	1.17	20.8	1.78	2.01	14.1	0.70	2.76	143	5.19	0.766	875	114

^a k_{on} values are expressed as ($\times 10^6 \text{ M}^{-1}\text{s}^{-1}$)

^b k_{off} values are expressed as ($\times 10^{-4} \text{ s}^{-1}$)

^c K_D was calculated by $k_{\text{off}}/k_{\text{on}}$

^dNB designates no binding

^eSPR steady state experiments revealed no binding, indicating a $K_D >0.1 \text{ mM}$ based on sensitivity limit of instrument

To determine whether the enhanced affinity to EDIII-DV4 conferred increased virus neutralizing activity, WT 4E11 and 4E-5A antibodies were assessed by a focus reduction neutralization test (FRNT) with DV1-4 (**Figure 4.4**). The data were fit to a standard four-parameter logistic model, and the FRNT₅₀, representing the mAb concentration which neutralized 50% of

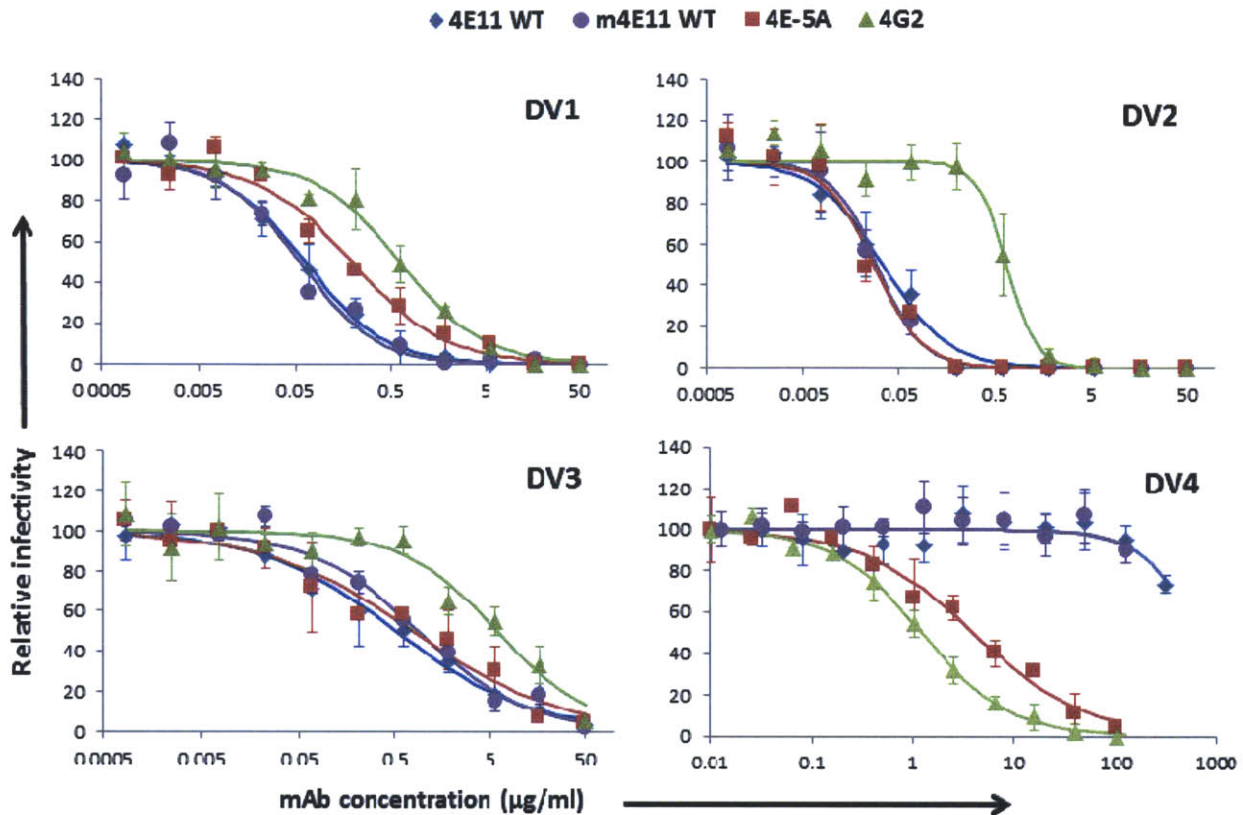


Figure 4.4 In vitro neutralizing activity of antibodies assessed by FRNT. Neutralization assays were performed with DV1-4 and antibodies 4E11 WT, m4E11 WT, 4E-5A, and 4G2. Serial dilutions of antibody were mixed with equal amounts of virus and added to Vero cell monolayers with a viscous overlay. After 4-6 days, cells were fixed and foci were immunostained and counted. Data points represent averages of duplicates with error bars representing standard deviation. A standard four-parameter logistic model was fit to the data using least squares regression. 4E-5A shows similar neutralizing activity to 4E11 and m4E11 for DV1-3 and a substantial increase in neutralizing activity to DV4. 4G2, a representative flavivirus fusion-loop specific antibody, demonstrates lower neutralizing activity for DV1-3 and only slightly higher activity to DV4 relative to 4E-5A.

virus, was determined (Table 4.5). Since WT 4E11 used in most experiments in this study was a human chimeric antibody (see Materials and Methods) and 4E11 was originally isolated from a mouse [16], an antibody harboring mouse constant regions with 4E11 variable domains (m4E11 WT) was also assessed for neutralizing activity. 4E11 and m4E11 showed no significant neutralization activity differences, indicating that the constant region change from mouse to human did not significantly affect antibody binding to the viruses, as anticipated. Neutralization activity of

4E11 was greatest for DV2 (0.034 $\mu\text{g/ml}$), with activities towards DV1, DV3, and DV4 lower by 1.8-, 15-, and >9,000-fold, respectively, demonstrating the relatively potent activity towards DV1-3 while very low activity towards DV4. The low activity of 4E11 for DV4, however, was specific, as an isotype-controlled unrelated mAb showed no neutralizing activity at a concentration of 312.5 $\mu\text{g/ml}$ (*data not shown*). 4E-5A neutralizing activity, relative to 4E11, was similar for DV2-3, slightly reduced for DV1 (~3-fold), and substantially greater for DV4 (>75-fold), indicating a general correspondence with the changes in affinity. Comparison to the flavivirus fusion loop-specific mAb 4G2 revealed that 4E11 and 4E-5A showed greater neutralizing activity for DV1-3, as anticipated, since fusion loop-specific mAbs display low neutralizing activities due to the inaccessibility of their epitope. For DV4, 4E-5A demonstrated slightly lower neutralizing activity compared to 4G2 (~3-fold). Overall, 4E-5A approximately maintains neutralizing activity to DV1-3 with a >75-fold increase to DV4. The results are in general agreement with 4E-5A affinity results with some small exceptions. Notably, 4E-5A affinity to EDIII-DV2 relative to 4E11 is increased ~10-20-fold, however this increased affinity did not translate into an increase in neutralizing activity. Additionally, 4E-5A affinity to EDIII-DV1 relative to 4E11 is unchanged (by competition ELISA) and ~3.5-fold lower (by SPR), and this small affinity change corresponds to a 3-fold decrease in neutralizing activity (see “4.4 Discussion” for further discussion). Collectively, these results demonstrate that the engineered affinity increases observed in 4E-5A translated to a substantial neutralization enhancement to DV4 while approximately maintaining DV1-3 neutralizing activities.

Table 4.5 Quantification of antibody neutralizing activity by FRNT₅₀.

Antibody	DV1		DV2		DV3		DV4	
	FRNT ₅₀ ($\mu\text{g/ml}$)	Relative activity ^a	FRNT ₅₀ ($\mu\text{g/ml}$)	Relative activity	FRNT ₅₀ ($\mu\text{g/ml}$)	Relative activity	FRNT ₅₀ ($\mu\text{g/ml}$)	Relative activity
4E11 WT	0.062	1.0	0.034	1.0	0.52	1.0	>312.5	1.0
m4E11 WT	0.055	1.1	0.030	1.1	0.88	0.6	>125	-
4E-5A	0.19	0.3	0.028	1.2	0.77	0.7	4.00	>75
4G2	0.62	0.1	0.67	0.05	5.85	0.09	1.23	>254

^aRelative activity defined as FRNT₅₀ of 4E11 WT divided by FRNT₅₀ of the test antibody

4.3.4 Structural analysis of 4E-5A antibody

To gain further structural insight into the five mutations of 4E-5A, a structural model of 4E-5A with EDIII of DV1-4 was generated using the four 4E11:EDIII models (Figure 4.5). As described above, the mutations localize to the periphery of the binding interface (Figure 4.2). An analysis of the predicted contacts formed by mutations to EDIII-DV4 revealed a predominance of electrostatic interactions (i.e., hydrogen bonds and salt bridges) (Table 4.5). Only one hydrophobic packing contact is predicted (VL S60W). The paucity of new hydrophobic contacts is consistent with the general localization of the residues near the periphery of the interface which generally is solvent accessible. Overall, two new salt bridges, two new hydrogen bonds, and a new hydrophobic packing contact are features of 4E-5A interaction with EDIII-DV4 compared to 4E11.

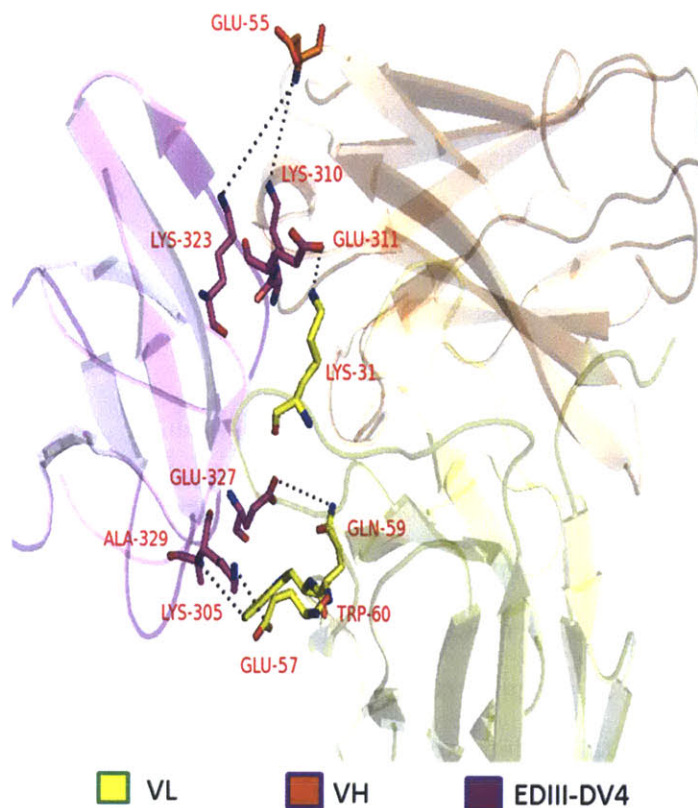


Figure 4.5 Structural prediction of 4E-5A and contacts formed by its five mutations. The five mutations of 4E-5A were substituted onto the 4E11:EDIII model. Intermolecular contacts are represented by dashed lines. VL domain and residues are represented in yellow, VH in orange, and EDIII-DV4 in purple.

The co-crystal structure of 4E11 in complex with EDIII of DV1-4 was recently published [33] and thus enabled comparison of the model predicted in this study to the experimentally determined structure. A reasonable confidence was associated with the model of 4E11:EDIII used in this study due to several reasons: (1) the modeling process took into account the functionally mapped epitope; (2) the final model was selected based on statistical physicochemical information

Table 4.6 Predicted hydrogen bond, salt bridge, and hydrophobic packing contacts formed by mutations in 4E-5A to EDIII-DV4.

Mutation	Predicted EDIII-DV4 contact(s)	Associated epitope residue(s)	Predicted WT residue contact
VH A55E	H-bond, salt bridge	K310, K323	None
VL R31K	Salt bridge	E311	Salt bridge
VL N57E	Salt bridge	K305	H-bond
VL E59Q	H-bond	E327	None
VL S60W	Hydrophobic packing	A329	None

of antibody-antigen interfaces, an approach which complements energy minimization used to generate model poses; (3) the final model had high correlation between experimentally determined energetic hot spots and predicted hot spots of the model; and (4) the model successfully led to the design of crossreactive-compatible DV4 affinity-enhancing mutations. The accuracy of the model was assessed by structural alignment with the solved crystal structure of 4E11 with EDIII of DV1-4 (**Figure 4.6**). The C_{α} backbone root mean square distance (RMSD) between the model of the crystal structure was $<1 \text{ \AA}$ for all four serotypes (0.812, 0.789, 0.834, and 0.89 \AA for serotypes 1-4, respectively), demonstrating good agreement of the model with the experimentally determined structure.

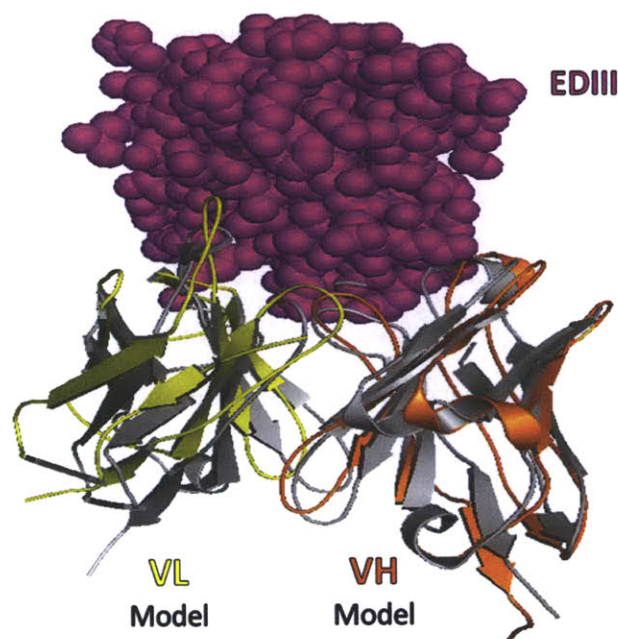


Figure 4.6 Alignment of 4E11:EDIII structural model with solved co-crystal structure. The structural models were aligned with the solved co-crystal structures of 4E11:EDIII-DV1-4 using PyMOL. The resultant alignment with EDIII-DV2 is shown. The model is colored (yellow represents VL and orange represents VH) and the antibody crystal structure is indicated in grey.

4.4. Discussion

4.4.1. Summary

In this study, with the aim of developing a broad spectrum potent neutralizing therapeutic antibody for clinical use, a structure-guided approach was undertaken to improve the neutralizing activity of the DV cross-reactive antibody 4E11. First, a structural model of 4E11 in complex with EDIII was generated, and validation of the model was performed by (1) analysis of interface physicochemical features of the model compared to a statistical database of antibody-antigen interfaces and (2) comparison to experimentally determined paratope and epitope binding hot spots. An empirical informatics approach was developed and implemented, which resulted in the identification of 87 mutations predicted to increase affinity of 4E11 to DV4 while not significantly affecting affinities to DV1-3. Mutations were experimentally tested, which resulted in the identification of 10 mutations with the targeted affinity profile. Mutations were characterized for affinity changes relative to WT 4E11, and combinations of mutations combinations were tested for further affinity enhancement. A quintuple mutant, termed 4E-5A, was shown to have increased affinity to DV4 by ~450-fold while approximately maintaining affinity to DV1-3 relative to WT 4E11. Increased affinity to DV4 translated to a >75-fold increase in neutralizing activity to DV4 while approximately maintaining neutralizing activity to DV1-3. The mutations in 4E-5A were predicted to localize at the periphery of the antibody-antigen interface, and resulted mostly in increased electrostatics interactions. Collectively, 4E-5A exhibits an interesting broad spectrum neutralization profile and is an antibody of interest for potential therapeutic development for treatment of dengue disease. This body of work has implications in a set of distinct but related areas:

- Properties of known cross-reactive neutralizing mAbs to DV (Section 4.4.2)
- Molecular factors governing neutralization potency of flavivirus antibodies (Section 4.4.3)
- Advancements in computational and experimental methodologies (Section 4.4.4)

- Clinical potential of antiviral mAbs for the prevention or treatment of dengue disease (Section 4.4.5)

4.4.2. Potent cross-reactive antibodies to DV

The combined breadth and neutralization potency of 4E-5A represents a new activity profile of DV-specific antibodies not yet observed from antibodies isolated from humans or animals infected with DV. Studies investigating the antibody response to DV infection have generally revealed a paucity of potentially neutralizing broad-spectrum mAbs [14, 30, 34-37]. In both mice and humans, a significant portion of isolated antibodies is directed against the highly conserved EDII fusion loop [34, 37-39]. This class of antibodies is generally complex-specific (i.e., reactive to DV1-4 complex), however they show low neutralizing activity due to the poor accessibility of this epitope in the mature virion structure [11]. EDIII-specific antibodies, in contrast, demonstrate higher neutralizing activity but typically lower cross-reactivity, and are often type-specific (i.e., reactive to only one serotype) [40, 41]. Cross-reactive EDIII-specific antibodies have been identified from DV-infected mice and humans, and biophysical studies have indicated that their epitopes generally localize to the A-strand of EDIII [13, 14, 28]. Cross-reactive A-strand antibodies tend to show higher neutralization potency than fusion loop-specific antibodies, however they typically neutralize only two or three serotypes (or very low neutralization activity to a fourth serotype, e.g., WT 4E11) [13, 14, 26-28, 30, 34]. Engineered mAb 4E-5A, having high neutralizing activity to DV1-2 (PRNT₅₀ < 0.1 µg/ml), moderate activity to DV3 (PRNT₅₀ < 1 µg/ml), and low neutralizing activity to DV4 (PRNT₅₀ < 10 µg/ml), is an A-strand EDIII antibody with neutralizing activity to all four serotypes and thus demonstrates an interesting profile of neutralizing potency and breadth of reactivity.

In contrast to findings of the properties of EDIII mAbs isolated from mice, a recent in-depth study of the human mAb response to DV infection identified a high level of broadly cross-reactive EDIII antibodies [38]. Two isolated EDIII-specific mAbs demonstrated moderate to low neutralization potency for all four serotypes, and two EDIII-specific mAbs exhibited high neutralization activities (comparable to serotype-specific EDIII antibodies) with subcomplex specificity (i.e., reactive to only two or three serotypes) [38]. Therefore, in contrast to mAbs thus far

characterized from DV infection of mice, EDIII-specific mAbs from human DV infection can possess broadly cross-reactive neutralization activity as well as high neutralization potency, though the latter may be limited to subcomplex specificity. Characterization of the structural and functional epitopes of these human cross-reactive EDIII mAbs would reveal interesting insights into neutralization mechanisms of broadly reactive and highly potent EDIII-specific mAbs and enable comparison to mouse cross-reactive mAbs which localize to the EDIII A-strand.

4.4.3. Molecular mechanisms of antibody neutralization potency

It was surprising that 4E-5A, while demonstrating 10-20-fold higher affinity to EDIII-DV2 than 4E11, exhibited the same neutralization potency as 4E11 to DV2, since increased affinity to a neutralizing epitope is likely to lead to increased neutralization activity [42-44]. These results indicate that, in the context of this epitope with DV2, affinity is not a limiting factor to increasing neutralization activity. However, a different affinity-neutralization activity correlation was observed for DV1: 4E-5A for DV1 consistently exhibited 2-4-fold lower neutralization activity than 4E11, which correlated well with a 3-fold reduction in EDIII-DV1 affinity relative to 4E11.

Studies investigating the molecular factors governing antibody neutralization potency of flaviviruses have revealed that antibody affinity controls the percentage of viral epitopes bound by an antibody, which thereby influences neutralization potency in a “multi-hit” model of virus neutralization (reviewed in [44, 45]). Thus, for an antibody which binds a given neutralizing epitope, increased affinity should translate to higher epitope occupancy on a DV particle and hence higher neutralization potency. For 4E-5A, the lack of increased neutralization activity for DV2 with increased affinity for EDIII-DV2 remains surprising in the context of this model. One possible explanation is that 4E-5A affinity to recombinant EDIII of DV2 is different than its affinity to its epitope in an intact virion. While such a difference seems unlikely, affinities of 4E11 and 4E-5A to DV2 can be experimentally determined and such studies would be of interest to perform. Another possible explanation for the apparent discrepancy is that affinity is not a limiting factor for 4E-5A-mediated neutralization of DV2, and therefore increased affinity registers no neutralization consequences. Such an explanation, however, appears inconsistent with the affinity-neutralization

results from DV1, in which for 4E-5A, a 3-fold decrease in affinity to EDIII-DV1 corresponded to a ~3-fold decrease in neutralization activity relative to 4E11. Overall, additional studies are required to further tease apart these apparent inconsistencies between affinity and neutralization activity for 4E-5A.

Affinity-enhancing mutations identified in this study provide a novel toolset to investigate molecular mechanisms of flavivirus neutralization potency by antibodies, and in particular, the role of affinity. While previous studies have drawn from correlations between affinities and neutralization activities with multiple antibodies and associated multiple epitopes to define such molecular factors [44, 46], 4E-5A (and related mutations) provides a system with a new level of control in which affinity can be systematically varied for a *fixed* epitope and then correlated with neutralization activity. Thus, 4E-5A and related mutations may be helpful in investigations to extend the understanding of molecular mechanisms which govern flavivirus neutralization by antibodies, studies which have implications for vaccine development and generation of therapeutic mAbs.

4.4.4. Computational and experimental method developments

In this study, a structure-guided rational design approach was undertaken to engineer increased affinity of the cross-reactive mAb 4E11. Success of such an approach was substantially dependent on (1) an accurate structural understanding of the 4E11:EDIII complex, (2) the ability to predict affinity-enhancing mutations, and (3) the accuracy of quantitative binding methods. Substantial advancements in these areas developed in this study contributed to the computational and experimental realization of a rationally re-designed cross-reactive mAb to DV.

First, at the inception of this study, no crystal structure of 4E11 or 4E11:EDIII complex was available, and consequently a computational structural model had to be developed. Importantly, a model which did not accurately reflect the true interaction would have significantly hampered or possibly prevented the ability to rationally design affinity-enhancing mutations. Methods to perform computational protein-protein docking have advanced significantly in recent years,

however substantial challenges remain, including the inability to confidently remove ineffective poses (i.e., false positives) from the pose which reflects reality [25]. Computational docking approaches typically utilize shape complementarity and energetics-based analyses to predict protein-protein molecular recognition. To improve upon the accuracy of these physical-based methods, complementary information was incorporated into the assessment of docking poses. Specifically, physicochemical features of antibody-antigen interfaces (e.g., number of contacts and interface surface area) were mined from the PDB, and the models were compared to the empirically derived statistical features. Such an approach led to the identification of four models having attributes significantly inconsistent with statistical features of antibody-antigen interfaces, leaving only one model in good agreement. The selected model was further validated by comparison to experimentally determined energetic hot spots of 4E11, and this final model was shown to be in good agreement with the solved crystal structure of 4E11:EDIII, which was later published [33]. The incorporation of empirical informatics of antibody-antigen interfaces, as developed in this study, directly aided in the *in silico* generation of an accurate 4E11:EDIII model. Additional studies are underway to assess the broader applicability of such an approach to improve computational antibody-antigen docking.

Second, antibody affinity enhancement by computational design remains a formidable challenge, with few studies achieving greater than ~10-fold improvement in affinity (summarized in **Table 4.7**). Previous studies have typically employed energetic minimization approaches for rational design and with antibodies which recognize a single antigen. In this study, rational design was employed for engineering 4E11, a cross-reactive antibody (i.e., binding to four serotypes), and to obtain a substantial increase in affinity improvement (>100-fold) since the affinity of 4E11 to DV4 is 1,800 to 130,000-fold lower than to DV1-3. As cross-reactive antibodies (inclusive of the case of 4E11) can make different contacts with their different antigens, rational design approaches applied to them must not only predict affinity-enhancing mutations but do so while not causing detrimental effects to contacts being made with other antigens, thus greatly increasing the complexity of design. Addressing these challenges was tractably approached by implementation of empirical informatics, in which the probability of paratope residue replacement was evaluated at

each instance using paratope-epitope pairwise propensities derived from known antibody-antigen structures. This empirical informatics approach benefited from the utilization of information directly from antibody-antigen structures and thus incorporated elements not easily recognized by general energetics methods (e.g., high prevalence of Tyr residues in paratopes). Additionally, an empirical informatics approach, as described here, has the distinct advantage of being less sensitive to precise atom coordinates in a structure, which is of particular benefit for this study of engineering 4E11, since the derived computational model of 4E11:EDIII does not carry the same atomic-level confidence of experimentally determined crystal structures. The application of an empirical informatics methodology and design of ~450-fold affinity improvement for a cross-reactive antibody represent new developments for antibody rational design (**Table 4.7**). Efforts are underway to look at the broader applicability of empirical informatics for affinity-enhancing mutation design for antibodies. It would also be of interest to combine empirical informatics with energetic minimization methodologies for rational design, as they represent different yet complementary approaches.

Table 4.7 Summary of studies employing rational design methods for antibody affinity improvement.

Study	Crystal structure?	Antigen	Modeling/design method	Number of mutations	Affinity improvement
Lippow, et al. <i>Nat Biotech</i> (2007) [47]	Yes	Single	Energetic minimization	6	140-fold
Clark, et al. <i>Protein Sci</i> (2006) [48]	Yes	Single	Energetic minimization	4	10-fold
Marvin, et al. <i>Biochemistry</i> (2003) [49]	Yes	Single	Energetic minimization	6	9-fold
Farady, et al. <i>Bioorg Med Chem Lett</i> (2009) [50]	Yes	Multiple (2)	Rule-/Energetics-based	1	~14-fold
Diskin, et al. <i>Science</i> (2011) [51]	Yes	Many (HIV gp120)	Structure-guided	1	~3-4-fold
This study	No	Multiple (4)	Empirical informatics	5	~450-fold

Third, the development of a method to rapidly and quantitatively determine mAb affinities to recombinant EDIII became a challenge during the course of this study. As mentioned above, EDIII indirect ELISA methods have been commonly employed in studies characterizing affinities of antibodies to flavivirus (including DV) recombinant EDIII proteins [26-30]. In this study with 4E11, initial investigations of antibody affinities by an EDIII indirect ELISA method demonstrated substantial discrepancies with those obtained by SPR. Such discrepancies have been noted more broadly with indirect ELISAs since they do not capture solution binding affinities (i.e., antigen is in an solid state, immobilized on the surface of the plate), and antigen proteins may be denatured upon adsorption to the plate surface [52]. A competition ELISA, which enables measurement of true solution dissociation constants [18], was developed and optimized to address this challenge and obtain accurate affinity measurements with higher throughput than by SPR.

The finding that the indirect EDIII ELISA method did not yield accurate results for 4E11 may be more broadly applicable to other EDIII-specific antibodies. For example, a recent study characterizing the structure and activity of a cross-reactive DV EDIII-specific antibody, 2H12, found affinity results determined by EDIII indirect ELISA to not correlate well with binding to intact virus nor neutralizing activity for DV1-4 [26]. A possible explanation for this apparent discrepancy may be related to inaccurate affinity estimates determined by EDIII indirect ELISA, an explanation that would be consistent with findings in this study of 4E11. The competition ELISA method developed in this study, which was cross-validated by SPR, may be broadly useful for researchers investigating affinities of flavivirus EDIII-specific antibodies.

4.4.5. Therapeutic potential of 4E-5A

The potential of a dengue antiviral therapeutic intervention in mitigating or preventing development of severe disease is supported by epidemiological observations that individuals with severe dengue disease (i.e., DHF/DSS) often have higher viremia levels by 1-2 logs compared to individuals with less severe DF [53, 54]. The protective activity conferred by antivirals, including antibodies, in animal models of DV infection further supports the potential of antivirals for dengue disease treatment in humans [30, 34, 55, 56]. However, only one clinical trial of antiviral treatment

of DV has been reported: chloroquine, an anti-malaria drug, was found to be ineffective in the time to resolution of viremia and time to resolution of NS1 antigenemia [57], however the antiviral effect of chloroquine *in vitro* is modest and has not been thoroughly studied [58, 59]. It thus remains unclear whether, and to what extent, specific antiviral therapy may be effective in reducing or preventing dengue severe disease. Importantly, DHF/DSS occurs in patients during defervescence and when viremia levels have dramatically decreased or are undetectable. Therefore, antiviral therapy likely would need to be administered prior to development of DHF/DSS state of disease. Clinically, such a therapeutic window of opportunity may be present when patients first seek medical attention upon development of DF signs and symptoms, as viremia is generally detectable during this phase. However, viremia levels wane rapidly, indicating a potentially short therapeutic window and requirement of rapid diagnostics.

In the absence of clinical information regarding the potential of antivirals to mitigate or prevent disease, insights may be gleaned from studies with animal models of DV infection. Interpretations of such studies, however, should be done cautiously as animal models, including non-human primates, do not faithfully recapitulate elements of human dengue disease. Despite this limitation, efficacy studies in animal models may provide additional information towards understanding the therapeutic profile of antiviral candidates. A variety of studies have demonstrated the protective role of antibodies in pre-exposure prophylactic and post-exposure therapeutic protection in DV infection of mice [30, 34, 35, 38, 55, 56, 60]. Since most studies have generally identified a correlation between *in vitro* neutralization potency and *in vivo* protection [34, 35, 61], protective capacity of mAbs can be estimated from their *in vitro* activity. 4E-5A, which demonstrates high neutralizing activity to DV1-2 (PRNT₅₀ < 0.1 µg/ml), moderate activity to DV3 (PRNT₅₀ < 1 µg/ml), and low neutralizing activity to DV4 (PRNT₅₀ < 10 µg/ml), may be predicted to have significant protective activity for DV1-2 however activity to DV3-4 would be less certain. Studies are underway to investigate the *in vivo* activity of 4E-5A.

The potential for antibodies to increase DV replication and hence disease burden in infected individuals (and as explained by the ADE theory) raises substantial challenges to development of a

clinically viable antibody therapeutic specifically for dengue infection. Multiple strategies involving removal or modification of antibody Fc regions provide means to reduce the potential of increased disease burden by antibody, with the rationale based on the hypothesis that ADE in humans occurs via antibody binding to Fc γ receptors on cell surfaces (**Figure 1.3**). Removal of an antibody Fc region [e.g., Fab or single chain fragment variable (scfv) forms] eliminates the potential for antibody fragments to bind Fc γ receptors, thus preventing ADE. However, such a modification diminishes Fc-mediated effector functions (i.e., activation of immune cells and complement) and the extended half-life of the antibody, which is mediated by Fc binding to the neonatal Fc receptor. Other strategies to prevent ADE include modification of the Fc region to specifically prevent binding to Fc γ receptors [38, 55, 62]. Such approaches retain the long half-life of the modified antibody but effector functions are removed which may decrease antiviral activity of a mAb *in vivo*. Indeed, a recent study demonstrated that poorly neutralizing cross-reactive antibodies provide protection *in vivo* in mice via Fc γ receptor effector functions, thus supporting a potentially substantial role of antibody effector functions in dengue immunity [63]. However, other studies have demonstrated that mAbs modified to prevent Fc γ receptor binding can confer *in vivo* protection, including in one mouse model system which captures ADE effects [38, 55]. Collectively, specific modification of the Fc region of a mAb provides an efficient means to reduce risk for ADE *in vivo*, however it remains unclear whether and to what degree the associated removal of Fc-mediated effector functions may reduce antiviral activity of a therapeutic mAb in humans.

The substantial antigenic heterogeneity between the four serotypes of DV has motivated multiple strategies for passive immunotherapy for dengue infection. One such strategy is the development of mAbs which neutralize a single serotype, with the rationale that serotype-specific antibodies demonstrate the most potent neutralization activities [35, 60, 64]. One such recently reported antibody, HM14c10, recognizes a quaternary epitope on the surface of DV and demonstrates potent *in vitro* and *in vivo* activity against multiple genotypes of DV1 [60]. Another strategy is the use of a cocktail of mAbs which, when combined, have neutralizing activity to all four serotypes [38]. In this study, a broad spectrum mAb, 4E-5A, was rationally designed with the aim of generating a mAb with potent neutralizing activity to all four serotypes. While such an approach

may yield mAbs with lower neutralization potency than the other strategies described, it offers the distinct advantage of being more economical than the development of multiple antibodies for the treatment of the four serotypes of DV. With the majority of the burden of dengue disease affecting developing regions, therapeutic cost becomes a paramount concern for effective and widespread use of a dengue therapeutic agent.

4.4.6. Overall significance and future directions

Overall, this study demonstrated the development and application of empirical informatics design methods to rationally redesign mAb 4E11 for significantly increased affinity and neutralizing activity to DV4 while approximately not changing affinity and activity to DV1-3. The quintuple mutant mAb 4E-5A exhibits a unique affinity and neutralizing activity profile towards the four serotypes of DV. These findings collectively provide the groundwork for: (1) further development and assessment of empirical informatics-based computational tools for antibody design and affinity enhancement, (2) more detailed investigation of the molecular mechanisms governing neutralization potency of flavivirus antibodies and particularly the role of affinity in affecting neutralization activity, and (3) the development of a broad spectrum neutralizing antibody for therapeutic and prophylactic treatment of dengue.

Attributions The work described in this chapter involved the participation of multiple individuals. Kannan Tharakaraman developed and implemented the computational studies. My contributions to these studies included the selection of 4E11 and overall design of the project as well as the design, development and implementation of experimental studies. Andrew Hatas and Yi-Ling (Joanne) Chen assisted with performing some neutralization, ELISA, and antibody expression experiments.

4.5. References

1. Beatty, M., G. Letson, and H. Margolis, *Estimating the global burden of dengue*. Am J Trop Med Hygiene, 2009. **81**(5): p. 231.
2. Gubler, D.J., *Epidemic dengue/dengue hemorrhagic fever as a public health, social and economic problem in the 21st century*. Trends in Microbiology, 2002. **10**(2): p. 100-103.
3. Mukhopadhyay, S., R.J. Kuhn, and M.G. Rossmann, *A structural perspective of the flavivirus life cycle*. Nat Rev Micro, 2005. **3**(1): p. 13-22.
4. Kuhn, R.J., et al., *Structure of Dengue Virus: Implications for Flavivirus Organization, Maturation, and Fusion*. Cell, 2002. **108**(5): p. 717-725.
5. Rey, F.A., et al., *The envelope glycoprotein from tick-borne encephalitis virus at 2.8 Å resolution*. Nature, 1995. **375**(6529): p. 291-298.
6. Crill, W.D. and J.T. Roehrig, *Monoclonal Antibodies That Bind to Domain III of Dengue Virus E Glycoprotein Are the Most Efficient Blockers of Virus Adsorption to Vero Cells*. Journal of Virology, 2001. **75**(16): p. 7769-7773.
7. Meulen, J.t., *Monoclonal antibodies for prophylaxis and therapy of infectious diseases*. Expert Opinion on Emerging Drugs, 2007. **12**(4): p. 525-540.
8. Casadevall, A., E. Dadachova, and L.-a. Pirofski, *Passive antibody therapy for infectious diseases*. Nat Rev Micro, 2004. **2**(9): p. 695-703.
9. Marasco, W.A. and J. Sui, *The growth and potential of human antiviral monoclonal antibody therapeutics*. Nat Biotech, 2007. **25**(12): p. 1421-1434.
10. Murphy, B.R. and S.S. Whitehead, *Immune Response to Dengue Virus and Prospects for a Vaccine**. Annual Review of Immunology, 2011. **29**(1): p. 587-619.
11. Cherrier, M.V., et al., *Structural basis for the preferential recognition of immature flaviviruses by a fusion-loop antibody*. The EMBO journal, 2009. **28**(20): p. 3269-3276.
12. Stiasny, K., et al., *Cryptic Properties of a Cluster of Dominant Flavivirus Cross-Reactive Antigenic Sites*. Journal of Virology, 2006. **80**(19): p. 9557-9568.
13. Lok, S.-M., et al., *Binding of a neutralizing antibody to dengue virus alters the arrangement of surface glycoproteins*. Nat Struct Mol Biol, 2008. **15**(3): p. 312-317.
14. Sukupolvi-Petty, S., et al., *Type- and Subcomplex-Specific Neutralizing Antibodies against Domain III of Dengue Virus Type 2 Envelope Protein Recognize Adjacent Epitopes*. Journal of Virology, 2007. **81**(23): p. 12816-12826.
15. Thullier, P., et al., *A recombinant Fab neutralizes dengue virus in vitro*. Journal of Biotechnology, 1999. **69**(2-3): p. 183-190.
16. Megret, F., et al., *Use of recombinant fusion proteins and monoclonal antibodies to define linear and discontinuous antigenic sites on the dengue virus envelope glycoprotein*. Virology, 1992. **187**(2): p. 480-491.
17. Saejung, W., et al., *Enhancement of recombinant soluble dengue virus 2 envelope domain III protein production in Escherichia coli trxB and gor double mutant*. Journal of Bioscience and Bioengineering, 2006. **102**(4): p. 333-339.
18. Friguet, B., et al., *Measurements of the true affinity constant in solution of antigen-antibody complexes by enzyme-linked immunosorbent assay*. Journal of Immunological Methods, 1985. **77**(2): p. 305-319.
19. Martineau, P., *Affinity Measurements by Competition ELISA*, in *Antibody Engineering*, R. Kontermann and S. Dubel, Editors. 2010, Springer: Berlin. p. 657-665.

20. Bobrovnik, S.A., *Determination of antibody affinity by ELISA. Theory.* Journal of Biochemical and Biophysical Methods, 2003. **57**(3): p. 213-236.
21. Marcatili, P., A. Rosi, and A. Tramontano, *PIGS: automatic prediction of antibody structures.* Bioinformatics, 2008. **24**(17): p. 1953-1954.
22. Lisova, O., et al., *Mapping to completeness and transplanted of a group-specific, discontinuous, neutralizing epitope in the envelope protein of dengue virus.* Journal of General Virology, 2007. **88**(9): p. 2387-2397.
23. Bedouelle, H., et al., *Diversity and junction residues as hotspots of binding energy in an antibody neutralizing the dengue virus.* FEBS Journal, 2006. **273**(1): p. 34-46.
24. Darnell, S.J., D. Page, and J.C. Mitchell, *An automated decision-tree approach to predicting protein interaction hot spots.* Proteins: Structure, Function, and Bioinformatics, 2007. **68**(4): p. 813-823.
25. Pons, C., et al., *Present and future challenges and limitations in protein-protein docking.* Proteins: Structure, Function, and Bioinformatics, 2010. **78**(1): p. 95-108.
26. Midgley, C.M., et al., *Structural Analysis of a Dengue Cross-Reactive Antibody Complexed with Envelope Domain III Reveals the Molecular Basis of Cross-Reactivity.* The Journal of Immunology, 2012. **188**(10): p. 4971-4979.
27. Wahala, W.M.P.B., et al., *Natural Strain Variation and Antibody Neutralization of Dengue Serotype 3 Viruses.* PLoS Pathog, 2010. **6**(3): p. e1000821.
28. Gromowski, G.D., N.D. Barrett, and A.D.T. Barrett, *Characterization of Dengue Virus Complex-Specific Neutralizing Epitopes on Envelope Protein Domain III of Dengue 2 Virus.* Journal of Virology, 2008. **82**(17): p. 8828-8837.
29. Gromowski, G.D. and A.D.T. Barrett, *Characterization of an antigenic site that contains a dominant, type-specific neutralization determinant on the envelope protein domain III (ED3) of dengue 2 virus.* Virology, 2007. **366**(2): p. 349-360.
30. Brien, J.D., et al., *Genotype-Specific Neutralization and Protection by Antibodies against Dengue Virus Type 3.* Journal of Virology, 2010. **84**(20): p. 10630-10643.
31. Wells, J.A., *Additivity of mutational effects in proteins.* Biochemistry, 1990. **29**(37): p. 8509-8517.
32. Northrup, S.H. and H.P. Erickson, *Kinetics of protein-protein association explained by Brownian dynamics computer simulation.* Proceedings of the National Academy of Sciences, 1992. **89**(8): p. 3338-3342.
33. Cockburn, Joseph J.B., et al., *Mechanism of Dengue Virus Broad Cross-Neutralization by a Monoclonal Antibody.* Structure, 2012. **20**(2): p. 303-314.
34. Sukupolvi-Petty, S., et al., *Structure and Function Analysis of Therapeutic Monoclonal Antibodies against Dengue Virus Type 2.* Journal of Virology, 2010. **84**(18): p. 9227-9239.
35. Shrestha, B., et al., *The Development of Therapeutic Antibodies That Neutralize Homologous and Heterologous Genotypes of Dengue Virus Type 1.* PLoS Pathog, 2010. **6**(4): p. e1000823.
36. de Alwis, R., et al., *In-Depth Analysis of the Antibody Response of Individuals Exposed to Primary Dengue Virus Infection.* PLoS Negl Trop Dis, 2011. **5**(6): p. e1188.
37. Crill, W.D., et al., *Humoral Immune Responses of Dengue Fever Patients Using Epitope-Specific Serotype-2 Virus-Like Particle Antigens.* PLoS ONE, 2009. **4**(4): p. e4991.
38. Beltramello, M., et al., *The Human Immune Response to Dengue Virus Is Dominated by Highly Cross-Reactive Antibodies Endowed with Neutralizing and Enhancing Activity.* Cell Host & Microbe, 2010. **8**(3): p. 271-283.
39. Lai, C.-Y., et al., *Antibodies to Envelope Glycoprotein of Dengue Virus during the Natural Course of Infection Are Predominantly Cross-Reactive and Recognize Epitopes Containing Highly*

- Conserved Residues at the Fusion Loop of Domain II.* Journal of Virology, 2008. **82**(13): p. 6631-6643.
40. Roehrig, J.T., *Antigenic Structure of Flavivirus Proteins*, in *Advances in Virus Research*. 2003, Academic Press. p. 141-175.
 41. Roehrig, J.T., R.A. Bolin, and R.G. Kelly, *Monoclonal Antibody Mapping of the Envelope Glycoprotein of the Dengue 2 Virus, Jamaica.* Virology, 1998. **246**(2): p. 317-328.
 42. Klasse, P.J. and Q.J. Sattentau, *Occupancy and mechanism in antibody-mediated neutralization of animal viruses.* Journal of General Virology, 2002. **83**(9): p. 2091-2108.
 43. Law, M. and L. Hangartner, *Antibodies against viruses: passive and active immunization.* Current Opinion in Immunology, 2008. **20**(4): p. 486-492.
 44. Dowd, K.A. and T.C. Pierson, *Antibody-mediated neutralization of flaviviruses: A reductionist view.* Virology, 2011. **411**(2): p. 306-315.
 45. Pierson, T.C., et al., *Structural Insights into the Mechanisms of Antibody-Mediated Neutralization of Flavivirus Infection: Implications for Vaccine Development.* Cell Host & Microbe, 2008. **4**(3): p. 229-238.
 46. Pierson, T.C., et al., *The Stoichiometry of Antibody-Mediated Neutralization and Enhancement of West Nile Virus Infection.* Cell host & microbe, 2007. **1**(2): p. 135-145.
 47. Lippow, S.M., K.D. Wittrup, and B. Tidor, *Computational design of antibody-affinity improvement beyond in vivo maturation.* Nat Biotech, 2007. **25**(10): p. 1171-1176.
 48. Clark, L.A., et al., *Affinity enhancement of an in vivo matured therapeutic antibody using structure-based computational design.* Protein Science, 2006. **15**(5): p. 949-960.
 49. Marvin, J.S. and H.B. Lowman, *Redesigning an Antibody Fragment for Faster Association with Its Antigen.* Biochemistry, 2003. **42**(23): p. 7077-7083.
 50. Farady, C.J., et al., *Improving the species cross-reactivity of an antibody using computational design.* Bioorganic & Medicinal Chemistry Letters, 2009. **19**(14): p. 3744-3747.
 51. Diskin, R., et al., *Increasing the Potency and Breadth of an HIV Antibody by Using Structure-Based Rational Design.* Science, 2011. **334**(6060): p. 1289-1293.
 52. Goldberg, M.E. and L. Djavadi-Ohanian, *Methods for measurement of antibody/antigen affinity based on ELISA and RIA.* Current Opinion in Immunology, 1993. **5**(2): p. 278-281.
 53. Vaughn, D.W., et al., *Dengue Viremia Titer, Antibody Response Pattern, and Virus Serotype Correlate with Disease Severity.* Journal of Infectious Diseases, 2000. **181**(1): p. 2-9.
 54. World Health Organization (WHO), *Dengue: Guidelines for Diagnosis, Treatment, Prevention and Control—New Edition.* 2009, UNICEF, UNDP, World Bank: Geneva.
 55. Balsitis, S.J., et al., *Lethal Antibody Enhancement of Dengue Disease in Mice Is Prevented by Fc Modification.* PLoS Pathog, 2010. **6**(2): p. e1000790.
 56. Deng, Y.-Q., et al., *A Broadly Flavivirus Cross-Neutralizing Monoclonal Antibody that Recognizes a Novel Epitope within the Fusion Loop of E Protein.* PLoS ONE, 2011. **6**(1): p. e16059.
 57. Tricou, V., et al., *A Randomized Controlled Trial of Chloroquine for the Treatment of Dengue in Vietnamese Adults.* PLoS Negl Trop Dis, 2010. **4**(8): p. e785.
 58. Randolph, V.B., G. Winkler, and V. Stollar, *Acidotropic amines inhibit proteolytic processing of flavivirus prM protein.* Virology, 1990. **174**(2): p. 450-458.
 59. Navarro-Sanchez, E., et al., *Dendritic-cell-specific ICAM3-grabbing non-integrin is essential for the productive infection of human dendritic cells by mosquito-cell-derived dengue viruses.* EMBO Rep, 2003. **4**(7): p. 723-728.
 60. Teoh, E.P., et al., *The Structural Basis for Serotype-Specific Neutralization of Dengue Virus by a Human Antibody.* Science Translational Medicine, 2012. **4**(139): p. 139ra83.

61. Oliphant, T., et al., *Development of a humanized monoclonal antibody with therapeutic potential against West Nile virus*. Nat Med, 2005. **11**(5): p. 522-530.
62. Goncalvez, A.P., et al., *Monoclonal antibody-mediated enhancement of dengue virus infection in vitro and in vivo and strategies for prevention*. Proceedings of the National Academy of Sciences, 2007. **104**(22): p. 9422-9427.
63. Vogt, M.R., et al., *Poorly Neutralizing Cross-Reactive Antibodies against the Fusion Loop of West Nile Virus Envelope Protein Protect In Vivo via Fcγ Receptor and Complement-Dependent Effector Mechanisms*. Journal of Virology, 2011. **85**(22): p. 11567-11580.
64. Shrestha, B., et al., *Complex phenotypes in mosquitoes and mice associated with neutralization escape of a Dengue virus type 1 monoclonal antibody*. Virology, 2012. **427**(2): p. 127-134.

5. Summary and significance

Proteins and polysaccharides are of growing importance as a source for novel therapeutic compounds due, in part, to their exquisite biological specificity, range of functionalities, and accumulating evidence of their clinical efficacy and safety. Proteins and polysaccharides in their natural form may demonstrate interesting “lead” activities by, for example, binding a therapeutic target. However, as they did not evolve for use as drugs, improvement in their properties, such as activity, affinity, specificity, and stability, among others, often is necessary to convert them to clinically viable compounds. In turn, characterization and rational engineering of proteins and polysaccharides that exhibit lead therapeutic activities are important steps towards the realization of new and improved clinically viable biopolymer drugs. However, owing to their large and structures, proteins and polysaccharides are faced with a unique set of challenges, compared to small molecules, in their discovery and development as safe, efficacious drugs.

In this thesis, we describe the implementation of structure-function relationship approaches to characterize and engineer polysaccharides and antibodies towards improving their therapeutic activity profiles. First, using an integrated approach, we engineer a modified pectin that exhibits significant *in vivo* anticancer activity, which we link to specific structural attributes and cellular functional mechanisms. These results improve our structure-function understanding of anticancer modified pectin, an important step towards the clinical use of this complex polysaccharide. Second, we employ orthogonal analytical approaches to identify and characterize oversulfated chondroitin sulfate, a glycan structurally related to heparin, as the major contaminant in batches of heparin drug product associated with an outbreak of adverse events. We link presence of the contaminant to activation of the contact pathway, thereby establishing a structure-function understanding of contaminated heparin and improving the safety profile of this polysaccharide drug. Lastly, we rationally design, using structure-based complementary approaches of energetics and empirical informatics methods, a broad spectrum neutralizing antibody to dengue virus. The engineered antibody demonstrates binding to all four serotypes of the virus and good *in vitro*

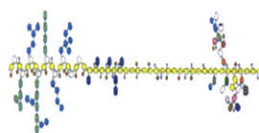
potency, an activity profile that lends itself as a potential lead molecule for further development as a therapeutic/prophylactic for treatment of dengue.

Beyond implications for the individual molecules studied herein (pectin, heparin, and dengue antibody), this thesis reveals broader insights thematic to structure-function investigations of polysaccharides and proteins. First, the use of multiple complementary structural methods, which alone only reveal limited information, substantially improve the accuracy of structural characterization through the provision of orthogonal types of information (**Figure 5.1**). In the cases of pectin and heparin, utilization of multiple analytical techniques, including CE, NMR, MS, and enzymatic digestion, was central to rapidly converging on key differences (i.e., between ACP and NCP for pectin, and heparin from OSCS) without requiring exhaustive characterization of all structural attributes of the multiple samples. For the engineered dengue mAb, empirical informatics of antibody-antigen structures provided complementary and critical insights when coupled with energetics-based methods for the generation of a 4E11:EDIII structural model and design of affinity-enhancing mutations.

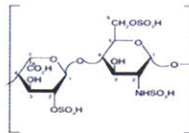
A second thematic insight from this thesis is the utility of statistical representation of complex structures, in contrast with complete structural elucidation or description, to rapidly develop robust structure-function relationships of polysaccharides and proteins (**Figure 5.1**). For pectin and heparin, statistical descriptions of structural attributes, such as fragmentation percentage and average sulfation density, helped facilitate an understanding of key structural differences of samples without demanding complete structural elucidation. In the case of engineering a dengue mAb, antibody-antigen interface structural features as well as paratope-epitope amino acid preferences were captured and implemented by statistical representation, an approach that enabled effective computational structural modeling and mutation design.

Focusing on the cases of pectin, heparin, and an anti-dengue antibody, this thesis has contributed to the development and implementation of structure-function approaches for characterizing and engineering polysaccharides and antibodies towards their safer and more efficacious clinical use. Findings described herein provide information towards directly improving

our ability to develop polysaccharide and antibody-based therapeutics to combat important medical diseases with unmet treatment needs.



Anticancer modified pectin



Contaminated heparin



Engineered dengue mAb

Use of complementary structural methods	Orthogonal analytical techniques for structure characterization	Orthogonal analytical techniques for structure characterization	Empirical information & energetics for modeling
Statistical representation of complex structures	Structural attributes as statistical features	Structural attributes as statistical features	Interface features and pairwise interactions as statistics

Figure 5.1 Summary of broader implications from this thesis regarding structure-function relationships of complex biopolymers.

List of Abbreviations

ACP	Activated citrus pectin
ADE	Antibody-dependent enhancement
AT	Antithrombin
BSA	Bovine serum albumin
C	Capsid
CDC	Centers for Disease Control
CDR	Complementarity determining region
CE	Capillary electrophoresis
COSY	Correlation spectroscopy
CRD	Carbohydrate recognition domain
DF	Dengue fever
dGalA	4,5-dehydrogalacturonic acid
DHF	Dengue hemorrhagic fever
DSS	Dengue shock syndrome
DV	Dengue virus
E	Envelope
EDI	Envelope protein domain I
EDII	Envelope protein domain II
EDIII	Envelope protein domain III
ELISA	Enzyme-linked immunosorbent assay
ER	Endoplasmic reticulum
Fc	Fragment crystallizable
FDA	Food and Drug Administration

FFU	Focus-forming units
FRNT	Focus reduction neutralization test
GAG	Glycosaminoglycan
Gal-1	Galectin-1
Gal-3	Galectin-3
GalA	Galacturonic acid
GlcA	Glucuronic acid
GlcNAc	N-acetylglucosamine
GlcNS	N-sulfonated glucosamine
HG	Homogalacturonan
HIV	Human immunodeficiency virus
HPLC	High pressure liquid chromatography
HS	Heparan sulfate
HSQC	Heteronuclear single-quantum correlation spectroscopy
HUVEC	Human umbilical vein endothelial cell
IdoA	Iduronic acid
JEV	Japanese encephalitis virus
K _D	Dissociation constant
LMWH	Low molecular weight heparin
M	Membrane
mAb	Monoclonal antibody
MALDI	Matrix-assisted laser desorption ionization
MS	Mass spectrometry
NCP	Native citrus pectin
NMR	Nuclear magnetic resonance

NS	Non-structural
OSCS	Oversulfated chondroitin sulfate
PBS	Phosphate-buffered saline
PDB	Protein data bank
PI3K	Phosphoinositide 3-kinase
PK	Pharmacokinetics
prM	Precursor membrane
PRSSV	Porcine reproductive and respiratory syndrome virus
RGI	Rhamnogalacturonan I
RGII	Rhamnogalacturonan II
Rha	Rhamnose
ROSEY	Rotating frame nuclear Overhauser effect spectroscopy
SEC	Size exclusion chromatography
TOCSY	Total correlation spectroscopy
UFH	Unfractionated heparin
WHO	World Health Organization
WNV	West Nile virus